ROMA TRE
UNIVERSITÀ DEGLI STUDI

DOCTORAL THESIS

An innovative architecture for an intelligent building energy management system

Author:
Fiorella LAURO

Supervisors:
Prof. Stefano PANZIERI
Roma Tre University
Prof. Stefano Paolo CORGNATI
Politecnico di Torino

A thesis submitted in fulfilment of the requirements
for the degree of Doctor of Philosophy in Computer Science and Automation

at the

Engineering Department
Section of Computer Science and Automation
Roma Tre University

JUNE 2016

ROMA TRE UNIVERSITY

Abstract

Engineering Department

Section of Computer Science and Automation

Doctor of Philosophy in Computer Science and Automation

An innovative architecture for an intelligent building energy management system

by Fiorella LAURO

Due to the increasing urbanization one of the main focuses of the environmental policy is constituted by the cities, where a better quality of life and lower energy consumption will be made possible by digital technology and innovation. Buildings are one of the main urban sectors involved in this challenge. The management systems of Smart Buildings look beyond the general objective to fulfill the occupants' comfort requirements and reduce the energy consumption. Smart Buildings are connected and responsive to the Smart Power Grid, and they interact with building operators and occupants to empower them with new monitoring levels and operational information on building performance. This work proposes a modular and hierarchical system architecture for the building energy management that accounts for the building operating conditions and the surrounding grid system. The research experiences described in this work constitute modules of this system acting at different levels and with different purposes. The first research experience is related to the regulation of the indoor temperatures of a multi-zones building on the basis of the occupancy profiles through an adaptive model predictive control law. Secondly a comprehensive fault detection and diagnosis methodology of anomalous building energy consumptions through artificial intelligence and data mining techniques is presented. Finally the results obtained by the application of this fault detection and diagnosis methodology to the electrical consumptions of several actual buildings are described.

Contents

List of Figures

List of Tables

List of Abbreviations

ADR	**A**ctive **D**emand **R**esponse
ANN	**A**rtificial **N**eural **N**etwork
ANNE	**A**rtificial **N**eural **N**etwork **E**nsemble
BEM	**B**asic **E**nsemble **M**ethod
BEMS	**B**uilding **E**nergy **M**anagement **S**ystem
CART	**C**lassification **A**nd **R**egression **T**ree
DBSCAN	**D**ensity-**B**ased **S**patial **C**lustering of **A**pplications with **N**oise
DR	**D**emand **R**esponse
DSO	**D**istribution **S**ystem **O**perator
DSM	**D**emand **S**ide **M**anagement
ECMS	**E**nergy and **C**omfort **M**anagement **S**ystem
EMPC	**E**conomic **M**odel **P**redicitive **C**ontrol
ENEA	Italian National Agency for New Technologies, Energy and Sustainable Economic Development
FDD	**F**ault **D**etection and **D**iagnosis
GESD	**G**eneralized **E**xtreme **S**tudentized **D**eviate
HVAC	**H**eating **V**entilation **A**ir **C**onditioning
ICT	**I**nformation and **C**ommunications **T**echnology
MAE	**M**ean **A**bsolute **E**rror
MAX	**M**aximum **A**bsolute **E**rror
MLP	**M**ulti-**L**ayer **P**erceptron
MPC	**M**odel **P**redicitive **C**ontrol
MVEM	**M**ajority **V**ote **E**nsemble **M**ethod
RES	**R**enewable **E**nergy **S**ources
RTP	**R**eal **T**ime **P**ricing
SG	**S**mart **G**rid
TOU	**T**ime **O**f **U**se
TSO	**T**ransmission **S**ystem **O**perator

Chapter 1

Buildings and energy: the current scenario

1.1 Introduction

Cities represent the biggest environmental policy challenge as they are responsible for about two-thirds of global energy consumption and about 80% of global carbon dioxide (CO_2) emissions [109]. Currently half the world's population lives in cities but urbanisation is set to increase: in 2050 cities will house three-quarters of the global population [1]. In order to deal with the urban growth new ways to manage cities and make them more effective are needed.

The convergence between the world of information and communications technology (ICT) and the world of energy (the *Energy 3.0*) is creating the conditions for new services and new technologies, e.g. smart and interoperable meters, variable speed and intensity controlled devices for the lighting appliances, management and control systems of the building energy consumptions [52]. In the same way that the ICT revolution has been driven by people needs to produce information and customise their content, so too the energy revolution will enable energy self-production and customisation of energy usages and consumption.

Smart City and Energy 3.0 challenges will be made possible by technological aspects strictly related to the concept of Internet of Things (IoT): more efficient and miniaturized sensors that can register information about consumption and production of energy, weather and environmental conditions, traffic and people flows; networks that interconnect all objects to one another, tracking and exchanging this information in real time. Furthermore the use of open data will create new personalised services such as better transport connections, accident risk warnings, home monitoring, new tariffs offered by utilities, such as Time Of Use (TOU) pricing which will encourage end-users to use energy in off-peak times when it is cheaper. The interconnection between the several urban aspects and the possibility to offer urban services on demand allows to

define a city "smart". This ongoing innovation is changing the way we use energy and will lead both to a better quality of life and lower energy consumption.

This work focuses on a particular aspect of the Smart City, the Smart Building, with the main purpose to propose an innovative architecture for the building energy management that takes in account the operating conditions of the building and of the surrounding energy system that directly interacts with the building. This Introduction Chapter highlights how today Smart Buildings operate in the world of Energy 3.0. The key role that Smart Buildings play in their own energy management and in the energy balance of the grid system is described. In Chapter 2 an overview on the control strategies for the energy management in buildings and for the Demand Side Management context in which buildings are involved is illustrated, and a modular and hierarchical building management system is proposed. In this regard the research experiences carried out and shown in Chapters 3, 4 and 5 constitute modules of this system acting at different levels and with different purposes. In particular Chapter 3 proposes an adaptive model predictive control (MPC) law based on the occupancy profiles for the regulation of the indoor temperatures of a multi-zones building. For the results evaluation, distributed and decentralized MPC architectures are compared. Chapter 4 focuses on the fault detection process of anomalous building energy consumption using actual data through artificial intelligence and data mining techniques. The faults detected refer to both single and consecutive (trend) anomalous consumption values. Chapter 5 represents a sort of completion of the previous Chapter, since it presents the application and then the on-line implementation of a comprehensive fault detection and diagnosis methodology of anomalous actual building electrical consumption. Finally, in Chapter 6 conclusions and possible future works are drawn.

1.2 Smart Buildings and Smart Grids

The major challenge that identifies buildings as “Smart Buildings" is the fulfillment over the building lifecycle of the comfort and safety requirements while minimizing energy cost and environmental impact, supporting the electrical grid [52]. Thus the Smart Building concept takes on a local and global meaning, as discussed below.

1.2.1 A look inside the Smart Building

To reach the vision of "Smart Building" it is not enough for a building to simply contain the systems that provide comfort and safety (Fig. 1.1a). Modern buildings are complex concatenations of structures, mechanical devices, sophisticated control systems and technologies, developed and improved over time, that result in services for

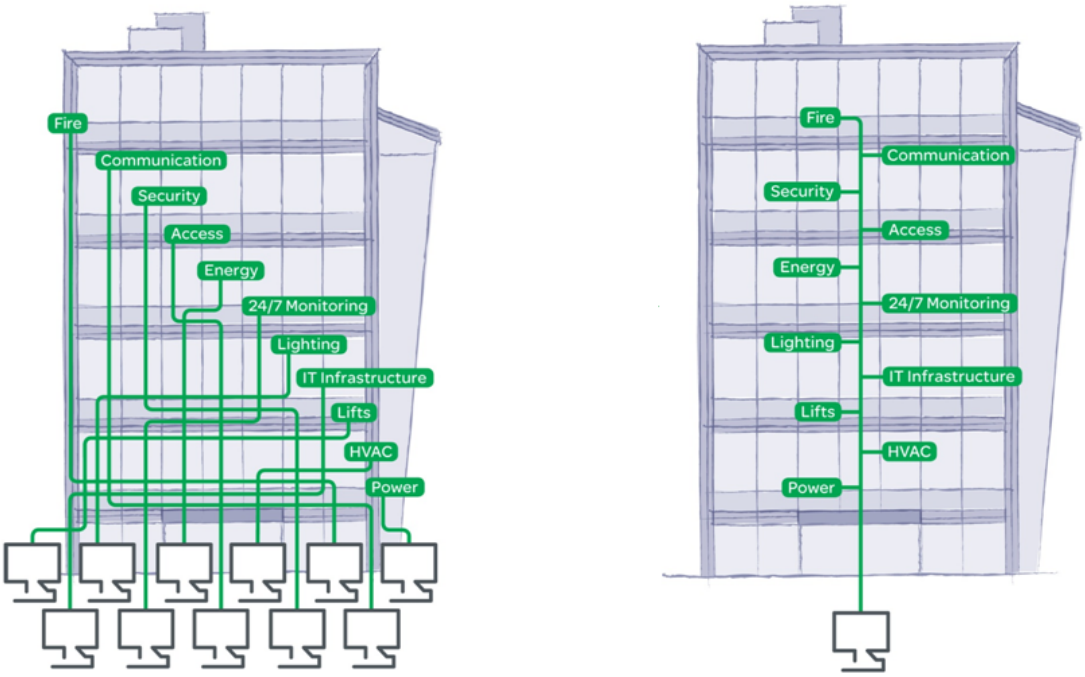

(A) Traditional design

(B) Integrated systems

FIGURE 1.1: Multiple systems in a building

the occupants (e.g. illumination, thermal comfort, air quality, physical security, sanitation). These systems may prove to be different data sources communicating through their own proprietary protocols, thus enabling the information exchange only in some directions. Multiple systems that operate simultaneously and individually can easily lead to complex troubleshooting, higher capital and operational expenditures and obstacles to achieving energy efficiency. Therefore it is necessary to connect the building systems in an integrated, dynamic and functional way (Fig. 1.1b). The building integrated systems have several advantages including:

- reduce the costs (both initial investments and ongoing operational expenses);
- increase the employee productivity;
- capitalize the on long-term financial value;
- create new revenue opportunities;
- enhance the building asset value;
- improve the customer experience.

The way to interoperable, connected devices and systems requires cooperation between different companies that often are historical business competitors. Anyway in the last years the adoption by many companies of some open standards such as BACnet, Modbus and LonWorks enabled the producers to make their contribution to a

functional whole [52]. The connection between all these features implies adding intelligence from the beginning of design phase through to the end of the building's useful life. Smart Buildings use ICT to connect all the equipment and systems so that they can share information to optimize total building performance. Examples are the thermal plant optimization process, that uses weather data and information about occupancy, or the lighting and heating/cooling control systems that act on the basis of occupancy data deriving from the building security system.

A Smart Building creates its management platform by connecting information of systems and components in an open format, allowing for the development of new applications that save time, energy and operating costs. People inside the Smart Building are a crucial component of its intelligence because energy use and occupant comfort require human involvement in the decision-making. A Smart Building provides intuitive tools designed to improve and enhance the activity of the people according to their needs. The facility managers can interact with these tools to do their jobs better, providing more comfort and more safety with less money, less energy and less environmental impact.

1.2.2 Beyond the walls of the Smart Building

The "Smart Grid" [8, 135, 52] is an emerging concept in recent years and consists of controls, computers, automation, new technologies and equipment working together with the electrical grid to respond digitally to the quickly changing electric demand. The Smart Grid represents a great opportunity to move the energy industry into a new era of reliability, availability and efficiency that will contribute to global economic and environmental health. This opportunity is not just about utilities and technologies; it is about giving consumers the information and tools they need to make choices about their energy use. The energy sector is experiencing a growing number of consumers producing their own energy, sharing it with one another and customising it for their own personal use. The Smart Grid will enable an unprecedented level of consumer participation, thus it is the ideal place for Smart Buildings to leverage the surrounding knowledge. Electricity markets are evolving toward "real time". In this scenario buildings can receive requests to reduce demand when wholesale prices are high or when grid reliability is jeopardized. In addition dynamic electric rates are a growing trend, then buildings more likely pay the actual cost of producing electricity at the instant it is used instead of the average cost over long time periods. Technology will be the key enabler, providing building operators with the tools and information they need to make smart choices, in this way building operators are not required to directly monitor markets and react to signals.

From the grid point of view, buildings are considered as load elements of the energy district ("micro-grid") in which they belong (see Fig. 1.2), operating in the overall grid connection mode. A micro-grid generally includes:

- load elements (e.g. buildings or groups of buildings also with different characteristics);
- Renewable Energy Source (RES) generation elements (e.g. solar panels, wind turbines);
- storage elements (e.g. electric vehicles).

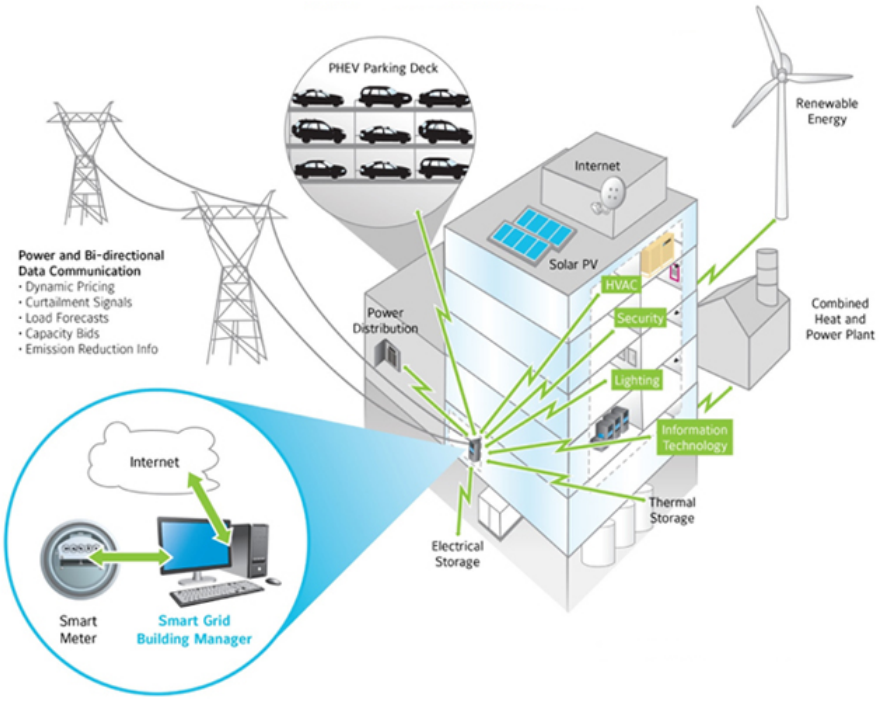

FIGURE 1.2: Smart Buildings and Smart Grid

Depending on the extent to which the load in the micro-grid can be controlled, the demand can be grouped into three categories [51]:

- Critical load: corresponds to non controllable devices, with a demand that must be supplied to avoid user's dissatisfaction (e.g. lighting);
- Adjustable load: corresponds to controllable devices (e.g. air conditioning). If necessary the consumption level of these devices can be remotely decreased for a specified time period in order to avoid load management problems;
- Shiftable load: corresponds to devices with a shiftable demand through the considered horizon (e.g. electric vehicle demand under some constraints).

The energy management of a micro-grid is based on an optimization model responsible for the overall coordination that changes depending on the adopted Demand Response (DR) policy (see Paragraph 1.3.1). The goal of the micro-grid optimization is to minimize the economic costs associated with the exchanged energy between the grid and the micro-grid. For instance, in the case of the TOU DR policy, the optimization model is based on three layers. The first layer optimization executes one-day-ahead considering daily forecasts regarding e.g. weather (then RES generation), demand, electric vehicles mobility (then storage) and energy price from the retail provider. The result of this optimization process is an optimal schedule for all the components of the micro-grid for the next 24 hours [51]. A further energy management layer minimizes the deviation with respect to the one-day-ahead optimal program (mostly caused by forecasts deviations) taking into account real measurements and short-term forecasts. This level is also responsible of the interaction with the Commercial Aggregator (see Section 1.3) through a flexibility forecaster tool [24]: this tool predicts the micro-grid's flexibility under a specific price incentive signal sent by the Aggregator on the basis of the micro-grid predefined energy consumption (purchased power from the grid). Finally, a real time energy management layer ensures balance between generation and demand against any unexpected issue (e.g. failures, unexpected loads, grid disconnection). These last two energy management layers have usually a control horizon of minutes order.

The benefits offered by the Smart Grid are not temporary and extend beyond the the entire lifetime of the Smart Building [52]. The electric grid becomes more robust and reliable. The carbon footprint is minimized as RES provide power, balanced with the information network that dinamically matches demand with variable supply. Electric vehicles move people, serving also as batteries (storage elements). Businesses operate at a new level of efficiency by using data in new ways, leveraging the connection between systems that until now have been entirely independent.

1.3 The Demand Side Management

Buildings are often characterized by a high simultaneous energy demand, that corresponds to a considerable peak demand effort in the energy distribution grid. Peak demand is a considerable issue for both suppliers and energy customers due to financial and capacity related aspects. Moreover, the profiles of users energy demand and energy produced from renewable sources typically do not match: the non-simultaneity between demand and supply causes imbalances in the electrical system, and the advantages that users can obtain are followed by drawbacks in the distribution grid [108].To overcome these problems current solutions are represented by energy accumulators and storage elements. However, especially in the electric field, these technologies do not allow for a proper balance of powers required by the the grid and they undermine

the reliability of the whole system. For this reason, in recent years the concept of Smart Grid (SG) was introduced, as an electrical system able to exchange not only energy flows but also information between the various components of the grid. In this regard it becomes possible to optimize energy consumptions with respect to energy availability using algorithms for the control of the SG [38, 125].

The Demand Side Management (DSM) is an approach that actively manage energy demand and supply in order to satisfy customers comfort requirements and in the meanwhile to achieve economics and consumptions savings from both the utility and the customer point of view [69]. Active Demand Response (ADR) is a particular case of DSM: the focus is on the short-term load handling. In particular, the goal is to follow a daily short-term schedule (e.g. hourly) which is periodically adapted according to external conditions (e.g. users behavior, weather conditions, market energy price, energy production available) such that the day-ahead load curve constraint is met. The DSM is aimed at modulating the shape of the load consumptions curve through direct and indirect operations affecting customers demand profile. Generally, the shape is modulated such that loads are shifted, peaks shaved or demand curve is flattened. DSM is an integrant part of SG and requires a proper ICT infrastructure (e.g. communication system, sensors, actuators, advanced processors, etc.) in order to achieve a dynamic control of the demand. The DSM, by promoting the interaction and responsiveness of the customers, determines short-term impacts on the electricity markets, leading to economic benefits for both customers and utility. Moreover, by improving the reliability of the power plant and, in the long term, by lowering peak demand, this strategy allows reduction of the overall plant, capital cost investments and postpones the need of network upgrades.

Energy systems are generally divided into five main sectors: Generation, Distribution/Transmission, Trading, Retailing, Consumptions. Generation main actors consist of power plants, providing energy through fossils or renewable sources. Distribution phase is based on Distribution System Operators (DSOs) and Transmission System Operators (TSOs), which in some cases redistribute energy to retailers [7]. However, wiring and retailing can be separated in some scenarios. Commercial Aggregators are responsible of trading phase, they sell energy to final users on a retail or wholesale market. Finally, the main actors of the consumption phase are customers, mostly related to commercial and residential building sectors. In this scenario, DSM plays an important role on retail phase: Commercial Aggregators trade energy according to dynamic deregulated markets in order to influence the demand curve by regulating customers behaviour through particular rates. Fig. 1.3 shows an example of scenario focused on a specific DSM application on buildings: the forecasted load curve can be used for adapting the daily buildings energy need in order to meet the required load hour by hour.

The DSM approach could lead to several benefits involving many aspects:

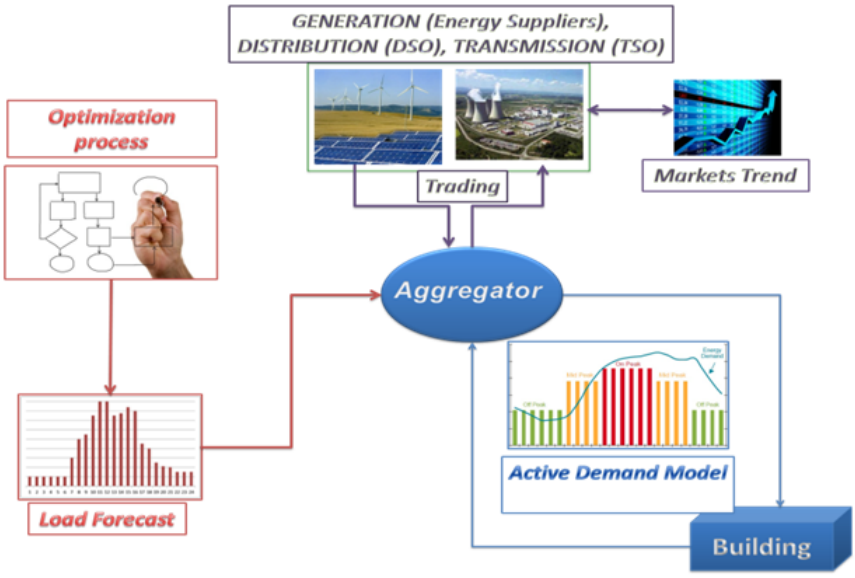

FIGURE 1.3: Example of an application scenario of DSM on residential and tertiary buildings

- *Reducing generation margin*. The total capacity of installed generation is generally larger than the system maximum demand in order to ensure the security of supply in case of exceptional events. It is estimated by Central Electricity Generating Board that margins account to 25%. Strbac [128] investigated the magnitude of shortages and their frequency in UK using a simplified generation model. According to his study, instead of dealing with such shortages by installing generation surplus systems that would be used very infrequently, it may be possible to identify house-holds that would be willing (for a fee) to forgo consumption relatively infrequently.

- *Improving transmission system*. Transmission infrastructures historically are designed for supporting large scale generation technologies. Moreover, for avoiding overloads due to circuit fails, they are based on a redundant network structure. The DSM approach can overcome those failures through load curtailing, allowing a proper design of the network.

- *Improving renewable sources usefulness*. The non-dispatchable and non completely predictable nature of renewable sources as wind and solar power, has somehow limited their penetration in energy markets and distribution supply. The DSM can improve their usefulness, rescheduling load peaks during high renewable supply and, on the other hand, decreasing demand during low renewable production.

Despite those advantages, also some drawbacks arise [108]. The current market structure is centralized and homogeneous, thus does not suit properly the flexibility required by DSM. Moreover, since benefits of the DSM affect a considerable amount of

different entities, it is challenging to identify a business model that justifies the investments [80]. Customers, especially in residential sector, do not always behave in economically rational manner: a study of Thorsnes et al. [130] demonstrated that price changes are not linearly related to consumptions changes, as the bill is not always the first concern of the customers.

The following Paragraph explains how the DSM acts in the energy distribution systems through the DR policies.

1.3.1 Demand Response policies

The DR indicates a specific tariff or program that allows end-use customers to change their normal patterns in order to respond to changes in price or availability of electricity on the markets [38]. End users can be directly or indirectly involved into the DR strategy. In the former scenario, they can perform load curtailment (e.g. dimming lights level, decreasing/increasing thermostat setpoints), consumption shifting (e.g. shifting heating/cooling phases into lower price time windows) or storage utilization. In the latter case, intermediary agents are involved, such as curtailment service providers, Commercial Aggregators of retail customers or DR providers [22].

DR policies can be divided into non-dispatchable, whose policies are proactive based and need to be properly scheduled, and dispatchable, namely reactive policies that enable to provide energy when actually needed. Among these two categories, different approaches were summarized in [125, 7].

Non-Dispatchable DR policies

The Dynamic Pricing is the main category, whose approach is to influence the demand by driving customers behaviour according to global load requirements through a dynamic energy price. Prices can vary on an hourly, daily or even a monthly basis. Lower fares during off-peaks periods encourage users to reschedule their activities. Most common dynamic pricing policies are:

- TOU: it is a very diffused tariff, generally daily changing with fixed blocks of pricing rates;
- Critical Peak Pricing: employed for commercial and industrial customers, it is an event-based tariff that triggers when critical peaks occur, and apply very high energy rates;
- Real Time Pricing (RTP): the rates change very fast, generally with hourly basis, depending to wholesale market prices.

Dispatchable DR policies

- Incentive Based: such approach is event based. A reward is guaranteed to customers for providing load reduction when particular events occur such as emergency, ancillary services or even interruptions. In Direct Load Control, customers allow a degree of control on their own equipment. Such approaches are very reliable, as the response of the users to events is fast and can overcome problems at system level.
- Demand Reduction Bids: customers actively propose a bid of a remunerated load reduction to the Commercial Aggregator.

Chapter 2

A modular and hierarchical architecture for the building energy management

2.1 Introduction

An efficient building energy management is essential for the reduction of power demands and greenhouse gas emissions, as the buildings sector accounts for about 40% of world total final energy consumption [26, 54].

The challenge of the last years concerning building control systems was to find a compromise between user comfort and energy consumption, building energy management systems (BEMS) in fact are also known as energy and comfort management systems (ECMS). These systems base their operations on intelligent control strategies, which use ICT infrastructure [123]. They commonly require functions including indoor comfort parameters (e.g. thermal, humidity, indoor air quality and illumination levels), occupant preferences and energy control [123].

The modern challenge for BEMSs is to actively interface with the grid energy management system. The BEMSs of buildings belonging to an energy district can be potentially involved in all the management levels and, depending on the size, complexity and tipology of the district, the number and the type of tasks delegated to BEMS can be different.

This Chapter presents an overview of the control strategies most used in recent years for building energy management and DSM. Then a model of system architecture for the building management on the basis of the energy current context described so far is proposed.

2.2 Control strategies for the energy management in buildings

The field of Smart Buildings encompasses an enormous variety of technologies, including energy management systems and building controls. BEMSs (or ECMSs or building energy and comfort management system, BECM) are control systems for individual buildings or groups of buildings that use computers and distributed microprocessors for monitoring, data storage and communication [98]. A BEMS consists of software and hardware; the software program is usually configured in a hierarchical manner, can be proprietary and can use Internet protocols and open standards.

The general objective of a BEMS is to fulfill the occupants' requirements for comfort while reducing energy consumption during building operations. In recent applications the energy market price variation is also taken into account [123]. Heating, ventilation, and air conditioning (HVAC) control, lighting control, hot water control and electricity control are commonly seen as required functions for the BEMS. Other common functions are the monitoring and control of fire systems and security systems. BEMSs provide the information and the tools that building managers need both to understand the energy usage of their buildings and to control and improve their buildings' energy performance.

For decades, BEMSs were employed for providing just enough energy to meet comfort standards. These energy efficiency measures contributed to sustainability goals, such as tracking and reducing greenhouse gas emissions, but building data were trapped within the BEMS and executive-level decision-makers could not measure and act on them. The "middleware" software level introduced in BEMS in recent years gathers data from all involved systems and merges it into a common platform for analytics and reporting [52]. One result is the web-based dashboard displays that offer a visual snapshot of which facilities are experiencing e.g. high energy usage, abnormal maintenance costs and many other situations that deserve prompt attention. When information is quickly available and can be accessed anywhere, energy managers are able to make better decisions that have an immediate impact on profitability. This feature results particularly useful when many buildings or geographic locations are involved.

There are numerous ways in which BEMSs act to reduce building operating cost, most of them involve optimized operation and increased efficiency [52]:

- optimized cooling and ventilation equipment: modeling loads dynamically allows the system to spend the minimum amount of energy and money to provide the comfort level desired;
- matching occupancy patterns to energy use: a Smart Building operates leaner (and save money) when there are less people inside;

- proactive maintenance of equipment: analysis algorithms detect problems in performance before they cause expensive outages, maintaining optimum efficiency along the way;
- dynamic power consumption: by taking signals from the electricity market and altering usage in response, a Smart Building ensures the lowest possible energy costs and often generates revenue by selling load reductions back to the grid.

BEMS can base their operations on building control schemes that can roughly be categorized as [123]:

- Conventional controllers, such as on/off switching controllers i.e. thermostats, Proportional (P), Proportional-Integral (PI), Proportional-Integral-Derivative (PID). The on/off controllers have been primarily used for indoor temperature regulation, however energy consumption and wastage are usually huge due to the substantial instabilities and frequent overshoot of the set points. Then they have been employed in various applications and disturbed environmental conditions, and have been poorly performing and generally have not been offered optimal control strategy. P, PI and PID controllers do not have any direct knowledge of the system to be controlled. They provide poor control performance for noisy and non-linear processes having large time delays when used alone. Thus, control designers turned to optimal, predictive and adaptive techniques. Due to various complications and implementation challenges, there has been no industrial development followed with these schemes. Since these are model-based control schemes, they require a model for building control strategy. These control strategies did not consider the comfort factor but were only concerned with energy consumption savings In addition they may not be user friendly, as the occupants are not able to participate in the configuration scheme.
- Intelligent controllers, such as Learning methods (i.e. artificial intelligence, fuzzy systems and neural networks), MPC methods and Agent based control methods. Various learning controls have been developed and successfully applied to electrical and mechanical systems, mostly in robotics, automation and manufacturing areas. Learning methods reach system stability and high performances through the unknown learning possibilities, which exist in system dynamics. These controls are designed like artificial intelligence having fewer requirements of the detailed models. In literature, the mainly employed control systems for BEMS are MPC [123, 72]. MPC methods (see Chapter 3) have high computational requirements, in addition to the need of a huge amount of data, expert monitoring and modelling. Although these issues have to be overcome, high energy saving can be reached since MPC involves information of dynamic modeling and occupancy predictions in contrast to rule-based control systems. Appreciable results in indoor comfort fulfilment and energy saving are obtained by agent based control

methods. Agents are generally virtual or physical entities that cooperate rationally. In control systems agents are usually arranged in multiple layers according to their functionality. These methods separate huge complex problems in different sub-problems to manage them as different physical or virtual agents. These different agents may communicate and co-operate each other and with their environment as well.

The several building aspects to manage recently led BEMS to the adoption of computational optimization method [123]. Building management optimisation is the process of minimizing an overall objective function that generally includes costs of building operation, user discomfort and unsafety with the constraint of environmental condition. The building management optimisation can be performed with respect to both design and control variables [50]. Although various optimization techniques have been established and reviewed, the genetic algorithm (GA) is the most recognized technique in building performance analysis. Various other strategies have included the Multi-objective Particle Swarm Optimization (MOPSO) in optimizing thermal, illumination and air quality comfort and building energy consumption and have also provided the opportunity for occupant preferences. Other strategies for optimization in the literature are the anytime optimization (AO), ordinal optimization (OO), femicon and meta-analysis. These strategies generally are aimed at making a Pareto optimal representative subset from which an appropriate solution can be driven by the decision-makers of the selected problem.

2.3 Control strategies for the Demand Side Management context

Several optimization approaches have been recently proposed for the energy management in the DSM context as described in [69], and some significant examples are presented below.

Faria et al. [36] used a simulation based analysis for minimizing the final users energy cost in a DR scenario. Simulator developed is based on Power System CAD for the network modeling and on MATLAB for DR plan management and users behavior modeling. Customers have been divided into five categories (domestic, small commerce, medium commerce, large commerce and industrial). Each one has its proper tariff plans and demand curve characterization. The simulator has been used for the fitness evaluation of a Particle Swarm based optimization.

Nguyen et al. [97] proposed a multi-objective optimization approach based on NSGA-II (non-dominated sorting genetic algorithm). The authors tried to optimize a four objective functions problem: maximizing Available Transmission Capacity (ATC) while

minimizing Expected Energy Not Supplied (EENS), Active Power Loss (APL) and DR programs capacity. ATC is a measure of the transfer capability in the physical transmission network for future commercial activities over already committed uses. Adequate ATC is needed to ensure all economic transactions to be achieved. EENS index evaluates composite system reliability for the power system [119]. APL provides an evaluation on the idle-time of the slack node in a transmission system. Finally, DR programs capacity represents the total power capacity available through DR plans. For the optimization phase, a binary coded parameterization has been used, since the problem described is discretized.

Schibuola et al. [120] showed how control strategies aimed at DR management within dynamic price-driven electricity markets may ensure good performances. A typical apartment with HVAC system was simulated and actual prices and weather conditions were considered. The HVAC consists of a heat pump coupled with a solar thermal plant and a photovoltaic (PV) system. In particular three control strategies were applied, whose action is based on the cost of electricity (absolute and relative to the following 12 h) and on the level of the local electricity generation from PV. The simulations showed that through proper control strategies is possible to achieve relevant money savings and high degrees of energy self-consumption.

Gelazanskas [38] proposed a MPC strategy aimed at keeping actual load curve as close as possible to desired one, and based on a Neural Network model predicting future price to be used for achieving desired load amount. Input variables are time, weather conditions, desired and actual load.

Since most promising improvements on DR context can be achieved through fast changing dynamics such as RTP, the MPC approach can be suitable for such problems [108, 72] on the basis of the perfect knowledge of the system (i.e. the responsive appliances). Moreover inputs constrained and known disturbances simplify its application. Significant peak demand reduction were shown by several studies of model-based DR control with a time-varying rate [79]. Economic MPC (EMPC) is gradually becoming popular in reducing energy end demand costs for buildings subject to variable energy prices, such as TOU prices or RTP. The energy prices are employed directly in the objective function of the EMPC problem. The model considers how energy prices can be designed in order to achieve a specific objective, which often is the minimization of peak energy demand. EMPC is a useful tool for managing building energy systems (e.g. HVAC) and it is effective for both the operating systems based on a variable pricing structure and the determination of the optimal variable prices for a given system [25]. Using these techniques, in a closed loop control scheme is possible to exploit the dynamic effects of the system to properly match the supply.

Night pre-cooling or pre-heating in buildings was an important way to shift energy demand for decades. The EMPC technique was successfully used to reduce further more

peak demand through a more accurate adjusting of temperature set-points in HVAC systems, as described in [79]. In this work the authors propose a closed-loop control system based on an EMPC technique to reduce energy and demand costs for HVAC systems of commercial buildings considering real-time uncertainties and constraints. The economic objective function in MPC accounts for the daily electricity costs and the optimization problem aimed at minimizing them. It was shown by a weekly simulation that under the TOU electrical pricing structure, EMPC brings substantial cost savings by automatically triggering pre-cooling effect and shifting the peak demand away from on-peak hours.

Oldewurtel et al. [100] showed that in the building HVAC control the peak electricity demand relative to a given reference load curve can effectively be reduced by incorporating an appropriate electricity RTP tariff directly into the cost function of a MPC strategy. They proposed an hourly-based electricity tariff for end-consumers, designed to reflect costs of electricity provision, based on spot market prices as well as on electricity grid load levels. They used least-squares support vector machines for electricity tariff price forecasting, and thus provide the MPC controller with the necessary estimated time-varying costs for the whole prediction horizon. In the given context, the hourly pricing provides an economic incentive for a building controller to react sensitively with respect to high spot market electricity prices and high grid loading, respectively. By simulations it was shown that a grid-friendly behavior was rewarded.

Zong et al. [145] presented an example of a MPC for electrical heaters control to maximize the use of local generation (e.g. solar power) in an intelligent building. The MPC is based on dynamic power price and weather forecast, considering an optimization objective such as minimum cost and minimum reference temperature error. The authors demonstrated that this MPC strategy can realize load shifting in periods with low prices and maximize the PV self-consumption in the residential sector. They expect that this demand side control study can considerably save energy, as the end users can avoid high electricity price charge at peak time, and improve grid reliability, when there is a high penetration of Renewable Energy Sources in the power system.

In [25] an EMPC problem is presented to determine optimal prices that minimize the peak electricity demand. The system was a simulated community of 900 residential homes where thermostat set-points could be automatically controlled. The key feature of this formulation considers a centralized problem (e.g., minimizing peak electricity demand) and implements it in a decentralized framework using pricing. For the presented cluster of homes, the optimal pricing profiles were relatively low prices for every hour except for the peak hour. This pricing structure was able to reduce peak demand by 9.6% when implemented in a decentralized control considering the minimum cost EMPC formulation, compared to the 10% peak reduction with the centralized control and minimum peak demand formulation.

In their work, Mendoza-Serrano and Chmielewski [87] discussed the effect of thermal energy storage in reducing operating costs related to HVAC systems for building temperature control. In particular they used the EMPC in combination with thermal energy storage to time-shift power consumption away from periods of high demand to periods of low energy cost. Dynamic electricity pricing and weather condition forecasts were incorporated within the methodology. The authors also considered the capital costs associated with thermal energy storage and proposed an optimization framework aimed at providing the proper balance between equipment costs and operational savings.

The work of Ma et al. [78] presents an EMPC for the optimization of the set-points in HVAC systems for load shifting and cost minimization under the TOU price policy. In order to ensure the proper building operations, the economic objective function accounted for: the combination of energy and demand costs with a TOU rate structure; a dynamic thermal process and power model of the building thermal mass dynamics; a set of constraints. The effectiveness of EMPC in energy cost savings was demonstrated using simulation: the EMPC strategy was capable of shifting the peak demand in off-peak hours and reducing energy costs compared to a baseline case for the building.

2.4 The proposed system architecture

A tertiary building that interacts with the energy market with a classic consumer profile is considered. The goal is to define a BEMS model valid in this scenario and that in future works can be extended for buildings involved in micro-grid context.

The proposed BEMS strategy is shown in Fig. 2.1. It is based on a system architecture that is modular from the features point of view and hierarchical [19, 89] depending on the control frequency and the objective.

The high level of the architecture is constituted by a predictive optimal control framework that minimizes the economic cost of the building operation (thus the consumption) while respecting the occupant comfort and safety. The optimization starts from building and weather measured historical data and building situation assessment, and considers weather and occupancy forecasts for the next e.g. 24 hours, together with the energy price forecasts offered by the energy retailer. To this end, the framework takes into account the price differences between the peak and off-peak periods of the day. The final result is the optimal energy schedule (e.g. reference settings of room thermostats) for the desired timestamp within the 24 hours optimization horizon.

The middle level consists in the "middleware" software level of BEMS described in Section 2.2 and is aimed at offering a building Decision Support System (DSS) framework. The DSS framework supports the energy manager and users in the decision-making activities and facilitates the organizational processes through a valuable consulting tool.

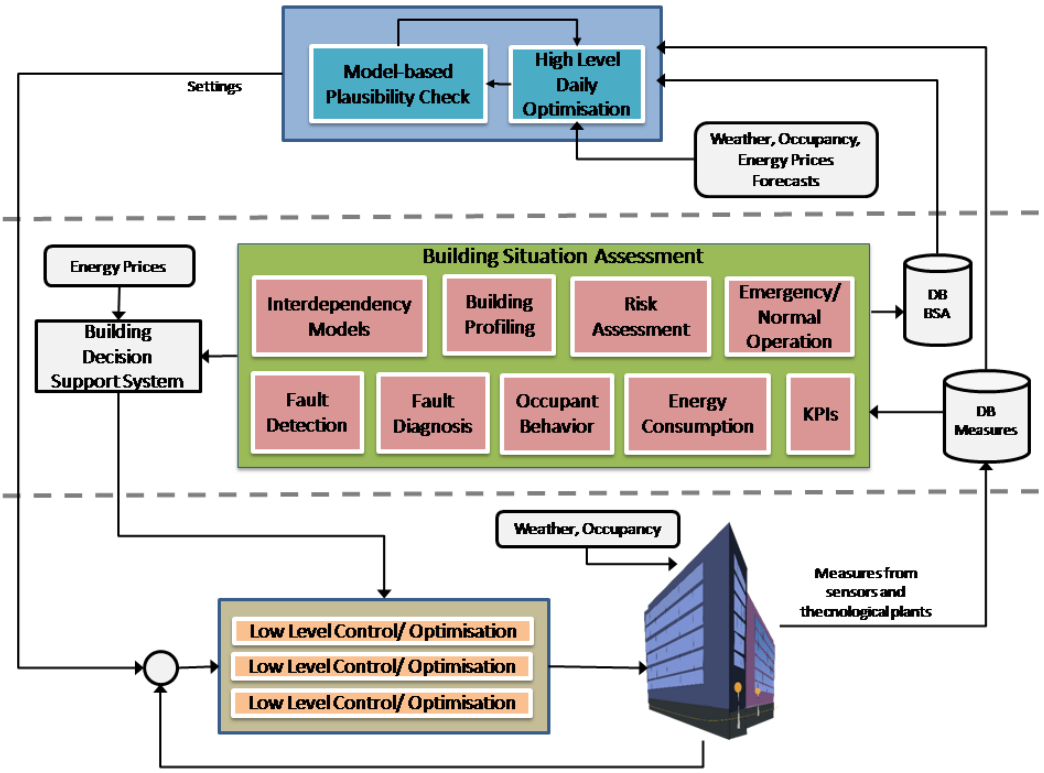

FIGURE 2.1: A system architecture for building energy management

This tool provides an immediate report about the building operating situation from different points of view: energy, security, general management. Several software modules contribute to the building situation assessment starting from the actual building measurements: energy consumption modeling, building energy profiling, Key Performance Indicators (KPI), fault detection, fault diagnosis, interdependency models, occupant behavior analysis, emergency/normal operation and risk assessment. The building situation assessment contributes as input to the optimization process of the high level. The DSS framework is also characterized by a reactive aspect based on the building situation assessment and further actual conditions e.g. energy prices. In this case the DSS acts on the low level control process and intervenes when emergencies, breakdowns and wastefulness occur or when the one-day-ahead plan cannot be followed because of unforecasted events, deciding whether some appliances have to be switched on or off. The middle level applications run with a frequency of some hours/minutes depending on the particular task.

Finally, the low level is in charge of following the one-day-ahead optimal schedule by varying and adapting the building settings on the basis of the actual conditions (weather, occupancy) and of the building DSS outcomes of the middle level. In order to do this, classical (e.g. Proportional Integral Derivative) or intelligent (e.g. Model Predictive) controllers are used, as described in Section 2.2. The control frequency in this case is small (typically minutes,seconds) and acts taking into account the ongoing

building operating conditions.

The next Chapters represent implementation and application examples of different modules operating at different levels of the building management architecture so far described. In Chapter 3 an adaptive MPC law adjusts the indoor temperatures of a multi-zones simulated building on the basis of the current occupancy profiles of each zone: thus this control strategy can be placed in the low level framework. Chapter 4 focuses on the fault detection process of anomalous building energy consumption using actual data through artificial intelligence and data mining techniques. Chapter 5 represents a sort of completion of the previous Chapter, since it presents the application and the on-line implementation of a comprehensive fault detection and diagnosis methodology of anomalous actual building electrical consumption. The fault detection and diagnosis methodology carried out offers a valuable analysis tool of the operating conditions of building and its appliances in the short and long term, then it constitutes an important application to be hosted in the middle level of the DSS framework.

Chapter 3

Model predictive control for thermal regulation in buildings

3.1 Introduction

More than 50% of the buildings sector energy consumption is due to heating, ventilation and air conditioning (HVAC) systems [26, 54]. In recent years, many studies were performed in order to optimize the energy efficiency of indoor heating systems, but the controllers most commonly used are still PID and thermostats. Thus, the challenge for HVAC system control is to find a compromise between the user thermal comfort and the energy consumption. In this respect, two principal approaches were proposed in literature: Artificial Intelligence (AI) [14, 73, 95] and MPC approaches.

The MPC [15] is able to predict the thermal system dynamics including disturbances and to apply an appropriate control action, it also avoids large oscillations and easily handles multi-input multi-output (MIMO) systems. On the other hand, the MPC relies on the physically based mathematical model of the HVAC system and building dynamics, not always so simply to obtain. In MPC the control sequence is calculated by solving an optimization problem, in particular, minimizing a cost function over a specified horizon. At every simulation step, only the first element of the control sequence is applied to the system as, at the next instant, a new optimization is performed based on current measurements.

For HVAC systems control, several formulations of cost functions, prediction models and configurations were presented in literature to minimize the consumption and to guarantee a desired comfort level. A centralized MPC based on the Predictive Mean Vote comfort index for the thermal regulation of a building is given in [23]. In [114] a MPC centralized controller for ventilation systems with reference to a non linear thermal model is showed. Reference [105] shows the development of a SMPC (Stochastic Model Predictive Control) that takes in account the forecasts of external temperature and occupancy for a single – zone building. In [111] a dynamic programming of MPC

cost function is proposed, with variable weighting coefficients depending on the occupancy and in a distributed approach. A comparison between MPC centralized and distributed approaches is present in [90], where the building occupancy profile is known in advance, thus in inoccupation periods there is no temperature set-point and only consumption is minimized. Evolutions of [90] are described in [91, 93], where different decompositions for the optimization problem are used, so as to ensure a greater efficiency in the DMPC (distributed MPC) strategy. Interesting is also [92], that proposes dynamic prediction horizons depending on the occupancy profile known in advance. Reference [34] instead demonstrates how MPC can be applied to different elements of an HVAC system, i. e. the fan speed.

This Chapter proposes two innovative MPC laws for the regulation of the indoor temperatures of a three-zones building. In particular two adaptive MPC strategies are proposed to achieve even higher performances ensuring temperature regulation on the basis of occupancy and energy price profiles. The experimentation is carried out considering the thermal coupling between the zones, thus comparing two possible MPC architectures (distributed and decentralized) in order to evaluate the best one in terms of control results (consumed energy and comfort). The comfort requirements are defined by operative air temperatures derived from more general temperature bands, according to the international standards [133, 127].

3.2 Temperature regulation in a multi-zone office building on the basis of the occupancy level

An adaptive MPC approach for thermal regulation in a multi-zone building is presented below [67]. The approach can be defined "adaptive" because at every simulation step the information about the occupancy level of each zone is used for calculating the proper control action with a prediction horizon of 10 minutes, resulting also in an energy consumption reduction. In particular, a dynamic temperature set-points strategy is adopted. Initially the thermal coupling between the zones is considered, implementing a distributed MPC architecture. Then a decentralized MPC architecture (without considering the thermal coupling between the zones) is also analysed. The results are evaluated in terms of energy consumption and comfort level defined by the indoor operative temperatures. In the experimentation an entire working day with four different time periods, correspondent to different occupancy levels for each zone, is considered. For the results evaluation, two performance indices are adopted.

This paragraph is organized as follows. Section 3.2.1 introduces the building and HVAC system models used for prediction and simulation. Section 3.2.2 compares the investigated MPC strategies and Section 3.2.3 describes the improvements proposed for an adaptive distributed MPC on the basis of four occupancy levels ranging between 0

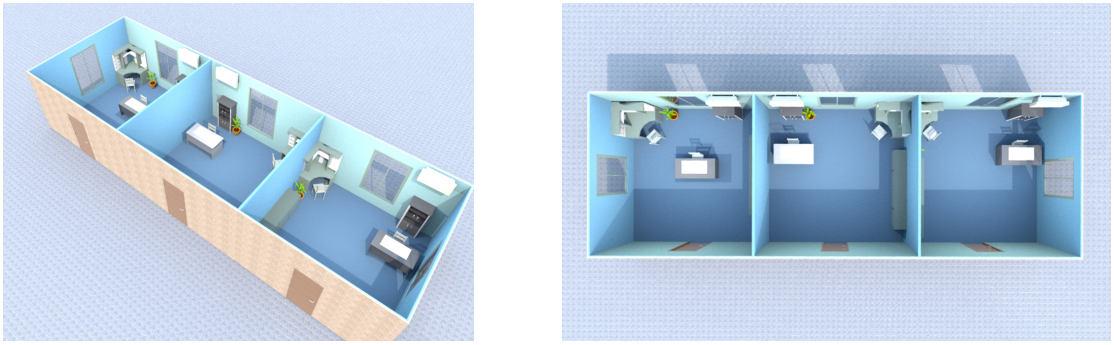

(A) (B)

FIGURE 3.1: The case-study building

and 1. The efficiency of the proposed control strategy is illustrated by a performances comparison in Section 3.2.4.

3.2.1 Building and HVAC system models

The MPC is characterized by the use of a prediction model and the optimization of an objective function based on that prediction. Several models can be used for the prediction of the system evolution under certain disturbances. In this work the state space model is used, obtained directly from the differential equations that describe the thermal model of building and HVAC system.

The focus is on an office building consisting of three rooms of the same dimensions, each room is occupied by an employee and constitutes a building "zone" (see Fig. 3.1). Generalization for buildings with several zones can be easily achieved.

The HVAC system is constituted by three identical electrical fan-coils, one per zone, operating in the "winter season" mode. Fan-coils have a maximum level of air mass flow rate, M_{dot}, which is specified in Table 3.1, and a minimum level, which is 0, when they are off.

The thermal coupling factor between rooms of the building is very important because it affects the internal temperature. For the sake of simplicity, only the thermal influences between rooms through internal walls are considered. Thus, the air temperature of a zone i, $T_{r,i}$, is related to the heat flow from the heater, Q_h, the heat losses to the environment, Q_l, and to the adjacent zones j, $Q_{r,i,j}$, as described in Eq. 3.1:

$$\dot{T}_{r,i} = \frac{\dot{Q}_h}{M_{air} \cdot c} - \frac{\dot{Q}_l}{M_{air} \cdot c} + \frac{\sum_{j=1}^{n} \dot{Q}_{r,i,j}}{M_{air} \cdot c} \tag{3.1}$$

where M_{air} is the mass of air inside the zone and c is the heat capacity of air at a constant pressure (see Table 3.1).

Parameter	Zone	Total building
Walkable area (m^2)	25	75
Width (m)	5	5
Length (m)	5	15
Height (m)	3	3
Thickness of internal walls (m)	0.1	-
Thickness of external walls (m)	0.2	-
Thermal conductivity coefficient of internal walls (W/mC)	0.36	-
Thermal conductivity coefficient of windows (W/mC)	0.078	-
Thermal conductivity coefficient of external walls (W/mC)	0.038	-
Maximum air mass flow rate M_{dot} (kg/min)	9.18	-
Mass of air M_{air} (kg)	91.87	275.62
Heat capacity of air c (J/kgK)	1005.4	-
Fan-coil hot air temperature T_h (°C)	40	-

TABLE 3.1: Building and heaters characteristics

A fan-coil i blows hot air at temperature T_h (40 °C) at an air mass flow rate depending on the MPC control signal $u_{c,i}$ variable between 0 and 1, as showed in Eq. 3.2:

$$\dot{Q}_h = (T_h - T_{r,i}) \cdot (M_{dot} \cdot u_{c,i}) \cdot c \tag{3.2}$$

The heat losses of the zone i to the external environment, characterized by the temperature T_{out}, are expressed by Eq. 3.3:

$$\dot{Q}_l = \frac{(T_{r,i} - T_{out})}{R_{eq}} \tag{3.3}$$

where R_{eq} is the equivalent thermal resistance of the external walls. Equation 3.4 illustrates the heat losses of the zone i to the adjacent zones j:

$$\dot{Q}_{r,i,j} = \frac{(T_{r,j} - T_{r,i})}{R_{wallij}} \tag{3.4}$$

where R_{wallij} is the equivalent thermal resistance of the internal walls.

In order to identify the state space model of the "building and heaters" system described above, some definition was made about the model: the states x_i are the indoor air temperatures of the three zones, $T_{r,i}$; the inputs u_i are the control signals of the fan-coils of the three zones calculated by the MPC controller, $u_{c,i}$; the input u_d is the disturbance constituted by the external temperature, T_{out}; the outputs y_i are the indoor air temperatures of the three zones, $T_{r,i}$.

The resulting three differential equations of the state space model are non-linear. Thus, the main idea is to approximate this non-linear system by a linear one around an equilibrium point, obtaining a model as showed in Eq. 3.5:

$$\begin{cases} \dot{x} = A \cdot x + B_c \cdot u_c + B_d \cdot u_d \\ y = C \cdot x \end{cases} \tag{3.5}$$

where A, B_c, B_d and C are the corresponding matrices obtained by the linearization process. The temperature used in the experimentation below as basic set-point temperature (22 °C), is chosen as equilibrium point. In the experimentation, only variations of a few degrees are considered, thus the linear and the non-linear approaches should not lead to very different results.

3.2.2 Model predictive control configurations

The state space model described in the previous section was the one used within MPC to ensure a good prediction of system future evolutions. Table 3.2 shows the MPC parameters values used in the experimentation.

Parameter	Value
Sampling time (min)	1
Control action interval (min)	1
Prediction horizon N_p (min)	10
Control horizon N_c (min)	4

TABLE 3.2: MPC parameters

In the following sections the decentralized and distributed MPC architectures, applied to the case-study building, and for completeness the centralized one are illustrated, in order to highlight benefits and drawbacks of each architecture.

Centralized model predictive control

In the centralized control structure, the entire multi-zone system is controlled by one MPC law (see Fig. 3.2). The controller takes in account all the dynamics of the system, all their interactions and the disturbances. The prediction model includes the thermal coupling factors, thus the measured temperatures of each zone, for the computation of the outputs prediction.

In the centralized MPC the control performances are good. However, the computational demand grows exponentially with the system size, in this case the number of the zones in the building. This control strategy is very accurate but a failure of the central controller could cause the failure of the entire building heating system.

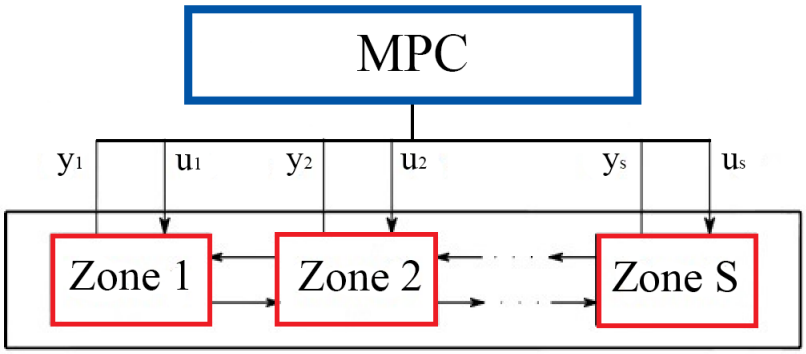

FIGURE 3.2: Centralized MPC

Decentralized model predictive control

The decentralized MPC approach is the simplest and therefore the most used multi-zone building thermal control structure. As shown in Fig. 3.3, each zone temperature is regulated by an independent controller that doesn't account for what's happening in the other zones, since the thermal influences among the zones are considered as external unknown perturbations. As the thermal coupling is ignored by the prediction model, when these influences are important they will not be quickly rejected.

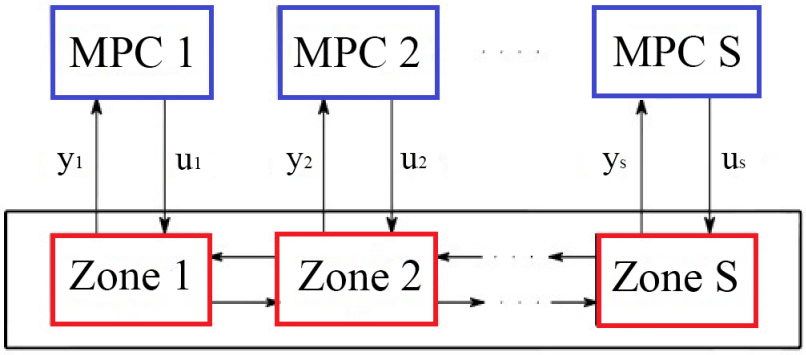

FIGURE 3.3: Decentralized MPC

With reference to the linearized state space model (Eq. 3.5), the dynamic matrix A_i of the single controller has dimensions 1x1. It considers only the temperature variation of the zone i as described in Eq. 3.6:

$$A_i = -\frac{\bar{u}_i \cdot M_{dot,i}}{M_{air,i}} - \frac{1}{M_{air,i} \cdot c \cdot R_{eq,i}} \tag{3.6}$$

where $\bar{u}_i$ is the control input value in the equilibrium point.

Also the input matrices are characterized by one single element and are defined by Eq. 3.7 and Eq. 3.8:

$$B_{c,i} = -\frac{T_{h,i} \cdot M_{dot,i}}{M_{air,i}} - \frac{\bar{x}_i \cdot M_{dot,i}}{M_{air,i}} \tag{3.7}$$

$$B_{d,i} = -\frac{1}{M_{air,i} \cdot c \cdot R_{eq,i}} \tag{3.8}$$

where $\bar{x}_i$ is the state value in the equilibrium point.

Once the prediction model is defined, the vector of the future outputs is calculated as described in Eq. 3.9:

$$Y_i = F_i \cdot x_i(k) + \Phi_i \cdot U_{c,i} + \Phi_{d,i} \cdot U_{d,i} \tag{3.9}$$

where $U_{c,i}$ and $U_{d,i}$ are respectively the Ncx1 vectors of the future control signal and disturbances evaluated by the i-th MPC controller and the matrices F and Φ are defined by Eq. 3.10 and Eq. 3.11 as follows:

$$F = \begin{vmatrix} CA \\ CA^2 \\ CA^3 \\ \vdots \\ CA^{N_p} \end{vmatrix} \tag{3.10}$$

$$\Phi = \begin{vmatrix} CB & 0 & 0 & \cdots & 0 \\ CAB & CB & 0 & \cdots & 0 \\ CA^2B & CAB & CB & \cdots & 0 \\ \vdots & \vdots & \vdots & \vdots & \vdots \\ CA^{N_p-1}B & CA^{N_p-2}B & CA^{N_p-3}B & \cdots & CA^{N_p-N_c}B \end{vmatrix} \tag{3.11}$$

This MPC configuration has the great advantages to divide the computational cost and ensure a good fault tolerance, but generally it offers the worst control performances.

Distributed model predictive control

A distributed MPC approach [96] is the best solution for large-scale dynamically coupled building systems. It is structured as a decentralized law, with a local controller for each zone that exchanges information related to its future behavior (see Fig. 3.4). Each

local controller uses the future output prediction of the neighbor zones for the prediction of the future thermal exchanges, in order to calculate the most suitable current control law.

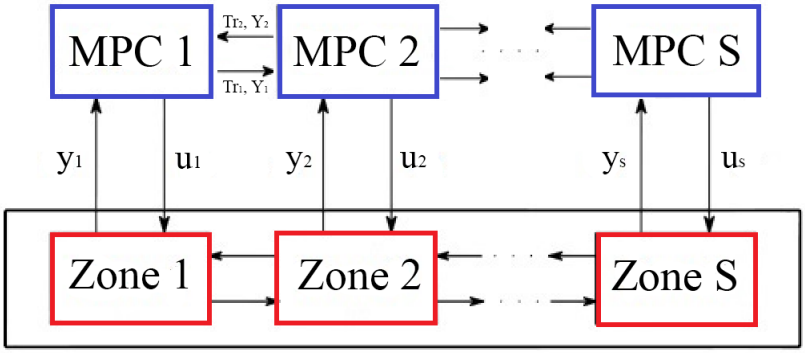

FIGURE 3.4: Distributed MPC

As compared with the decentralized approach, the linearized state space model presents additional terms in order to evaluate the effect of the thermal exchanges with the neighbor zones on the temperature variation. Assuming that the i-th zone has n neighbor zones, the following equations (Eq. 3.12, Eq. 3.13) highlight the differences with the state space model of the previous paragraph:

$$A_i = -\frac{\bar{u}_i \cdot M_{dot,i}}{M_{air,i}} - \frac{1}{M_{air,i} \cdot c \cdot R_{eq,i}} - \sum_{j=1}^{n} \frac{1}{M_{air,i} \cdot c \cdot R_{wallij}} \tag{3.12}$$

$$B_{d,i} = \left| \frac{1}{M_{air,i} \cdot c \cdot R_{eq,i}} \quad \frac{1}{M_{air,i} \cdot c \cdot R_{walli1}} \quad \cdots \quad \frac{1}{M_{air,i} \cdot c \cdot R_{wallin}} \right| \tag{3.13}$$

In this case the $B_{d,i}$ matrix is a vector: the first term is related to the disturbance due to external temperature T_{out}, the other terms to the disturbances due to the n neighbor zones. Similarly the vector of disturbances $U_{d,i}$ contains $N_c(1+n)$ elements.

The collaboration among the local control laws permits the improvement of global system performance compared to decentralized structure. On the other hand, the computational demand is significantly reduced compared to the centralized case.

3.2.3 Adaptive model predictive control

The distributed MPC strategy described above allows the reduction of the errors with respect to a given reference temperature. In this section an adaptive MPC strategy is proposed in order to further lower consumption. The adaptive control is based on the occupancy level of each zone of the building: the idea is to ensure the comfort only

when actually needed from the users, thus reducing the energy consumption. A development of works [90, 91, 93] is proposed, in which during the inoccupation periods only consumption was minimized (corresponding to the absence of temperature setpoint). The innovative aspect of the proposed approach is the identification of several occupancy levels between 0 and 1, in spite of the only two levels (1 for occupancy and 0 for inoccupation) proposed in previous literature. In fact, the momentary absence of the employee from his office rarely results in a complete absence for the whole day (e.g. lunch break). With an adaptive MPC based on the total absence/presence of the employee, when the employee is back the zone could be cold and reaching the reference temperature may take a long time.

In the case-study building the occupancy data are recorded with a 10 minutes timestamp and are obtained from two different information sources:

- Badge data: indicate if each employee is in the building or not;
- Presence sensors: indicate if there is at least one person in the related monitored zones.

Crossing these two measurements, four occupancy levels are defined for each zone of the building, as shown in Table 3.3.

Occupation level	**Badge**	**Presence sensor**
1	Yes	Yes
0.7	Yes	No
0.3	No	Yes
0	No	No

TABLE 3.3: Occupation levels

An adaptive MPC strategy is built on the basis of these occupancy levels, as explained in the following paragraph.

Dynamic temperature setpoints

When the occupancy level is not 1, the reference to an ideal temperature is useless and expensive, thus a lower temperature setpoint is a good idea to decrease energy consumptions. For a simple and immediate choice of the dynamic temperature setpoints, the percentage p_i of the ideal reference temperature is used for each occupancy level i respectively, as shown in Table 3.4.

Hence, at the instant k the controller takes in account the reference temperature value expressed by Eq. 3.14:

$$rif(k) = rif_{comf} \cdot p_i(k) \tag{3.14}$$

Occupation level	p_i	Temperature setpoint (°C)
1	1	22
0.7	0.9	19.8
0.3	0.8	17.6
0	0.5	11

TABLE 3.4: Adaptive MPC, first test: dynamic temperature set-points

where rif_{comf} is the temperature setpoint that corresponds to the maximum comfort for the occupants (22 °C). When the occupancy level is 0, the set-point temperature of 11 °Cinvolves the switching off of the heater, as can be observed also in the experimentation carried out in Section 3.2.4.

3.2.4 Results discussion

The building and HVAC system model, used for the prediction phase in the previous sections, is adopted also for the simulation step. All the results are obtained implementing the MPC strategies, described in Sections 3.2.2 and 3.2.3, and such model in Matlab and Simulink. The experimentation is carried out considering an entire working day with four different time slots correspondent to four occupancy levels for each zone, as showed in Table 3.5.

ZONE	Time slot			
	7:30-12:10	12:10-14:00	14:00-19:45	19:45-20:30
1	1	0.7	1	0.3
2	0	0	0	0
3	0.7	0.7	1	0.7

TABLE 3.5: Adaptive MPC, first test: occupation levels during the experimentation day

The disturbance constituted by the external temperature during the experimentation day ranges between 7 and 19 °C(see Fig. 3.5). At every simulation step, the external temperature is taken as constant value during the whole prediction horizon.

For the results evaluation, two performance indices are adopted.

For the comfort, when the occupancy level is maximum, the average distance from reference temperature in the whole building is used, as illustrated in Eq. 3.15:

$$MAE_{TOT} = \frac{\sum_{i=1}^{3} MAE(i)}{3} \tag{3.15}$$

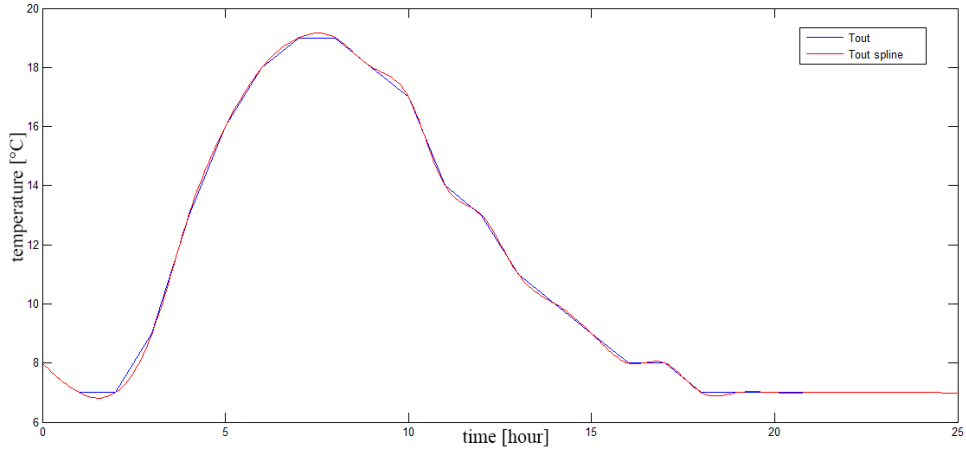

FIGURE 3.5: External temperature

where $MAE(i)$ is the average distance from reference temperature in the zone i, calculated as in Eq. 3.16:

$$MAE(i) = \frac{\sum_{j=1}^{n} |T_{r,i} - rif_{comf,i}|}{n}, \forall occupancylevel_i(j) = 1 \tag{3.16}$$

where n is the number of iterations.

The performance index for the consumption is the total air mass produced by fan-coil units in the whole building, as showed in Eq. 3.17:

$$M_{TOT} = \sum_{i=1}^{3} M_{tot}(i) \tag{3.17}$$

where $M_{tot}(i)$ is the total air mass produced by fan-coil unit in the zone i, as expressed in Eq. 3.18:

$$M_{tot}(i) = \sum_{i=1}^{n} u(j) \cdot M_{dot} \tag{3.18}$$

The MPC strategies just described are compared with two other correspondent MPC approaches defined, for the sake of simplicity, "non-adaptive": in these cases the MPC controllers consider only if the building zones are occupied or not, then the temperature set-point is 22 °Cwhen the zone is occupied (the occupancy level is greater than 0), 11 °Cotherwise (the occupancy level is equal to 0). Trough this comparison it is possible to obtain a better evaluation of the results. Fig. 3.6 and Fig. 3.7 show the temperature evolutions in each zone of the building during the experimentation day, resulting from the application of adaptive and non-adaptive MPC strategies respectively.

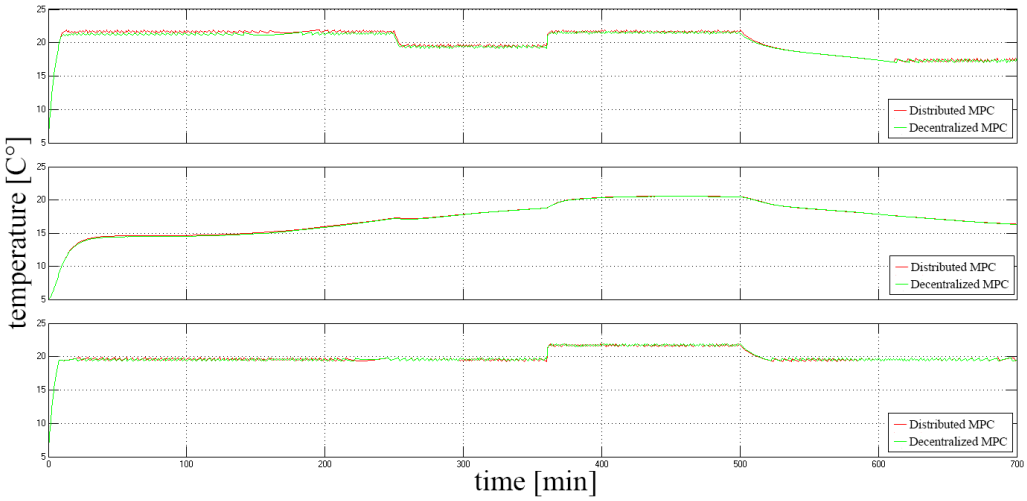

FIGURE 3.6: Adaptive MPC, first test: temperature behaviour for each zone obtained with distributed and decentralized strategies

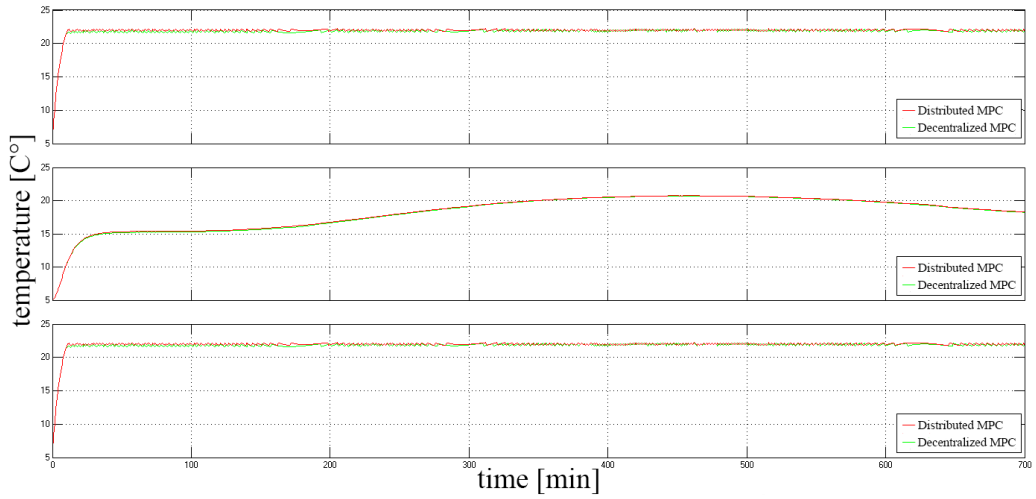

FIGURE 3.7: Non-adaptive MPC, first test: temperature behaviour for each zone obtained with distributed and decentralized strategies

Both configurations follow very well the temperature set-point in each time slot of the day. This is also evident from MAE_{TOT} results reported in Table 3.6: each configuration reports very small temperature errors and, as expected, distributed MPC presents smaller errors than decentralized one.

The control action evolutions in each zone of the building, resulting from the application of adaptive and non-adaptive MPC strategies, are illustrated in Fig. 3.8 and in Fig. 3.9 respectively.

For a more realistic simulation, only five possible values between 0 and 1 with a step of 0.25 were defined for the control signal (output of the MPC controller). It can be noticed that the non-adaptive MPC signals present no peaks in their evolution, since the temperature setpoints don't change during the day. Looking at Table 3.6, the great

Dynamic Temperature Setpoints		
	MAE_{TOT} [°C]	$M_{tot}[kg]$
Distributed	0.084	3029
Decentralized	0.130	2954
Non-adaptive MPC		
	MAE_{TOT} [°C]	$M_{tot}[kg]$
Distributed	0.073	4223
Decentralized	0.105	4117

TABLE 3.6: Adaptive MPC, first test: results comparison

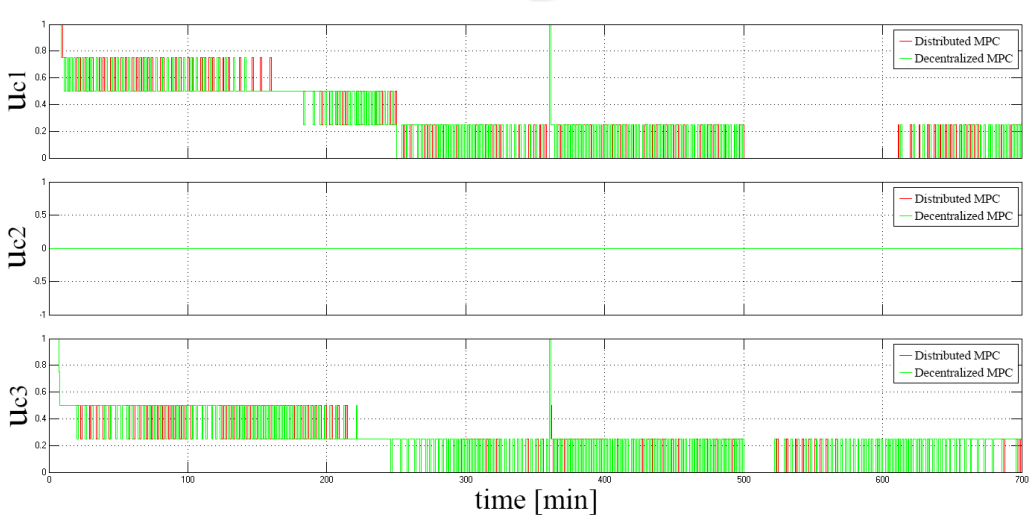

FIGURE 3.8: Adaptive MPC, first test: control behaviour for each zone obtained with distributed and decentralized strategies

advantage of using an adaptive MPC strategy is evident. M_{tot} results confirm that the control effort, and then the energy consumption, of an adaptive MPC configuration is much lower than that of a non-adaptive one.

It can also be observed that the central zone, characterized by occupancy 0 for the whole day, reaches anyway temperatures of about 20 °Cdue to the thermal exchanges with zone 1 and zone 3. These conditions represent the worst situation for the distributed controls of zone 1 and zone 3 compared to decentralized ones from the consumption point of view. Anyway, as Table 3.6 illustrates, the performances of the distributed MPC strategies in terms of consumption are good.

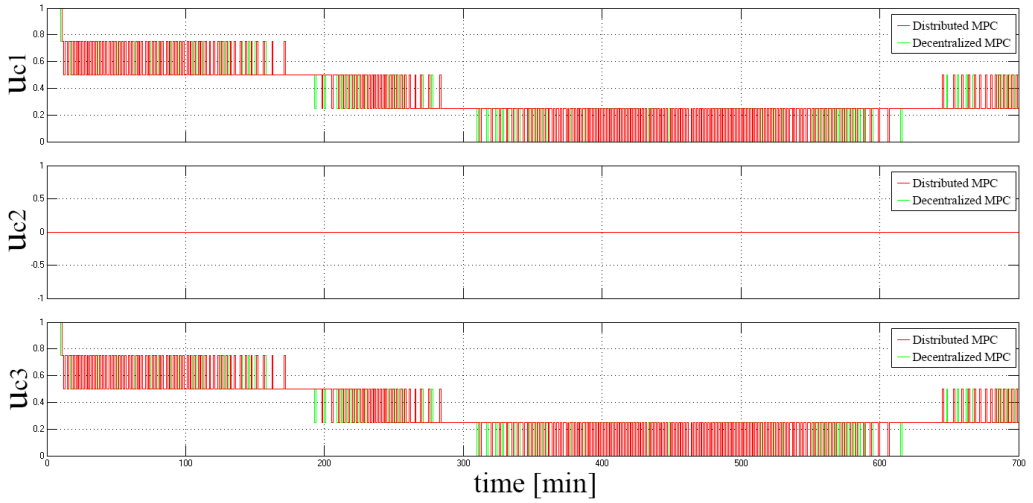

FIGURE 3.9: Non-adaptive MPC, first test: control behaviour for each zone obtained with distributed and decentralized strategies

3.3 Temperature regulation in a multi-zone office building on the basis of the occupancy level and the energy price

In this Section a development of the adaptive MPC approach for the thermal regulation in a multi-zone building so far described is proposed. The main idea is the achievement of even higher performances ensuring temperature regulation on the basis of occupancy and energy price profiles. According to Chapter 2, a reference scenario for the MPC strategy here introduced may occurr when the energy prices are decided for the next day involving all the actors of the energy market. From the buildings (users) point of view, the next day the goal is to follow the day-ahead load curve based on e.g. weather and occupancy forecasts and energy prices definitions. A possible application consists in adapting the established daily schedule of the temperature set-points (based on the the defined energy prices and resulting from the high level control process) according to the actual occupancy data (low level control).

Then, at every simulation step, the information about the energy price and the occupancy level of each zone is used for defining the correspondent temperature set-points and so for calculating the proper control action. As in the previous experimentation, the distributed and decentralized MPC architectures are compared and the results are evaluated in terms of energy consumption and comfort level defined by the indoor operative temperatures. The MPC parameters, the building and HVAC system models used for prediction and simulation and the four occupancy levels ranging between 0 and 1 for each zone of the building (Table 3.3) are the same as the previous Section.

3.3.1 Experimentation and results discussion

Even in this experimentation case an entire working day (750 min, i.e. 12 hours and 30 min) is considered, in particular consisting of different time slots with different occupancy levels for each zone, as showed in Table 3.7. The central zone (zone 2) is occupied for most of the day, in this way compared to the previous experimentation is possible to get a more comprehensive assessment of the performance of distributed and decentralized MPC strategies.

	Time slot			
	7:00-11:10	**11:10-13:00**	**13:00-15:20**	**15:20-19:30**
Occupancy level zone 1	1	0.7	1	0.3
	7:00-17:00			**17:00-19:30**
Occupancy level zone 2	1			0
	7:00-13:00		**13:00-15:20**	**15:20-19:30**
Occupancy level zone 3	0.7		1	0.7

TABLE 3.7: Adaptive MPC, second test: occupancy levels during the experimentation day

Three energy price levels are considered possible: high, medium and low. During the experimentation day, the following energy price profile is defined (Table 3.8):

	Time slot		
	7:00-11:10	**11:10-15:20**	**15:20-19:30**
Price level	HIGH	LOW	MEDIUM

TABLE 3.8: Adaptive MPC, second test: energy price profile during the experimentation day

The temperature set-points change on the basis of the combination of occupancy level of the specific zone and energy price. For high, medium, low energy price the temperature set-points are showed in Tables 3.9, 3.10, 3.11 respectively. When the occupation level of the zone is greater than 0 the temperature set-point can assume values in the range 19 - 22 °C, when the zone is unoccupied the temperature set-point is 11 °Cinvolving the switching off of the heater.

Occupation level	p_i	**Temperature setpoint (°C)**
1	0.9545	21
0.7	0.9091	20
0.3	0.8636	19
0	0.5	11

TABLE 3.9: Adaptive MPC, second test: dynamic temperature set-points for high energy price

Occupation level	p_i	Temperature setpoint (°C)
1	1	22
0.7	0.9091	20
0.3	0.8636	19
0	0.5	11

TABLE 3.10: Adaptive MPC, second test: dynamic temperature set-points for medium energy price

Occupation level	p_i	Temperature setpoint (°C)
1	1	22
0.7	0.9545	21
0.3	0.9091	20
0	0.5	11

TABLE 3.11: Adaptive MPC, second test: dynamic temperature set-points for low energy price

Figures 3.10 and 3.11 indicate the temperatures and the control signals of each zone of the building obtained applying the MPC distributed and decentralized strategies so far described.

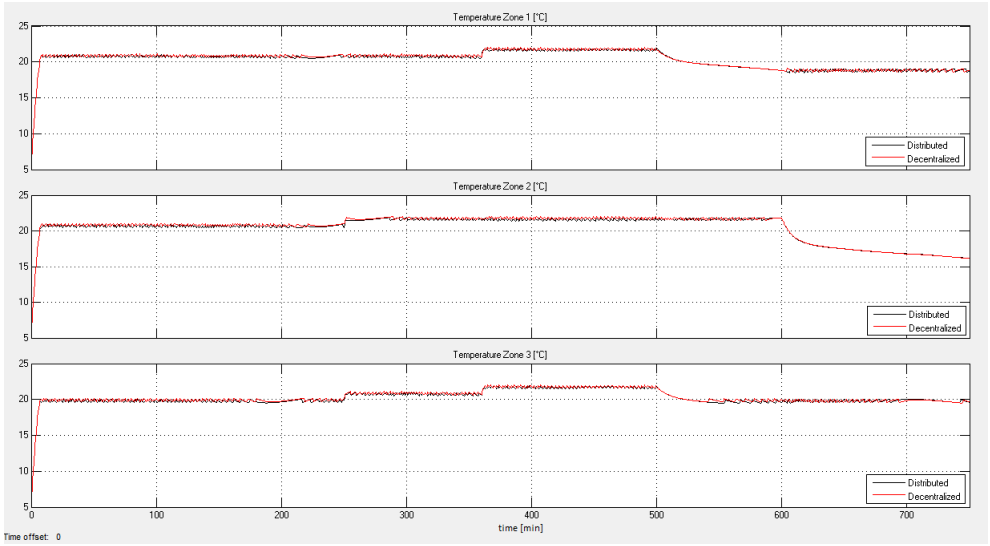

FIGURE 3.10: Adaptive MPC on the basis of occupancy level and energy price, second test: temperature behaviour for each zone obtained with distributed and decentralized strategies

For the performance evaluation, the presented distributed and decentralized MPC approaches are compared with the non-adaptive ones and the adaptive ones based only on the occupancy levels introduced in the previous Section. Figures 3.12 and 3.13 illustrate the temperatures and control signals evolutions of non-adaptive MPC approaches.

In the case of adaptive MPC strategies based on the occupancy level of each zone of the building, the chosen temperature set-points are the same of the medium energy price

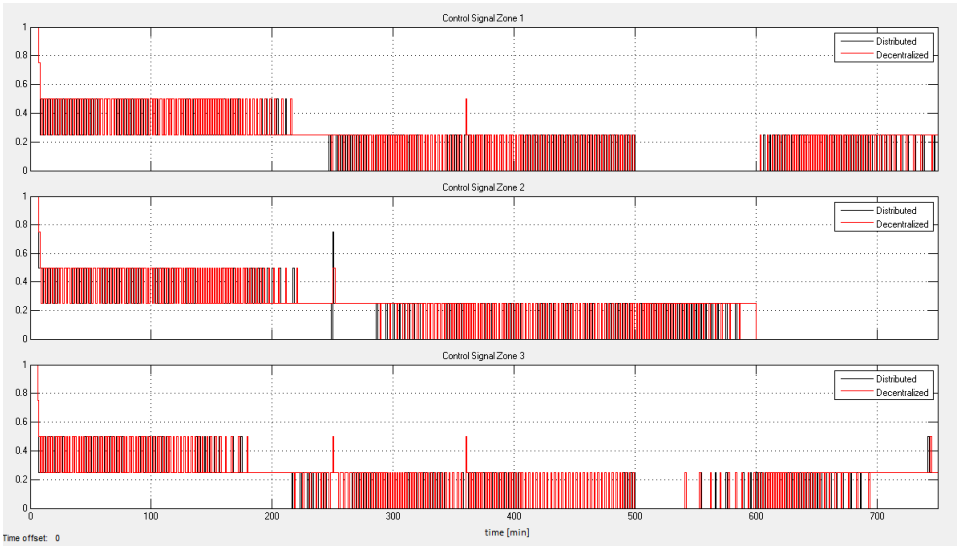

FIGURE 3.11: Adaptive MPC on the basis of occupancy level and energy price, second test: control behaviour for each zone obtained with distributed and decentralized strategies

case (see Table 3.10). The resulting temperature and control signal evolutions for each zone of the building during the experimentation day are reported in Fig. 3.14 and 3.15 respectively.

For the results evaluation, the two performance indices of the previous Section are adopted: for the comfort, when the occupancy level is maximum, the daily average distance of actual indoor temperatures from the ideal temperature set-point (22 °C) in the whole building, MAE_{TOT}; for the consumption, the total air mass flow rate through fan-coil units in the entire building, M_{tot}, evaluated for the whole experimentation day and for the time slots correspondent to the variations of the energy price level in the third MPC configuration. Table 3.12 summarizes the results of the experimentation day.

Non-adaptive MPC					
	$\mathbf{MAE_{TOT}[^\circ C]}$	$\mathbf{M_{tot}[kg]}$	$\mathbf{M_{tot}[kg]}$ **7:00-11:10**	$\mathbf{M_{tot}[kg]}$ **11:10-15:20**	$\mathbf{M_{tot}[kg]}$ **15:20-19:30**
Distributed	0.1764	4881	2896	858	1127
Decentralized	0.09334	4992	2949	895	1148
Adaptive MPC: dynamic temperature setpoints according to occupancy levels					
	$\mathbf{MAE_{TOT}[^\circ C]}$	$\mathbf{M_{tot}[kg]}$	$\mathbf{M_{tot}[kg]}$ **7:00-11:10**	$\mathbf{M_{tot}[kg]}$ **11:10-15:20**	$\mathbf{M_{tot}[kg]}$ **15:20-19:30**
Distributed	0.1727	4090	2692	725.4	672.6
Decentralized	0.1109	4184	2745	757.4	681.6
Adaptive MPC: dynamic temperature setpoints according to occupancy and energy price levels					
	$\mathbf{MAE_{TOT}[^\circ C]}$	$\mathbf{M_{tot}[kg]}$	$\mathbf{M_{tot}[kg]}$ **7:00-11:10 High price**	$\mathbf{M_{tot}[kg]}$ **11:10-15:20 Low price**	$\mathbf{M_{tot}[kg]}$ **15:20-19:30 Medium price**
Distributed	0.3812	3936	2465	796.4	674.6
Decentralized	0.3155	4021	2511	833	677

TABLE 3.12: Adaptive MPC, second test: results comparison

The great advantage of using an adaptive MPC strategy is evident: the results related to M_{tot} confirm that the control effort, and then the energy consumption, of an adaptive MPC configuration is much lower than non-adaptive strategy. Looking at Table 3.12, is

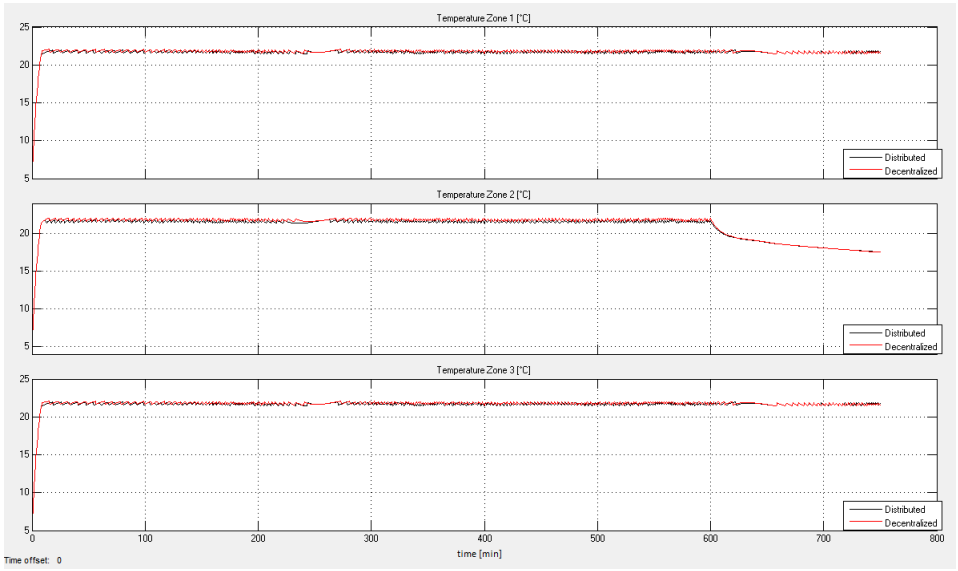

FIGURE 3.12: Non-adaptive MPC, second test: temperature behaviour for each zone obtained with distributed and decentralized strategies

also evident the advantage of using a distributed MPC strategy (that considers the thermal coupling between the zones of the building) than a decentralized one (that doesn't consider the thermal coupling between the zones of the building): the consumptions are lower in spite of little higher temperature errors.

The adaptive MPC with dynamic temperature set-points according to occupancy and energy price levels is the MPC configuration that presents the lowest consumption global index, M_{tot}. In particular, compared to MPC strategy with dynamic temperature set-points according to occupancy levels, it is important to observe that the consumption is lower in the time slot correspondent to the high energy price and is higher in the time slot correspondent to the low energy price. From the other hand, the average temperature error MAE_{TOT} in this MPC configuration is higher because, when the energy price level is HIGH and the occupancy level is maximum, the temperature set-point is 21 °C, then the distance from the ideal indoor comfort temperature (22 °C) is higher as well.

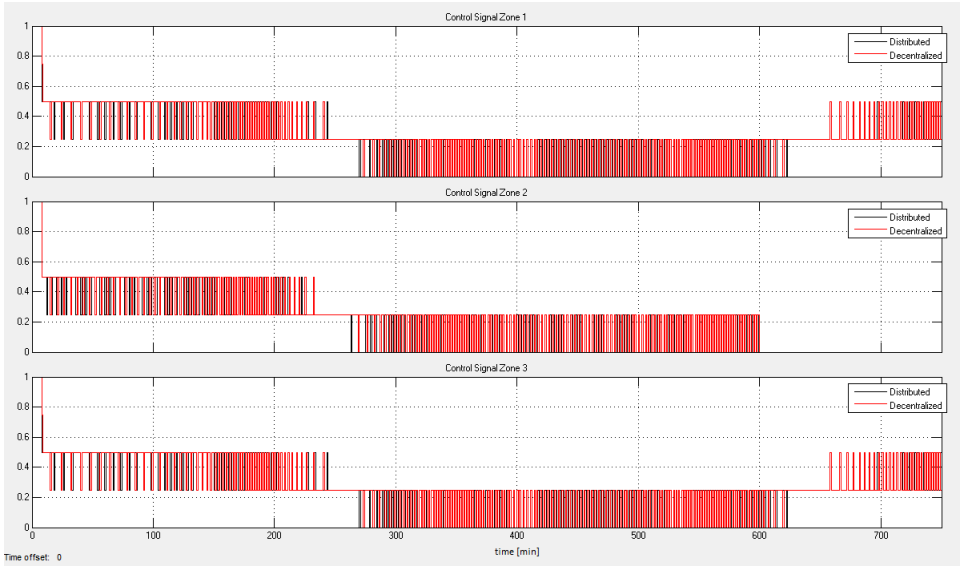

FIGURE 3.13: Non-adaptive MPC, second test: control signal behaviour for each zone obtained with distributed and decentralized strategies

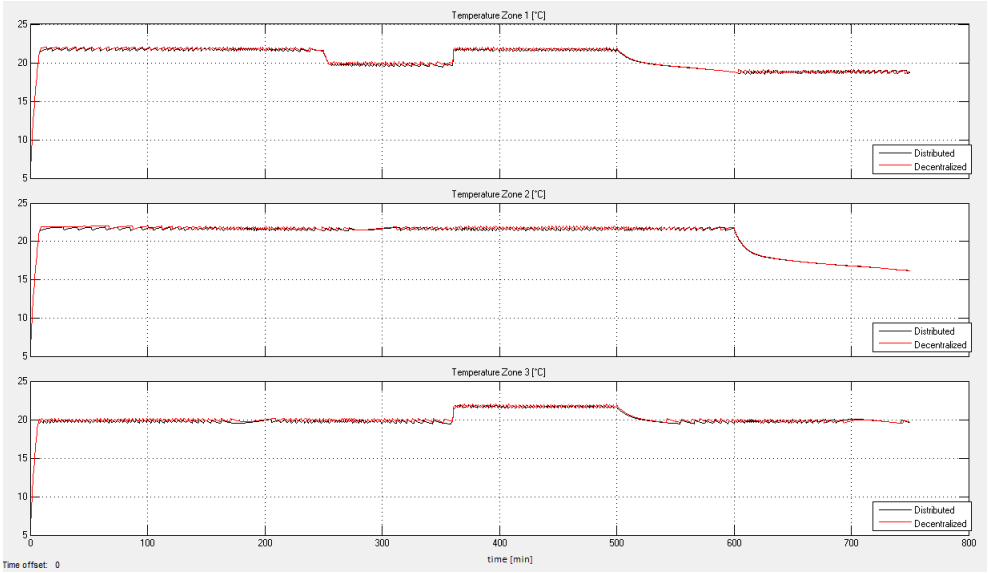

FIGURE 3.14: Adaptive MPC on the basis of occupancy level, second test: temperature behaviour for each zone obtained with distributed and decentralized strategies

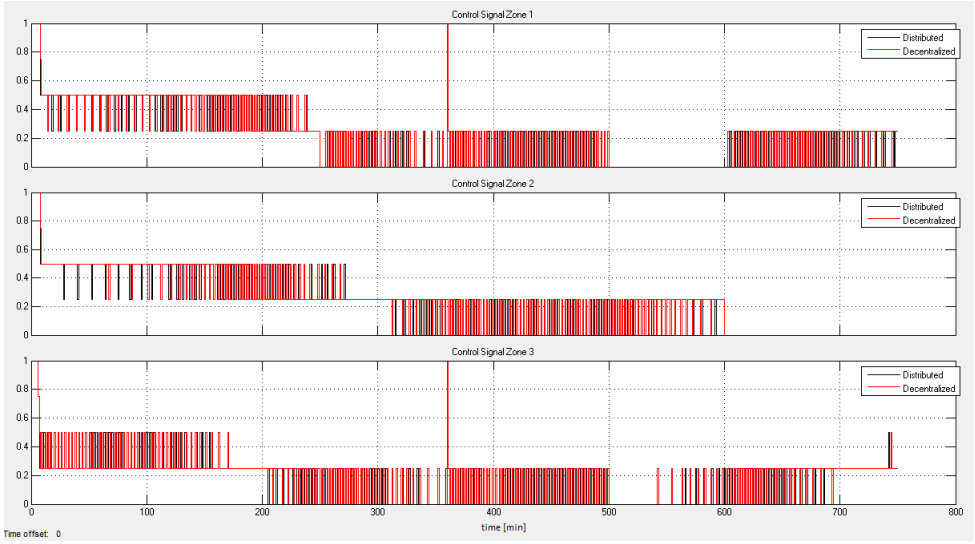

FIGURE 3.15: Adaptive MPC on the basis of occupancy level, second test: control behaviour for each zone obtained with distributed and decentralized strategies

Chapter 4

Fault detection analysis of building consumptions

4.1 Introduction

Buildings are becoming more and more complex energy systems consisting of several elements i.e. heating/cooling systems, ventilation systems, lighting and control systems etc. In addition, buildings have multifarious activities and the occupants may have different demands from a building. Even though building ramification is growing, communication between the participants and the building elements during the building life is poor [29]. The building energy system and the monitoring of its energy and environmental performance has been the subject of great interest in recent years. There is an increasing awareness that many buildings do not perform as intended by their designers. Typical buildings consume 20% more energy than necessary due to faults occurring at a different level of the building life cycle i.e. from construction to operations [47, 137]. The BEMS collects and stores massive quantities of energy consumption data. The general goal of BEMS (control of energy uses and costs, while maintaining indoor environmental conditions to meet comfort and functional need) can not be achieved without uncovering valuable information from the tremendous amounts of available data and transform it into organized knowledge [29]. Hence significant potential exists for better use of BEMS data through fault detection analysis in order to improve operations and save energy. There is an increasing need for automated fault detection tools in buildings. The total energy request in buildings can be significantly reduced by detecting abnormal consumption effectively. Numerous models are used to tackle this problem but either they are very complex and mostly applicable to components level, or they can not be adopted for different buildings and equipment.

Fault detection is the determination that the operation of a building is incorrect or unacceptable from the expected behavior [46]. The pattern recognition-based methods, which belong to the history-based methods category [57], are advantageous for fault

detection since they do not require a deep understanding of physics of the concerned system(s) and can be applied to different levels. Seem [121] proposed a pattern recognition algorithm for automatically determining the days of the week with similar energy consumption profiles. Seem [122] also presented a method for converting the energy consumption data into information and accounted for weekly variation in energy consumption by grouping the days of week with similar power consumption. Liu, Chen, Mori, & Kida [76] classified the building lighting power data considering the number of people and then implemented a robust statistical algorithm to detect the outliers. Fontugne et al. [37] used the Strip, Bind and Search (SBS) method to build sensor traces in order to identify abnormal device usage in buildings.

In the recent years the application of artificial intelligence [101, 106] became one of the most important topics in fault detection. Chen, Wang, & van Zuylen [20] described the density based local outlier approach and compared it with two further algorithms, the statistics-based approach and the distance-based approach, for detecting and analyzing the outliers in traffic data sets for an application to intelligent transportation systems. The experimental results reveal that this method of outlier mining is feasible and more valid then the other two methods presented to detect outliers. Cao et al. [16] proposed a density-similarity-neighbor-based outlier mining algorithm for the data preprocess of data mining technique. They performed the experiments on synthetic and real datasets to evaluate the effectiveness and the performance of the proposed algorithm; the results verified that the proposed algorithm has a higher quality of outlier mining and do not increase the algorithm complexity. Chen, Miao, & Zhang [21] introduced a neighborhood-based outlier detection algorithm that integrates rough-set-granular technique with the outlier detecting. The experimental results show that neighborhood-based metric is able to measure the local information for outlier detection. The detected accuracies based on the neighborhood outlier detection are superior to the k-nearest neighbor for mixed dataset, and a little better than recurrent neural network for discrete dataset. Alan, & Catal [2] proposed an outlier detection approach using both approaches software metrics thresholds and class labels to identify class outliers. The experiments revealed that their novel outlier detection method improved the performance of robust software fault prediction models based on Naive Bayes and Random Forests machine learning algorithms. Razavi-Far et al. [113] focused on the development of a pre-processing module to generate the latent residuals for sensor fault diagnosis in a doubly fed induction generator of a wind turbine. The inputs of the pre-processing module were batches of residuals generated by a combined set of robust observers to operate point changes. The outputs of the pre-processing module were the latent residuals progressively fed into the decision module, a dynamic weighting ensemble of fault classifiers that incrementally learned the residuals-faults relationships and dynamically classified the faults including multiple new classes. The results of simulations confirmed the effectiveness of the approach, even in the incomplete scenarios due to sensor failures.

Many theoretical studies in the application research of artificial intelligence are focused on Artificial Neural Networks (ANNs) [126, 61] and a large number of papers on the application of ANNs for fault detection have been published. For instance, Rossi et al. [118] proposed an effective modeling technique for determining baseline energy consumption of a CHP plant subjected to a retrofit. The study aimed to recreate the post-retrofit energy consumption and production of the system in case it would be operating in its past configuration (before retrofit). Two different modeling methodologies were applied to the CHP plant: thermodynamic modeling and artificial neural networks. A high level of robustness was observed for neural networks against uncertainty affecting measured values of variables used as input in the models. The study demonstrated the great potential of neural networks for assessing the baseline consumption in energy intensive industry and for overcoming the limited availability of on-shelf thermodynamic software for modeling all specific typologies of existing industrial processes. Dodier, & Kreider [30] created a whole-building energy software for detecting energy use problems. The software uses ANNs models as energy end-use predictors to evaluate the expected energy end-use in relation to the measured one, considering weather, time of the day and other features of building energy use that are time- and day-dependent. The software generates detection messages as "lower than normal" and "higher than normal" energy ratio. Mavromatidis et al. [85] developed a diagnostic tool for a supermarket using the ANN models. This tool evaluates, on the basis of suitable explanatory variables, the energy consumption of each supermarket subsystem to provide the energy baseline, and then performs the fault detection analysis. The actual energy consumption is compared to the predicted consumption and the performance is labeled as Bad/Average/Good. If five or more consecutive points greater than the upper or lower prediction bound occur, the likelihood of a fault occurrence is high.

As demonstrated above, few papers are focused on artificial intelligence and data mining techniques applied to the specific sector of building energy consumption fault detection. The present Chapter is devoted to the problem of fault detection using actual building energy consumption data through simplified robust algorithms. Section 4.2 provides a description of the of eight adjacent buildings (hereafter referred as cluster of buildings) whose monitored data are used for the experimentation. In Section 4.3 recorded data with a 15 minutes timestamp of active electrical power for lighting and total active electrical power of the mentioned buildings are analyzed. The proposed methodology [17], starting from the previous experience of [59], uses statistical pattern recognition techniques and ANN ensembles coupled with two different outliers detection methods for fault detection. A comparison of results obtained through these methods is carried out to minimize the number of false outliers and to improve the robustness of the fault detection analysis. In addition, in Section 4.4 an analysis of the thermal energy data of a building of the cluster in the winter season is performed. The objective is the automatic definition of the shape and the size of the building thermal

energy daily profile for detecting possible anomalies in the energy demand time trend.

4.2 Cluster of buildings and data description

The cluster of buildings under investigation is located within the Italian National Agency for New technologies, Energy and Sustainable Economic Development (ENEA) Casaccia Research Center and includes buildings F66 - F67 - F68 - F69 - F70 - F71 - F72 - F73, positioned in two different blocks. A first block, consisting of three contiguous buildings is oriented along the axis NW-SE, while the second block consists of 5 buildings and its main orientation is NE-SW as shown in Fig. 4.1.

FIGURE 4.1: The cluster of buildings

The eight buildings have similar characteristics both from a structural and HVAC point of view. Moreover all the buildings are offices and hence serve the same purpose. They consist of a single floor except building F67, which also includes a basement. The buildings are composed of a concrete external wall with a thickness of 30 cm, and an internal paneling of insulating material of about 5 cm. The windows are sliding with an aluminum frame. The control of solar radiation in the offices is obtained through external venetian blinds. All the buildings are served by a centralized heating and cooling plant located in a technical room in which the carrier fluids are produced. At the building level is located a technician room in which the heating / cooling sub system and the air handling unit are placed. At the level of the individual building, the electrical panel includes a counter-general of the total electricity supplied to the building, plus a breakdown of artificial lighting, plug load and overall conditioning system electrical lines.

Each building is equipped with an advanced monitoring system aimed at collecting energy consumption (electrical and thermal) and the environmental conditions. Active electrical power for lighting and total active electrical power consumption of each

building with 15 minutes timestamp is analyzed in this experimentation. Furthermore number of occupants, global solar radiation, average indoor and outdoor temperatures, time, date and day of the week (Sun-Sat = 1-7), are recorded and considered as independent variables. The monitoring and actuation system developed is structured in five logical layers:

- fieldbus layer, directly interface to sensor network through a BEMS;
- sensor and actuator layer, containing applications that interface database of data warehouse layer with BEMS;
- application layer, containing diagnostics and control logics applications;
- presentation layer, that is a web interface to users.

4.3 Fault detection analysis

One of the effective ways of analyzing large data is to identify recurring patterns in the raw data. Clustering and classification are two common techniques used for finding hidden patterns in data sets. Discovering the patterns in data before applying the outliers detection algorithm is very useful to find anomalies in the building energy consumption. Outliers are cases that have data values very different from the data values for the majority of cases in the data set. Statistical-based [139], distance-based [112], deviation-based [4] and density-based [35] outliers detection methods are mainly discussed in recent times.

4.3.1 Pattern recognition techniques and outliers detection methods

The pattern recognition techniques and outliers detection methods employed for fault detection are briefly explained below. As shown in Fig. 4.2 and fully explained in the next paragraph, first, a classification and clustering of 15 minutes timestamp recorded data using CART (Classification And Regression Tree), K-Means and DBSCAN (Density-Based Spatial Clustering of Applications with Noise) algorithms are respectively carried out. With CART and K-Means methods, the detection of evident outliers in each class and cluster respectively is performed using generalized extreme studentized deviate (GESD) algorithm. In the DBSCAN method the outliers are directly detected analyzing a particular cluster (cluster-0), in which they are isolated. Second, the ANN Ensemble (ANNE) approaches are introduced and their capability for energy fault detection is demonstrated. The fault detection is performed analyzing the magnitude of the residual generated by ANNE using an algorithm capable to detect peaks in a data set and the GESD method. Finally, the results obtained by each method are compared to improve the fault detection analysis.

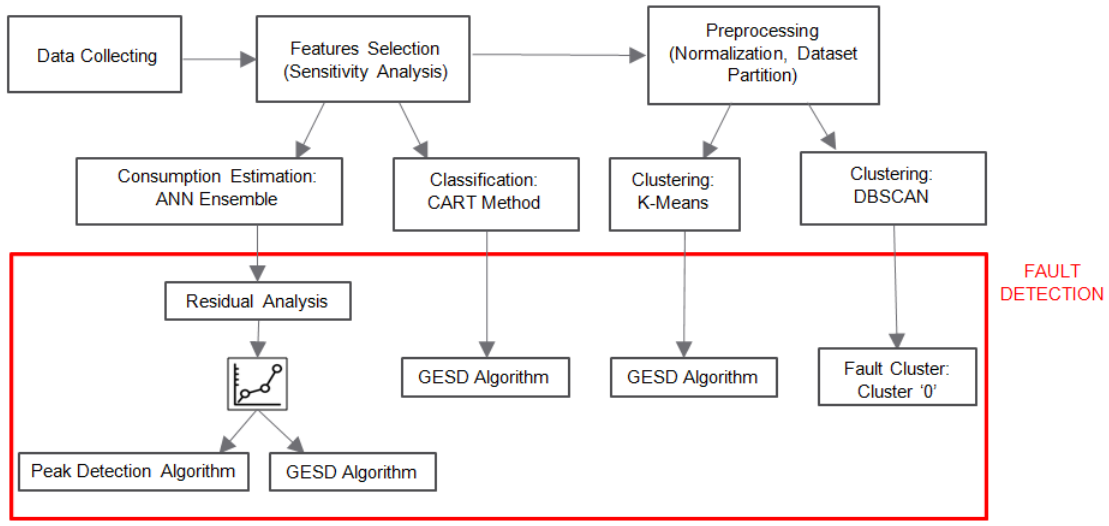

FIGURE 4.2: The fault detection methodology

Classification and regression tree

The CART algorithm is based on classification and regression trees. A CART is a binary decision tree that is constructed by splitting a parent node into two child nodes repeatedly, beginning with the root node that contains the whole learning sample. The CART method can easily handle both numerical and categorical variables and is useful in robust detection of outliers. The proposed method is aimed at the identification of decision trees from which it is possible to identify rules based on the values assumed by the independent variables for the classification of data and the subsequent and effective identification of anomalies. Therefore it is particularly suitable for conducting analysis of fault detection in real time. CART methodology generally consists of three parts:

- construction of maximum tree;
- choice of the right size tree;
- classification of new data.

The detailed approach is described in "Classification and Regression Trees (CART) Theory and Applications" [131].

Clustering

Clustering is concerned with grouping together objects that are similar to each other and dissimilar to the objects belonging to other clusters. It is useful for extracting information from unlabeled data. The selected algorithms can be classified into two categories: (i) partitioning methods and (ii) density-based methods. These methods

require the definition of a metric to compute distances between objects in the dataset. In this case study, distances between objects are measured by means of the Euclidean distance computed on normalized data.

K-Means is selected for this study, which belongs to partitioning methods category. It requires as input parameter, k, the number of partitions in which the dataset should be divided. It represents each cluster with the mean value of the objects it aggregates, called centroid. The algorithm is based on an iterative procedure, preceded by a set-up phase, where k objects of the dataset are randomly chosen as the initial centroids. Each iteration performs two steps: in the first step, each object is assigned to the cluster whose centroid is the nearest to that object; in the second step, centroids are relocated, by computing the mean of the objects within each cluster. Iterations continue until the k centroids do not change [55].

DBSCAN [35] is the density-based method considered in this study. The method requires two input parameters: a real number, r, and an integer number, $minPts$, used to define a density threshold in the data space. A high density area in the data space is an n-dimensional sphere with radius r which contains at least $minPts$ objects. DBSCAN is an iterative algorithm which iterates over the objects in the dataset, analyzing their neighborhood. If there are more than $minPts$ objects whose distance from the considered object is less than r, then the object and its neighborhood originate a new cluster. DBSCAN is effective at finding clusters with arbitrary shape, and it is capable of identifying outliers as a low density area in the data space. The effectiveness of the algorithm is strongly affected by the setting of parameters r and $minPts$.

Artificial neural networks and basic ensemble method

ANNs [126, 3] are data modeling and decision making tools which can be used to model complex relationships between inputs and outputs or to find patterns in data. ANNs are referred also as black-box or data-driven models and they are mainly used when analytical or transparent models can not be applied. ANNs essentially contain masses of parallel, interconnecting information processing units, technically known as "neurons", which interact with one another and can be located in multi-layers. For example, a typical structure consists of an input layer, an output layer and one or more intermediate layers, where the hidden neurons are located. The neurons can be combined in various ways to form different types of interconnecting structures: the connections between units define the network topology or architecture. The feedforward structures are mainly featured in FDD research papers. In feedforward ANN the data processing can extend over multiple (layers of) units, but no feedback connections are present, i.e., connections extending from outputs of units to inputs of units in the same layer or previous layers. These models are also known as Multi-Layer Perceptrons (MLP) [117], since the basic structure is the perceptron [116].

The term "ensemble" describes a group of learning machines working together on the same task: the goal is to obtain better performances than those which could be obtained from any of the constituent models. In the last years, several ensemble methods have been carried out [62, 77, 12]. The non-generative ensemble method seeks to combine the outputs of the machines in the best way. In the case of ANNs, they are trained on the same data, they run together and their outputs are combined in a single one. Basic Ensemble Method (BEM) [107, 11] is the simplest way to combine a group of neural networks as an arithmetic mean of their outputs. This method can improve the global performance, although it does not take into account that some models can be more accurate than others, and it has the advantage to be very easy to apply.

Outliers' detection methods

An outlier is an observation (or subset of observations) which appears to be inconsistent with the remainder of that set of data. Outliers arise because of human error, instrument error, changes in behavior of systems or faults in systems. In this study GESD and Peak Detection methods are used to detect abnormal consumption. Both methods allow to find multiple outliers in a data set.

Generalized extreme studentized deviate many-outlier method

In order to perform the GESD method, two parameters need to be set:

- the probability α of incorrectly declaring one or more false outliers;
- an upper limit n_u of the expected number of potential outliers.

On the basis of the indications of [18], the expected number of potential outliers is evaluated finding the largest integer that satisfies the inequality (Eq. 4.1):

$$n < 0,5 \cdot (n-1) \tag{4.1}$$

where n is the number of observations in the data set X: $x1$, $x2$, $x3$, ..., xn, and for the probability α values between 5% and 10% are chosen.

The method allows detecting the outlier values in a data set through the calculation and comparison of the two following important parameters:

- the $i-th$ extreme studentized deviate R_i, determined from (Eq. 4.2):

$$R_i = \frac{|x_{e,i} - \bar{x}|}{s} \tag{4.2}$$

  where $x_{e,i}$ is the extreme element in set X that is furthest from the average $\bar{x}$ of elements in set X and s is the standard deviation of elements in set X;

- the $i-th$ critical value λ_i, determined from (Eq. 4.3):

$$\lambda_i = \frac{t_{n-i-1,p}(n-i)}{\sqrt{(n-i-1+t^2_{n-i-1,p})(n-i+1)}} \tag{4.3}$$

where $t_{n-i-1,p}$ is the student's t-distribution with $(n-i-1)$ degrees of freedom, and the tail area probability p is determined from (Eq. 4.4):

$$p = 1 - \frac{\alpha}{2 \cdot (n-i+1)} \tag{4.4}$$

Peak Detection Method

Identifying and analyzing peaks in a given time-series is important in many applications such as building energy consumptions. In order to avoid subjectivity and to devise algorithms for the automatic detection of peaks in any given time-series, it is important to define the notion of the peak. A peak is defined as an observation that is inconsistent with the majority of the observations of a data set. Not all local peaks are true: a local peak is true if it is a reasonably large value even in the global context.

The implemented method, *Peak Detection*, is based on the use of a peak function, which associates a score (S value) with every element of the given time-series [102]. The mean m' and the standard deviation s' of all positive values of the peak function are computed. A given point x_i in the time-series is a peak if its score S_i is positive and satisfies the condition (Eq. 4.5):

$$S_i - m' > h \cdot s' \tag{4.5}$$

where h is a user-specified constant, tipically 1 <= h <= 3 according to [102]. Particularly, the peak function computes the average of the maximum among the signed distances of a given point x_i in a time-series X from its k left neighbors and the maximum among the signed distances from its k right neighbors, as expressed by Eq. 4.6:

$$S_i = \frac{max\{x_i - x_{i-1}, x_i - x_{i-2}, ..., x_i - x_{i-k}\} + max\{x_i - x_{i+1}, x_i - x_{i+2}, ..., x_i - x_{i+k}\}}{2} \tag{4.6}$$

The score S is an index that allows to quantify the severity of the outliers and then provides information about the priorities for actions to be associated with each outlier.

In addition to the outliers' detection methods and once the outliers are detected, another synthetic index, modified z-score ($Mzscore$, z_m), is used to quantify how far and

which direction an outlier is from the mean value of typical observations. z_m is defined as (Eq. 4.7):

$$z_m = \frac{x_{outlier} - \bar{x}_{robust}}{s_{robust}} \tag{4.7}$$

where $x_{outlier}$ is a raw value of an outlier, $\bar{x}_{robust}$ is the mean value of non-outliers in the data set X and s_{robust} is the standard deviation of non-outliers in the data set X.

4.3.2 Methodology

The proposed approach, illustrated in Fig. 4.2, is applied to each building of the cluster for both winter and summer data. This Paragraph contains the application of each method described in Paragraph 4.3.1.

For all the simulations performed, the values of the active electrical power for lighting and the total active electrical power of each building are considered as dependent variables. The independent variables considered are: date, day of the week, time of the day, average indoor temperature, average outdoor temperature, number of occupants and global solar radiation. The selection of the appropriate independent variables to consider was conducted on the basis of a sensitivity analysis and on the basis of the experience on this issue. The results are obtained for both time periods (Jan-Feb and May-Jun). The choice of time periods has also allowed to assess the types of fault found in the periods in which weather conditions relating solar irradiance are different. The selected time periods, in fact, presenting different availability of natural light, were used to verify potential fault associated with the behaviour of the occupants in the management of artificial lighting.

The first analysis of fault detection is carried out by applying the GESD algorithm to each class identified by the CART method. The major steps adopted for CART analysis used for fault detection are summarized below:

- sensitivity analysis on monitoring data in order to identify the independent variables of greater importance on the variation of the dependent variables (active electrical power for lighting/total active electrical power);
- classification of data using the CART method and applying pruning methods (cross validation and number of samples in both parent and child nodes);
- application of GESD many outliers detection algorithm to each class;
- Use of dimensionless statistical indicator ($Mzscore$) to show the degree of importance or severity of each outlier identified in each class.

With regard to the analysis of clustering (KMeans and DBSCAN), in order to overcome the limitations of the algorithms that do not allow to consider time and day as independent variables, data sets are divided into the working period (from 07:30 to 17:30), the non-working period and the weekends. The approach adopted for the splitting of the data is the experience gained from some previous work [60] for which the partition of the data set in the daytime, nighttime and weekend proved not to be particularly effective for the nature of the fault in the type of buildings under investigation. It did not allow to evaluate the effectiveness of the outliers occurring in the early hours of the morning and at the end of the working hours. Before performing the clustering analysis, the recorded real data are normalized by means of the standard score ($z - score$) method. The analysis of fault detection was carried out by applying the GESD algorithm to each cluster found by K-Means. With DBSCAN method, in all discovered clusters, the cluster label zero contains all points identified as outliers or noise. To set the input parameters (r, $minPts$), different tests were carried out for all data (active electrical power for lighting and total active electrical power) by changing the values of these parameters. The results show that by keeping the value of one parameter constant and changing the value of other parameter the discovered clusters are different. For example, if the value of $minPts$ is kept constant and the value of radius r decreases, then the number of clusters and outliers increases. The results obtained from these tests are analyzed and the similarities within the clusters are investigated in order to select the appropriate values of both input parameters. The results show that DBSCAN is able to identify clusters with the same density and with very similar data. In any process, it was noted that if the value $minPts$ is kept constant and the value r grows then the number of outliers tends to decrease as the number of clusters can be identified. In addition, by setting the values $minPts > 3$ the process is stable and the number of the formed clusters is always equal to two, that's why it was not considered necessary to proceed with further sensitivity analysis on the parameters of clusterization.

Regarding the second part of the experimentation, the ANN ensemble was built according to BEM and combining 10 ANN models. The considered ANN features are:

- feed-forward MLP;
- 1 hidden layer consisting of 15 neurons;
- hyperbolic tangent as activation function for the hidden neurons;
- linear activation function for the output neurons.

For the ANN modeling, a single 15-minute consumption constitutes an output record as well as each single 15-minute independent variable constitutes an input record. Two different ANN BEM were built, trained and tested for each building of the cluster, according to the two different time periods considered (Jan-Feb and May-Jun) and to the availability of monitored data. Considering a timestamp of 15 minutes and a 2-months

period, the dataset related to each ANN BEM consists of about 5000 data records, of which 60% for the training data set, 10% for the validating data set and 30% for the testing data set. Many experiments were carried out with different number of hidden layers and neurons: finally, the selected ANN architecture was the one with the lower errors (according to the mean absolute error, MAE, and the maximum absolute error, MAX).Training was performed with MATLAB through the Levenberg-Marquardt algorithm stopping after 1000 iterations.The residuals were calculated by the difference between the real consumption and the consumption estimated by the ANN BEMs in the testing period for the fault detection analysis of each building.

4.3.3 Results and discussion

The results obtained from the analysis of fault detection conducted separately for each building, for the two dependent variables and for the two time periods are summarized and presented in this Paragraph.

Classification and clustering

With CART analysis, it was found that for all buildings, considering both the dependent variables active electrical power for lighting and the total active electrical power, the most influential variables are the number of occupants and the solar irradiance. During the summer, the independent variable outdoor temperature is particularly important too for the classification process. Furthermore, the number of classes identified for each examined case are between 5 and 10. In the Fig. 4.3, 4.4, 4.5, 4.6 the sequence graphs of both active electrical power for lighting and total active electrical power consumption and $Mzscore$ graphs for the selected classes with outliers are shown.

It is clear that the outliers in individual class are mostly peak values and can be easily located, while in sequence data the same is not possible. Each outlier identified by the GESD method is labeled with the time of the day, the day of the week and the date. It was verified that for all the simulations performed the index $Mzscore$ assumed extreme absolute values proving to be an excellent diagnostic marker for the analysis of fault detection. Moreover, for each building examined (relative to the total electrical active power for lighting) and for the selected classes with the method CART, in the Fig. 4.3 and 4.4 outliers identified that are common to both clustering methods applied are also highlighted. This type of analysis is particularly important because it allowed to verify the correctness of the data classification based on the outliers identified in the selected class and also identified through the clustering methods, K-Means and DBSCAN.

The following Tables (Tab. 4.1 and 4.2) show in detail the outliers identified by the methods K-Means and DBSCAN; the common outliers are highlighted for both active

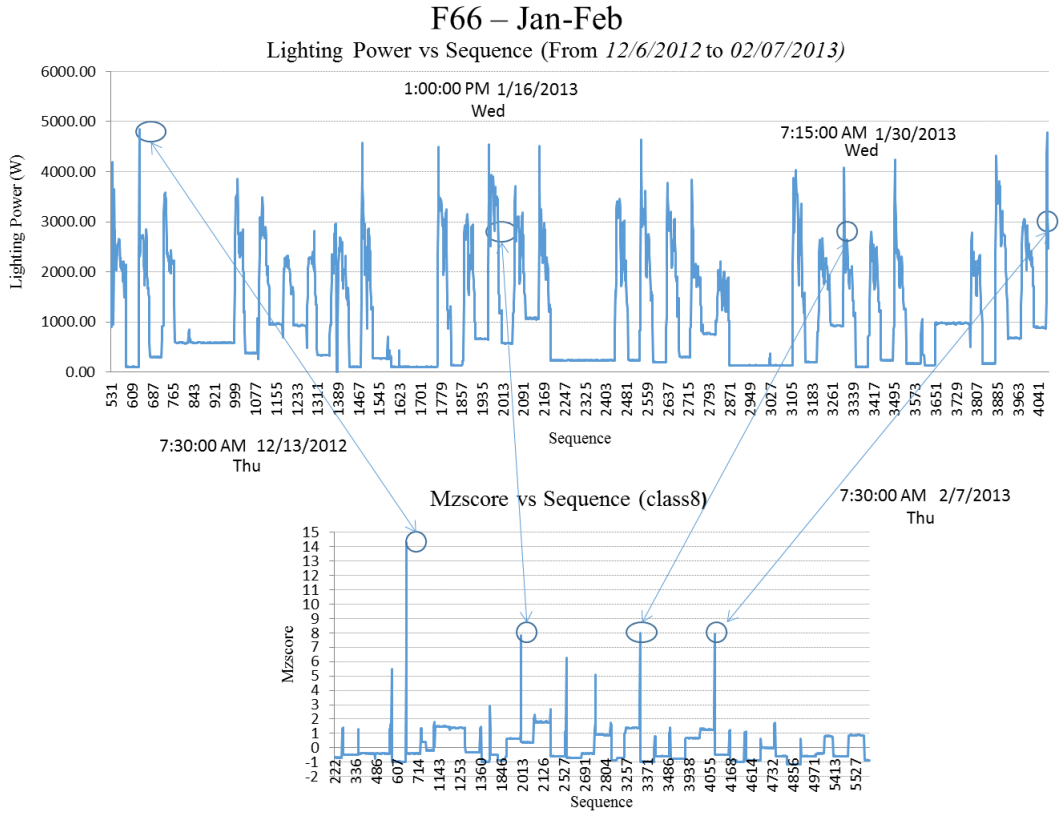

FIGURE 4.3: Segment of active electrical power for lighting sequence and Mzscore of a class data (CART) with evidence of major outliers identified with GESD (Building F66-winter data) [17]

electrical power for lighting and total active electrical power considering different periods of the day. It was observed that for buildings F69 and F72 (Jan-Feb) the outliers are common only for the active electrical power for lighting while for buildings F68, F71, F72 and F73 (May-Jun) outliers are common for both active electrical power for lighting and total active electrical power.

Further conducted analysis and reported in the Tables 4.3 and 4.4 relate to the identification of the outliers observed for the total active electrical power which are common to all three methods of data mining techniques. From these Tables it is observed that most common outliers are identified in the early morning.In general outliers are identified in three different periods of the day. The first period is early morning between 06:30 and 07:30. In the early morning both electrical power for lighting and total electrical power have the peaks at a very low presence of occupants. The second period in which many outliers are identified is between 12:30 and 13:30 during the lunch break. The third period is related to the end of working hours between 17:00 and 17:30, where it is observed that a decrease in the number of occupants of the building does not correspond to a decrease in power consumption for lighting and total power (which takes into account the plug load and air conditioning).

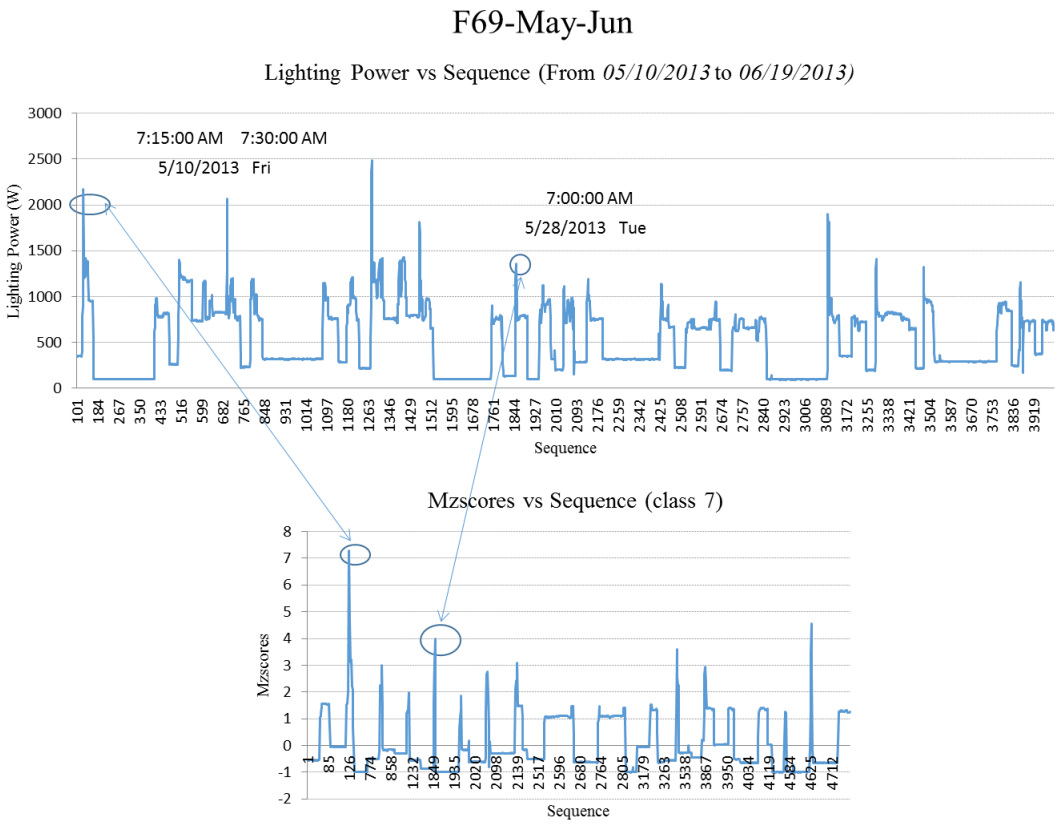

FIGURE 4.4: Segment of active electrical power for lighting sequence and Mzscores of a class data (CART) with evidence of major outliers identified with GESD (Building F69-summer data) [17]

Artificial neural network ensemble

The fault detection analysis conducted on the basis of the residuals obtained by the ANN BEMs consumptions modeling is described in this Paragraph. For the sake of simplicity, in the following only the results for the building F68 in summer season (May 2013 – June 2013) are shown.

A residual analysis on lighting active electrical power and total active electrical power was performed and for both cases the testing residuals with a timestamp of fifteen minutes are shown in Figure 4.7(a) and (b) respectively.

Then, the peak detection and the GESD methods were applied to active electrical power for lighting residuals: the detected faults are reported in Table 4.5. The testing period for building F68 is from 10/06/2013 to 20/06/2013.

The identified residual peaks include potential early morning faults for which very high power demand is observed with few people in the buildings (see Table 4.5). These situations correspond to "systematic" anomalies: the high consumption in the early morning is due to the cleaning staff that is not part of presence data. Table 4.5 shows

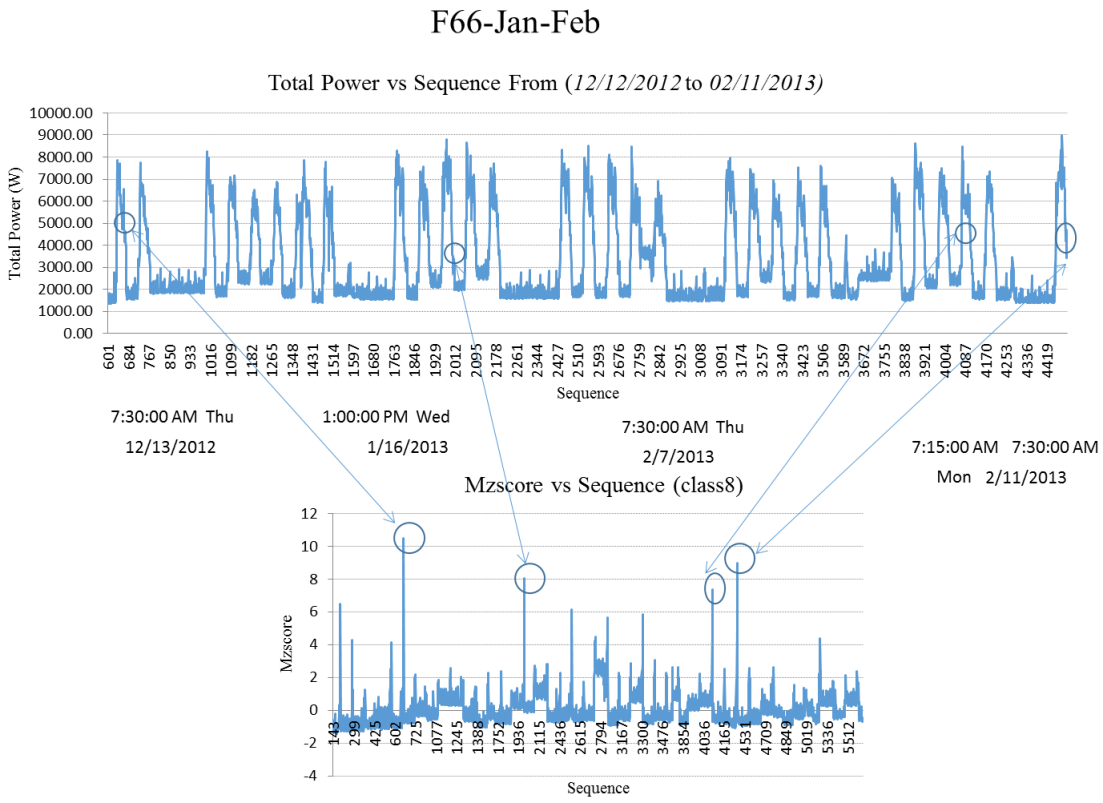

FIGURE 4.5: Segment of total active electrical power sequence and Mzscores of a class data (CART) with evidence of major outliers identified with GESD (Building F66-winter data) [17]

also that the Peak Detection Method performs better than the GESD method since it is able to detect a greater number of "not false positives" faults: it should be noticed that this conclusion is not general but it is specific to this particular type of fault detection application and strongly dependent on the dataset used. In Figure 4.8 an example of fault detected by the Peak Detection Method and not by the GESD method applied to building F68 residuals is shown: this situation correspond to a "real" anomaly because the lighting power consumption is high (1.28 kW) with respect to the time of the day and only one presence in the building.

The results confirm that the analysis of residuals generated through the ANN BEM and the application of the Peak Detection Method represents a useful and powerful technique for the peak building lighting fault detection.

The Peak Detection Method is also directly applied to the sequences lighting active power demand data. In Figure 4.9 is shown an example of outlier (5.17 kW) detected in the early morning for building F68 with the values of $Mzscore$ and S function indices.

However the data analysis showed that lighting power consumption is related to several variables i.e. people, solar radiation, day and time, so it can be inferred that in this specific application the extreme values are not always definite faults. Therefore

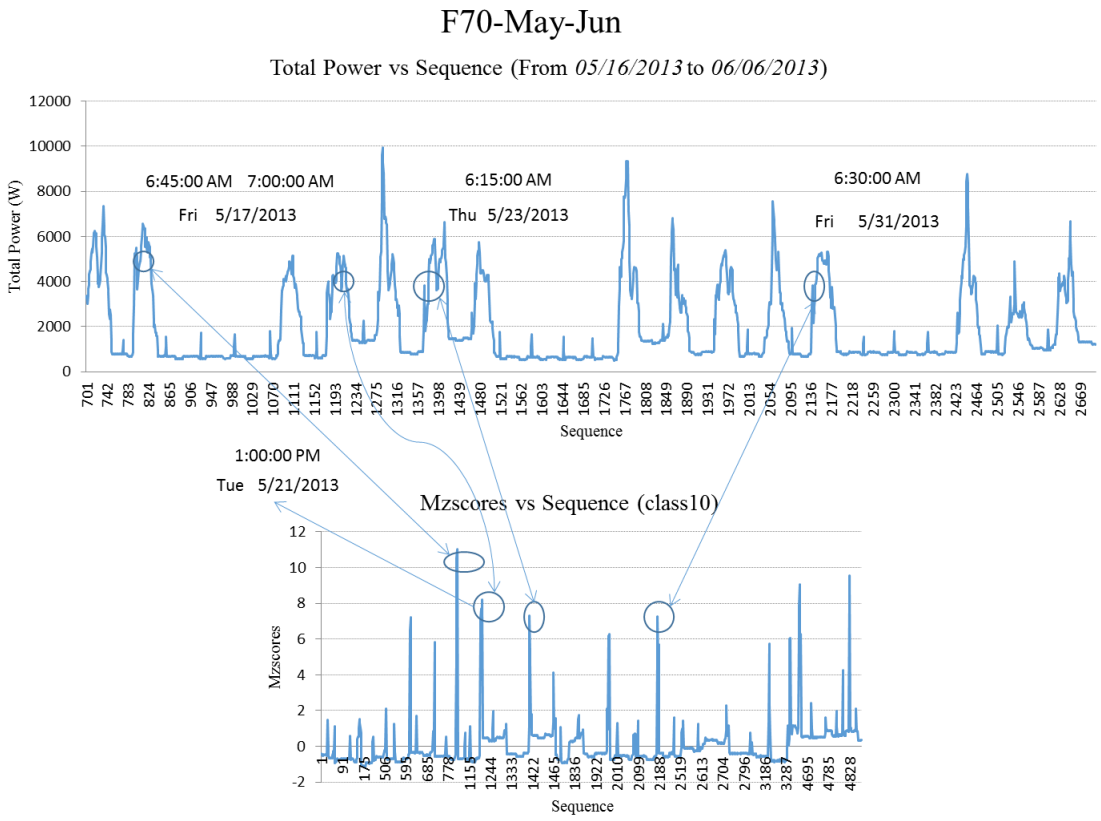

FIGURE 4.6: Segment of total active electrical power sequence and Mzscores of a class data (CART) with evidence of major outliers identified with GESD (Building F70-summer data) [17]

some false positives can be found when an "univaried" outlier detection method is applied without taking into account the effect of the independent variables. For this reason, a FDD process performed through a residual ANN BEM analysis is always recommended to avoid the occurrence of false positive faults.

Identification of common outliers

Following the various comparative analyses of the results obtained using the statistical pattern recognition techniques and the residuals analysis described in Paragraph 4.3.1, this Paragraph summarizes the anomalies identified through all proposed methods for some selected buildings belonging to cluster of buildings in the period May-Jun. The objective of this analysis is to improve the fault detection by minimizing the false anomalies and to identify the type of faults. Figure 4.10 shows the $Mzscore$ graph of a class (CART) with evidence of common outliers detected by CART and K-Means with GESD, DBSCAN and Peak Detection Method applied to ANN BEM residuals.

In Figure 4.11 the Mzscores of a class (CART) with evidence of common major outliers identified by ANN BEM residuals (GESD) and CART (GESD) are shown.

Date	Id Day	Time	Electric active Power [W]	Total electric active power [W]	Indoor temperature [°C]	People presence	Outdoor temperature [°C]	Global solar radiation [W/m^2]	Color legend
05/12/2012	4	7.30.00	2430.00	6311.39	16.15	1	6.20	141	
06/12/2012	5	6.45.00	300.00	2535.39	18.69	0	4.60	339	DBSCAN -Lighting Power
06/12/2012	5	7.00.00	175.00	1958.19	18.83	0	5.20	381	DBSCAN-Total Power
06/12/2012	5	7.15.00	135.00	2001.40	18.90	1	5.60	292	Common-DBSCAN&K-means
06/12/2012	5	7.30.00	450.00	2616.60	18.95	1	5.80	360	
07/12/2012	6	7.30.00	2615.00	5211.00	16.35	1	3.70	107	
13/12/2012	5	7.15.00	2515.00	4729.20	17.69	0	4.90	311	
13/12/2012	5	7.30.00	4855.20	7655.79	16.47	0	5.20	369	
14/12/2012	6	7.30.00	920.00	3181.10	19.51	1	9.70	512	
17/12/2012	2	7.15.00	585.00	2807.89	18.83	1	12.70	67	
17/12/2012	2	7.30.00	970.00	3406.19	19.02	1	13.10	466	
20/12/2012	5	7.30.00	845.00	3322.19	16.99	1	8.00	248	
08/01/2013	3	7.00.00	1470.00	3450.00	16.00	0	10.00	185	
08/01/2013	3	7.15.00	2640.00	4722.70	15.76	1	9.90	100	
08/01/2013	3	7.30.00	3065.00	5405.79	15.69	1	9.80	111	
16/01/2013	4	7.30.00	3510.00	6110.60	16.60	2	3.70	0	
24/01/2013	5	7.30.00	2655.00	6253.29	16.02	2	5.50	0	
30/01/2013	4	7.30.00	3590.00	6100.20	16.26	2	5.20	7	
07/02/2013	5	7.30.00	2885.00	5980.00	18.93	0	3.70	0	
11/02/2013	2	7.30.00	4445.20	6852.39	15.09	0	3.20	0	
13/02/2013	4	7.30.00	3185.00	7012.70	16.72	3	3.80	11	

TABLE 4.1: Outliers detected with KMeans (GESD) and DBSCAN methods for total electrical active power and active electrical power for lighting (Building F66-winter data)

Date	Id Day	Time	Electric active Power [W]	Total electric active power [W]	Indoor temperature [°C]	People presence	Outdoor temparature [°C]	Global solar radiation [W/m^2]	Color legend
17/05/2013	6	07:00:00	3235.00	4342.39	21.91	0	15.30	63	
23/05/2013	5	06:45:00	5165.20	6191.29	21.64	0	13.10	23	DBSCAN-total power
27/05/2013	2	06:45:00	4530.00	5791.39	20.07	0	9.40	28	Common-DBSCAN&K-means
27/05/2013	2	07:00:00	4785.20	5826.20	20.12	0	9.50	35	
27/05/2013	2	07:15:00	3840.00	4860.00	20.10	0	9.90	83	
29/05/2013	4	07:15:00	4160.00	5200.60	21.28	0	14.00	160	
04/06/2013	3	07:00:00	5015.20	6462.20	21.85	0	14.20	26	
10/06/2013	2	06:45:00	3640.00	4515.60	24.09	0	16.30	105	
10/06/2013	2	07:00:00	4140.00	5202.79	24.09	0	16.40	90	
10/06/2013	2	07:15:00	2910.00	4194.89	24.07	1	16.50	102	

TABLE 4.2: Outliers detected with KMeans (GESD) and DBSCAN methods for total electrical active power and active electrical power for lighting (Building F68-summer data)

These Figures confirm that most real abnormal consumption occurs during the early morning period. Furthermore, the outliers detected by the application of all proposed methods among the buildings are analyzed. It was observed that in all buildings the abnormal values detected are mainly of an identical nature. Most outliers are present during the same time periods and with a fewer number of people presence (see Table 4.6).

Figure 4.12 shows the active electrical power for lighting and the total active electrical power consumption against the number of people presence (9 and more) for the cluster of buildings (winter data and summer data).

The energy consumption of outliers shown in Table 4.6 is as high as peak operating hours and equals to the consumption of high number of people presence. Usually off-peak electric use in many buildings is 30-70% of peak use. From these results it can be concluded that outliers identified by all methods more likely correspond to values of real abnormal consumption, hence minimizing the number of false positives. Through

Date	Id Day	Time	Total electric active power [W]	Indoor temperature [°C]	People presence	Outdoor temparature [°C]	Global solar radiation [W/m^2]
02/12/2012	1	07:45:00	2517.00	22.75	0	8.80	0
02/12/2012	1	20:00:00	2588.50	21.90	0	6.20	0
14/12/2012	6	06:30:00	5514.50	18.94	0	8.50	91
14/12/2012	6	06:45:00	4492.10	18.30	0	8.60	103
17/12/2012	2	07:30:00	4815.60	19.67	1	13.10	466
14/01/2013	2	07:30:00	4498.20	19.40	0	9.00	0
19/01/2013	7	02:30:00	2529.89	20.09	0	0.40	0
19/01/2013	7	02:45:00	2403.50	20.06	0	0.20	0
19/01/2013	7	08:15:00	2606.89	19.83	0	2.60	12
19/01/2013	7	14:45:00	2699.10	21.31	0	4.50	51
20/01/2013	1	03:15:00	2628.19	20.04	0	9.20	0
22/01/2013	3	07:15:00	4694.20	18.76	0	4.00	0
05/02/2013	3	07:15:00	6533.60	19.19	0	5.90	0
05/02/2013	3	07:30:00	6010.50	19.03	0	5.90	0
07/02/2013	5	07:30:00	4765.60	20.93	1	3.70	0
13/02/2013	4	07:30:00	4558.00	21.64	1	3.80	11

TABLE 4.3: Common outliers identified with CART (GESD), KMeans (GESD) and DBSCAN for total electrical active power (Building F72-winter data)

Date	Id Day	Time	Total electric active power [W]	Indoor temperature [°C]	People presence	Outdoor temparature [°C]	Global solar radiation [W/m^2]
14/05/2013	3	07:30:00	3169.00	18.87	2	12.40	26
23/05/2013	5	06:45:00	4066.60	21.79	0	13.10	23
23/05/2013	5	07:00:00	4238.70	21.15	0	13.20	32
31/05/2013	6	06:45:00	3205.30	20.42	0	9.00	26
31/05/2013	6	07:00:00	4292.00	20.59	0	9.30	51
31/05/2013	6	07:15:00	4433.10	20.23	0	9.80	74
31/05/2013	6	07:30:00	4124.50	19.50	2	10.40	127
11/06/2013	3	07:15:00	3361.19	23.35	1	16.10	33
13/06/2013	4	07:15:00	3561.69	23.89	0	19.40	42
21/06/2013	6	07:30:00	3633.19	24.45	1	20.40	60
21/06/2013	6	15:15:00	918.40	25.64	6	29.30	747
27/06/2013	5	07:30:00	3271.80	20.01	2	17.10	35

TABLE 4.4: Common outliers identified with CART (GESD), KMeans (GESD) and DBSCAN for total electrical active power (Building F71-summer data)

the proposed approach, this abnormal consumption is avoidable resulting a significant amount of saved energy. Thus, once the ANN models are trained and the pattern recognition models are defined, all the simulations can be performed in minute order time. The proposed methodology allows to perform a fault detection analysis in "near" real time and can be easily implemented in BEMS as demonstrated in the next Chapter. Moreover, it should be recognized that the whole building data modeling approach is useful for indications of probable cause and additional field measurements are required to confirm the probable cause of anomalous consumption, as again confirmed in Chapter 5.

The results show the the effectiveness and usefulness of this data analysis approaches in automatic fault detection of anomalous energy consumption values. In particular the neural ensemble method has always proven to be more robust than the single neural model. The analysis of residuals (ANN BEM) coupled with the peak detection method has also allowed to identify outliers in relation to the boundary conditions of the buildings (occupants, indoor/outdoor temperatures, solar radiation, time and day). As a consequence the method is able to detect the outliers that much more likely reflect real anomalous consumption compared to outlier identified by statistical methods simply applied only to actual consumption data (univariate analysis). Since the

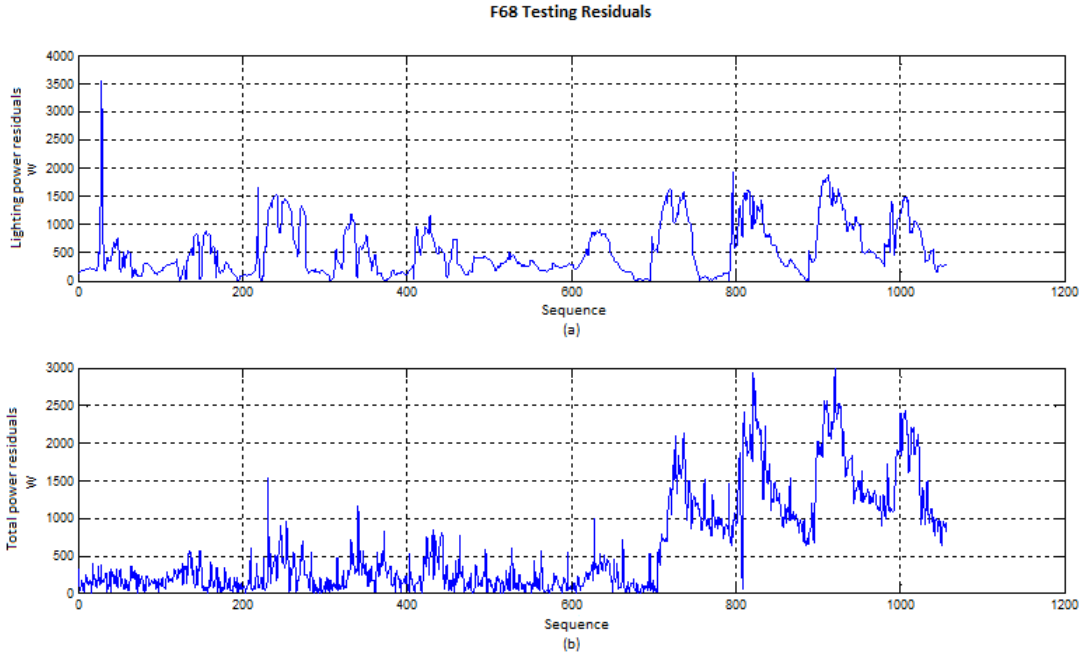

FIGURE 4.7: Testing residuals of building F68 [17]: (a) active electrical power for lighting; (b) total active electrical power

Date	Time	Power residual value [W]	S function value	Mzscore
Peak detection method				
10/06/2013	06:45	3088.68	2911.39	5.82
10/06/2013	07:00	3539.88	3362.59	6.85
12/06/2013	06:30	1670.47	1591.85	2.61
12/06/2013	20:00	1296.86	943.99	1.76
18/06/2013	06:45	1948.57	1648.96	3.24
21/06/2013	07:00	1414.58	936.35	2.03
Date	**Time**	**Power residual value [W]**		**Mzscore**
GESD method				
10/06/2013	06:45	3088.68		5.76
10/06/2013	07:00	3539.88		6.77

TABLE 4.5: Residual analysis and fault detection with ANN BEM for building F68

ANNs training set is characterized by a "fault free" hypothesis, the ANNs testing output allow the estimation of the normal consumption related to the input conditions and an high value of testing residuals represents rightly an anomalous consumption. The CART method algorithm coupled with GESD outliers detection algorithm is particularly robust and accurate in finding the outliers of active electrical power for lighting and total active electrical power. The method allows to determine more correctly if the energy consumption is significantly different from previous consumption with the similar boundary conditions. In the experimental results using K-Means approach some of the identified clusters are impure and outliers are often scattered and difficult to identify (the anomalous energy consumption values are disseminated). The DBSCAN method proved to be particularly suitable for grouping data into clusters characterized by the same density and with similar values. In addition, the method is effective in bringing together all the outliers in a one cluster (cluster-0). In general , it was found

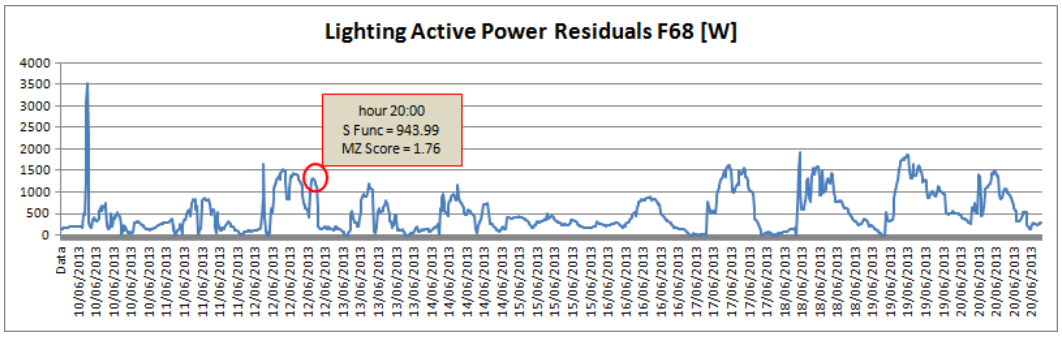

FIGURE 4.8: Example of fault detection through residual analysis of building F68 [17]

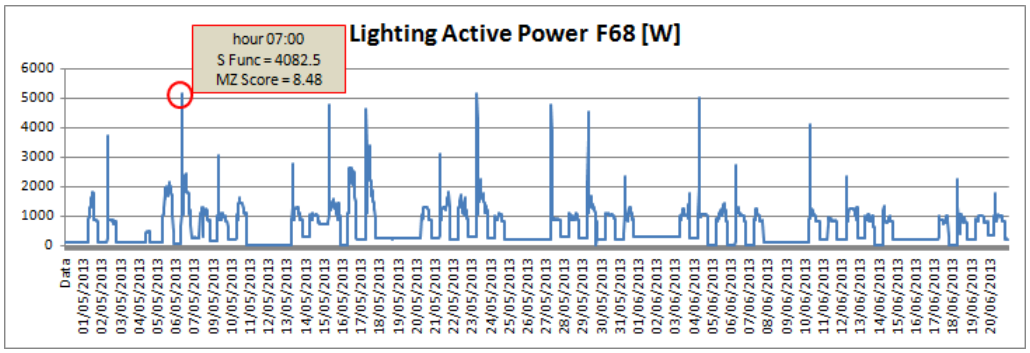

FIGURE 4.9: Example of fault detection through Peak Detection Method application to consumption data of building F68 [17]

that for clustering analysis a suitable splitting of data allows to overcome the inherent limitation of the algorithms (the time can not be considered as input variable in this algorithm). Since weather conditions change considerably on the basis of the period of the year and strongly influence electrical energy consumptions, all the described models have to be suitably built and trained for each season taking in account the different building operation conditions.

4.4 Building energy profiling and trend detection analysis

The fault detection analysis so far conducted in the cluster of buildings of ENEA Casaccia Research Centre included the development of robust methods for the automatic detection of anomalous singular values of electric consumption, taking account of the boundary conditions that determine them. This Section is instead focused on the development of a methodology and algorithms for the detection of anomalous thermal energy trend for the cluster of buildings. The development of processes that automatically identify anomalies connected to the energy demand time trend is important because it is linked to the possibility of obtaining significant energy savings. These methodologies constitute strategic and innovative applications in the fault detection

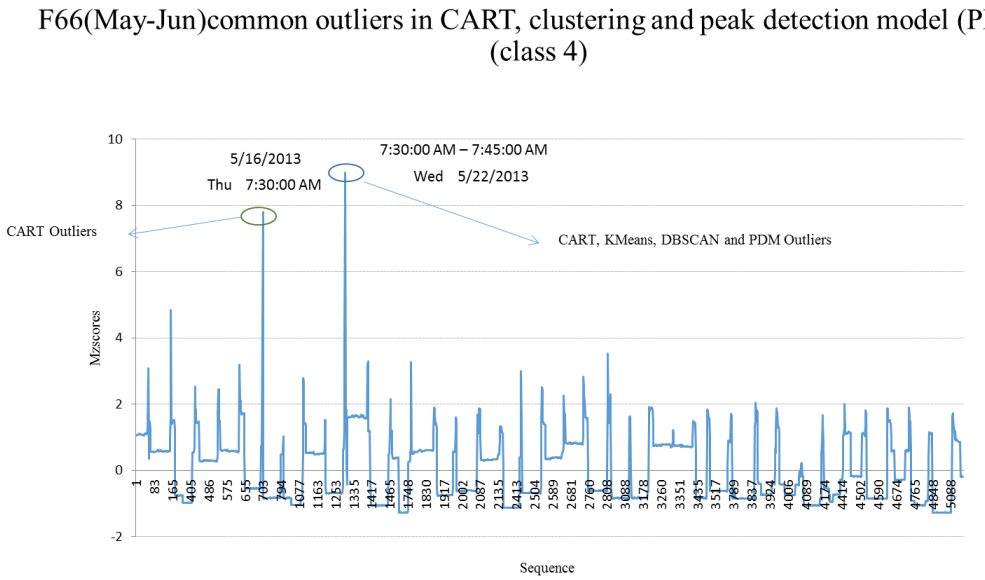

FIGURE 4.10: Mzscores of a class (CART) with evidence of common major outliers detected by CART and K-Means with GESD, DBSCAN and Peak Detection Method (Building F66) [17]

Date	Id Day	Time	Electric active power for lighting [W]	Total electric active power [W]	People presence	Outdoor temparature [°C]	Global solar radiation [W/m^2]
16/05/2013	5	07:30:00	4200.00	5950.29	1	13.40	39
16/05/2013	5	07:45:00	4695.20	7493.10	3	13.90	44
22/05/2013	4	07:30:00	4165.20	7422.79	2	13.90	65
22/05/2013	4	07:45:00	4615.20	6718.20	2	14.00	97
31/05/2013	6	07:30:00	1690.00	4124.50	2	10.40	127
11/06/2013	3	07:15:00	1145.00	3361.19	1	16.10	33
21/06/2013	6	07:30:00	750.00	3633.19	1	20.40	60
27/06/2013	5	07:30:00	815.00	3271.80	2	17.10	35
28/06/2013	6	07:45:00	645.00	4215.39	1	17.00	74
29/05/2013	4	07:30:00	1885.00	6035.79	1	14.10	76

TABLE 4.6: Some common outliers detected by all methods among the cluster of buildings

research area: the anomalous trends of energy consumption are some of the main factors to detect since they could represent symptoms of failure or bad management and then causes of energy waste. In the following Paragraphs the conceptual framework for the methodology development is first described, then an application case of the developed procedure to the thermal energy required for the environmental heating of a building of the cluster (building F66) is presented.

4.4.1 Methodology framework

The first part of the process developed (Phase 1 and Phase 2 illustrated in Fig. 4.13) had the goal of identifying the typical and fault-free daily consumption profiles. These profiles are used as reference or benchmark trends in order to identify the condition of "anomalous" for the testing energy demand time trend. The data set was processed in

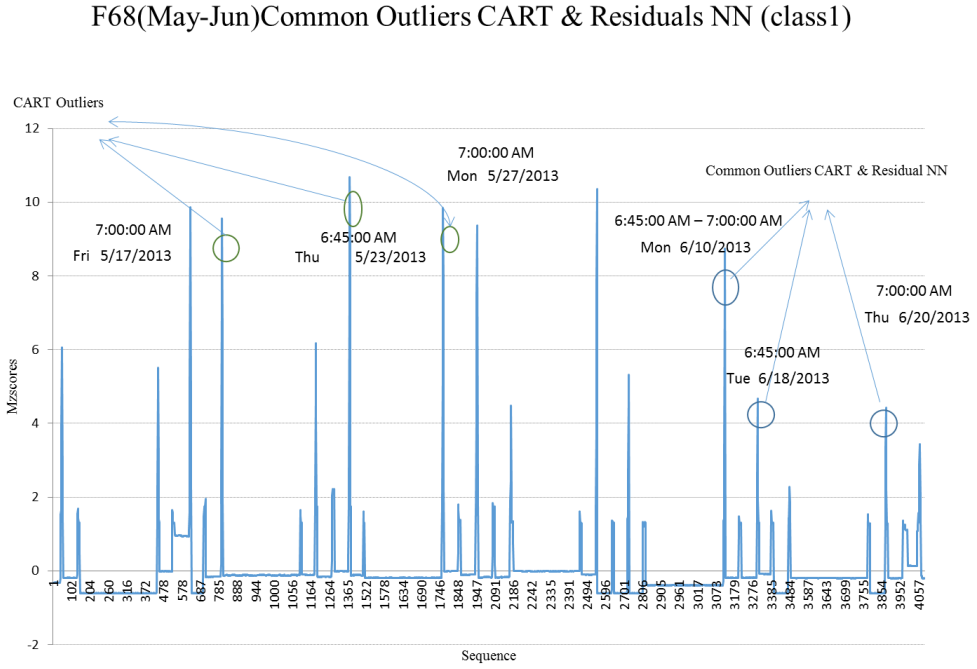

FIGURE 4.11: Mzscores of a class (CART) with evidence of common major outliers identified by ANN residuals (GESD) and CART (GESD) (Building F68) [17]

order to obtain hourly average thermal power values. For this purpose a "data preparation" analysis (data cleaning, missing data covering and outlier detection) was initially conducted on the data set. Then a descriptive statistical analysis was carried out in order to identify correlations between the variables, variation range, occurrence frequencies and a visualisation analysis of the hourly average thermal power values was also realized through box plots and scatter plot representations. Basing on the results obtained from these previous steps, the data set was partitioned in three different sub-data sets. The K-Means clustering algorithm (already presented in Section 4.3.1) was applied to each sub-data set, considering for each day the hourly average thermal power as the only variable. This step allowed to identify, for each sub-data set, homogeneous groups of thermal power profiles that could be labeled through a categorical variable relative to the reference cluster. Successively some dimensionless factors capable of synthetically representing the shape of a daily profile of hourly average power were identified. These factors are based on the ratio between typical power or energy of the profile under observation. Therefore, for each sub-data set and for each cluster, the "shape" factors for each hourly average thermal power daily profile were calculated. For each sub-data set a classification tree through the CART algorithm (also introduced in Section 4.3.1) was then developed, using as predictors the shape factors and as target (or variable to classify) the reference cluster. In other words, on the basis of the shape factors values corresponding to the profile under observation the classifier is able to

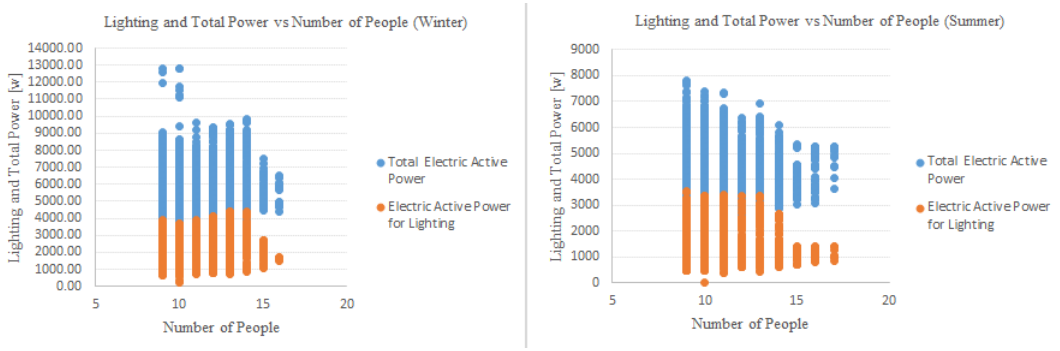

FIGURE 4.12: Scatter plots showing active electrical power for lighting and total active electrical power vs number of people [17]

associate it to one or more reference cluster. The calculation of the median profile of the thermal power hourly profiles within each end node of each classification tree led to the determination of the benchmark profiles. Within each end node the confidence interval with a probability of 95% was also calculated, resulting in the determination of an upper and lower profile for the benchmark profile representing its uncertainty.

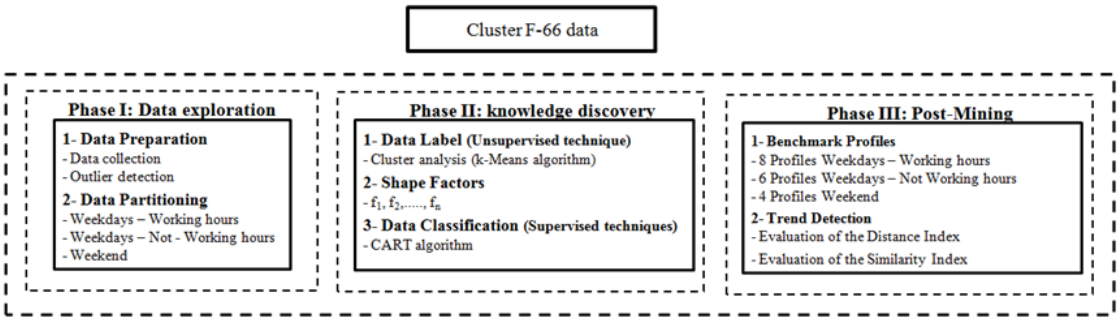

FIGURE 4.13: Logic framework of the trend detection process

In order to activate the trend detection process, the procedure requires that the testing profile through the classifier is associated, and then compared, to one of the previously identified benchmark profiles. Once the benchmark profile with its relative uncertainty is decided, the trend detection analysis is based on the evaluation of two different indicators that define and quantify the potential anomaly of the trend (Phase 3 in Fig. 4.13). The first indicator involves calculating the norm of residuals and indicates the deviation of the thermal power absolute values of the testing profile. The second indicator instead is based on the evaluation of the incidence angle for each hour between the testing profile and the benchmark profile. The possibility that for every hour the benchmark profile and testing profile present or opposing trends (for example, one descending and the other ascending) or diverging trends (same sign of the angular coefficients of the profiles but different values) occurs through this second indicator.

4.4.2 Experimentation and results discussion

The details of the phases of the trend detection methodology briefly described above are provided below also through an application case study. In particular, the heating power required during some months of the winter season 2014-2015 was analyzed. Building F66 belonging to the cluster of buildings of ENEA Casaccia (see Section 4.2) was used as reference.

Identification of similar consumption profiles through clustering analysis

The data set was first object of a data preparation procedure. In particular, in order to obtain a data set without outliers and, finally, fault free benchmark profiles, all the outliers that make a thermal power profile an anomalous profile were eliminated, i.e. infrequent values or values affected by measurement errors. This procedure was carried out through the use of statistical techniques (outlier detection methods).

Once obtained a robust data set, a clustering analysis using the k-Means algorithm was applied with the purpose of identifying groups of similar days with reference to the hourly average daily profile of thermal power required for environmental heating. The data set was previously divided into three distinct sub-data sets: the first related to the working hours (from 8:00 to 17:00) of the working days (Monday-Friday), the second related to the non-working hours (from 17:00 to 8:00) of the working days, the third related to weekend and public holiday days. This subdivision was made by observing the power profiles that showed significantly different characteristics throughout the three periods. After a sensitivity analysis regarding the variables which influence the heating energy consumption, the nature of the available data revealed that the more correct clustering operation could base on the only variable constituted by the hourly average thermal power. The analysis of the available data is in fact resulted in a weak relationship between the thermal power required for heating and the other monitored variables (internal temperature, external temperature, solar radiation, occupancy). The k-Means algorithm proved particularly effective in identifying homogeneous clusters of typical profiles for each sub-data set analyzed. The number of identified clusters is 3 for data set relative to working weekdays during working hours, 3 for working weekdays during non-working hours and to 2 for public holidays and weekends.

Figures 4.14, 4.15 and 4.16 present the heating power similar profiles grouped into one of the identified clusters for each of the sub-data sets, and in particular for working weekdays during working hours, working weekdays during non-working hours and public holidays and weekends respectively. Considering these Figures it's evident that the cluster algorithm is highly effective in grouping similar days in terms of power profiles for each sub-data set.

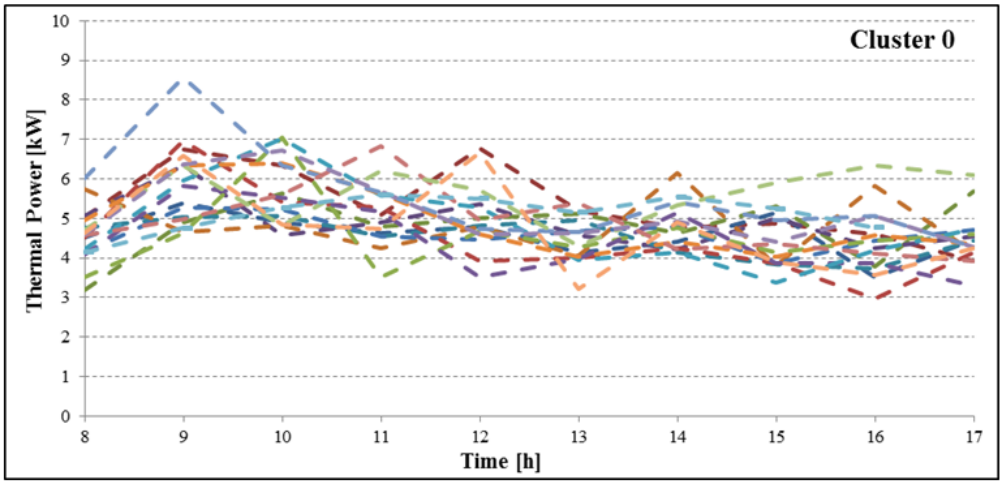

FIGURE 4.14: Hourly average thermal power profiles belonging to a reference cluster (working weekdays during working hours)

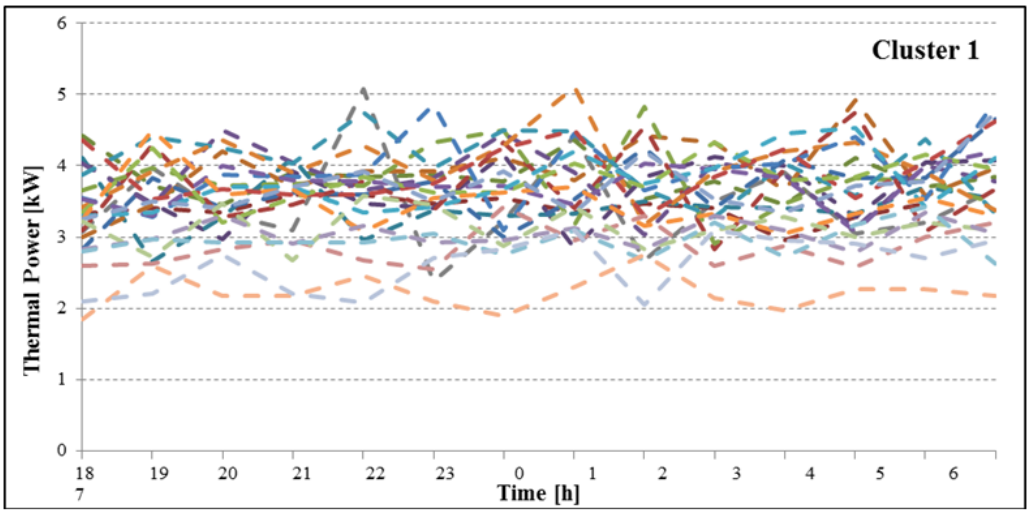

FIGURE 4.15: Hourly average thermal power profiles belonging to a reference cluster (working weekdays during non-working hours)

The clustering algorithm's effectiveness is also demonstrated by the SVD (Singular Value Decomposition) values, shown in Figures 4.17 and 4.18 for working weekdays during working hours and working weekdays during non-working hours respectively. It is possible to observe that objects within each cluster are characterized by high similarity, while they are different between a cluster and another. The identification of the reference clusters for each sub data set was a preliminary and fundamental operation for the construction of a classification tree. In fact labeling the similar profiles with the corresponding reference cluster allowed to use this categorical variable in the classification tree.

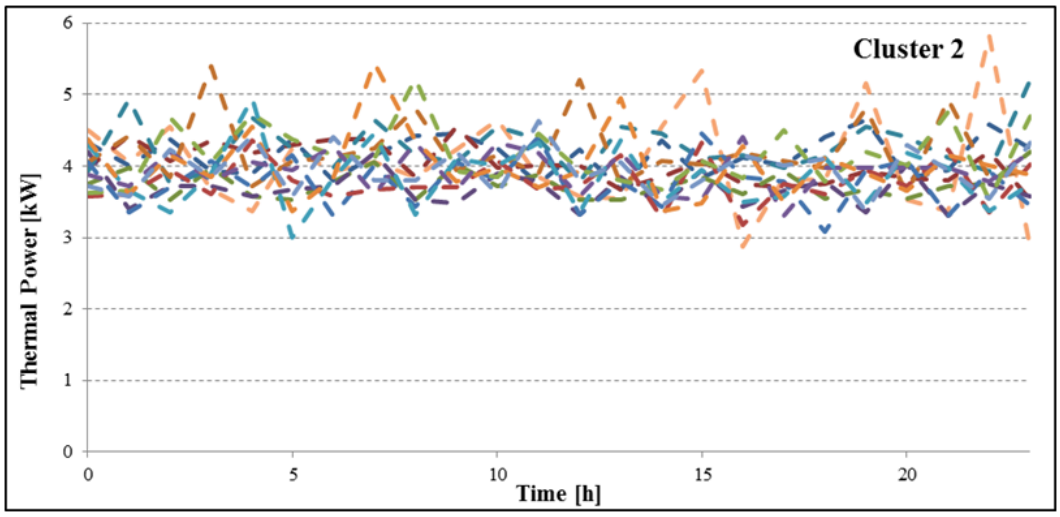

FIGURE 4.16: Hourly average thermal power profiles belonging to a reference cluster (public holidays and weekends)

Shape factors evaluation

In order to identify the variables useful for leading the supervised classification process, several factors capable of concisely representing the shape of the hourly average power profiles for each sub-data set were defined on the basis of a sensitivity analysis. The defined shape factors are presented in Tables 4.7, 4.8 and 4.9 with respect to the three analyzed sub-data sets. The shape factors are dimensionless indicators ranging from 0 to 1 characterized by the ratio between hourly average power or energy of the daily profile.

Factor	Definition	Acquisition period
Daily P_{avg}/P_{max}	$f_1 = P_{avg,day,w}/P_{max,day,w}$	Working hours (10 h, 8:00-18:00)
Daily P_{min}/P_{max}	$f_2 = P_{min,day,w}/P_{max,day,w}$	Working hours (10 h, 8:00-18:00)
Daily P_{min}/P_{avg}	$f_3 = P_{min,day,w}/P_{avg,day,w}$	Working hours (10 h, 8:00-18:00)
Work Impact	$f_4 = 10/24 \cdot P_{avg,work}/P_{avg,day}$	1 day (working hours 10 h, 8:00-18:00)
Lunch Impact	$f_5 = 2/24 \cdot P_{avg,lunch}/P_{avg,day}$	1 day (lunch hours 2 h, 12:00-14:00)

TABLE 4.7: Shape factors for working weekdays during working hours

Factor	Definition	Acquisition period
Daily P_{avg}/P_{max}	$f_1 = P_{avg,day,nw}/P_{max,day,nw}$	Non-working hours (14 h, 18:00-8:00)
Daily P_{min}/P_{max}	$f_2 = P_{min,day,nw}/P_{max,day,nw}$	Non-working hours (14 h, 18:00-8:00)
Daily P_{min}/P_{avg}	$f_3 = P_{min,day,nw}/P_{avg,day,nw}$	Non-working hours (14 h, 18:00-8:00)
Night Impact	$f_{4'} = 14/24 \cdot P_{avg,night}/P_{avg,day}$	1 day (non-working hours 14 h, 18:00-8:00)

TABLE 4.8: Shape factors for working weekdays during non-working hours

In particular f_1 factor is defined as the ratio between the average and the maximum daily powers, f_2 factor as the ratio between the minimum and the maximum daily powers and f_3 factor as the ratio between the minimum and the average daily powers. f_4 and f_5 factors instead describe the thermal power impact of working period and lunch period respectively on the daily profile: f_4 factor is defined as the product of

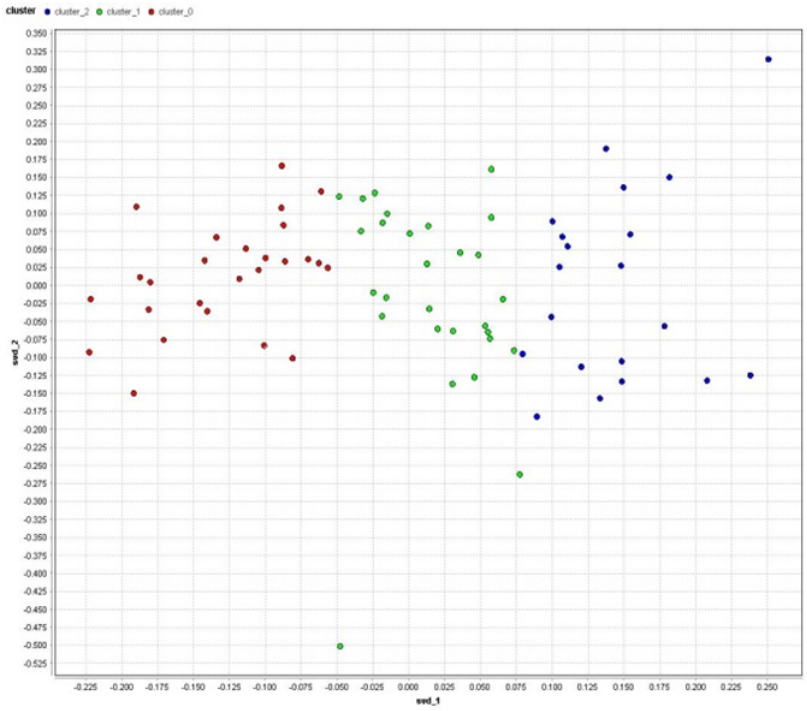

FIGURE 4.17: Objects representation within an identified cluster (working weekdays during working hours)

Factor	Definition	Acquisition period
Daily P_{avg}/P_{max}	$f_1 = P_{avg,day}/P_{max,day}$	1 day
Daily P_{min}/P_{max}	$f_2 = P_{min,day}/P_{max,day}$	1 day
Daily P_{min}/P_{avg}	$f_3 = P_{min,day}/P_{avg,day}$	1 day

TABLE 4.9: Shape factors for public holidays and weekends

the ratio of the average power during the working hours and the daily average power, and the ratio between the number of working hours and the number of hours in a day, while the f_5 factor as the product of the ratio of the average power during the lunch hours and the daily average power, and the ratio between the number of lunch hours and the number of hours in a day. The number of working and lunch hours was obtained through the direct analysis of the available data set. Finally the $f_{4'}$ factor (night impact) is defined as the product of the ratio of the average power during the non-working hours and the daily average power, and the ratio between the number of non-working hours and the number of hours in a day.

Through testing analysis, the dimensionless factors described above proved excellent descriptors of the shape of the thermal power daily profiles. The shape factors were calculated hour by hour for each thermal power profile relatively to each sub-data set considered and then used as variables (predictors) to classify the profiles in relation to the identified clusters. The construction of the classifier is illustrated in the next Section.

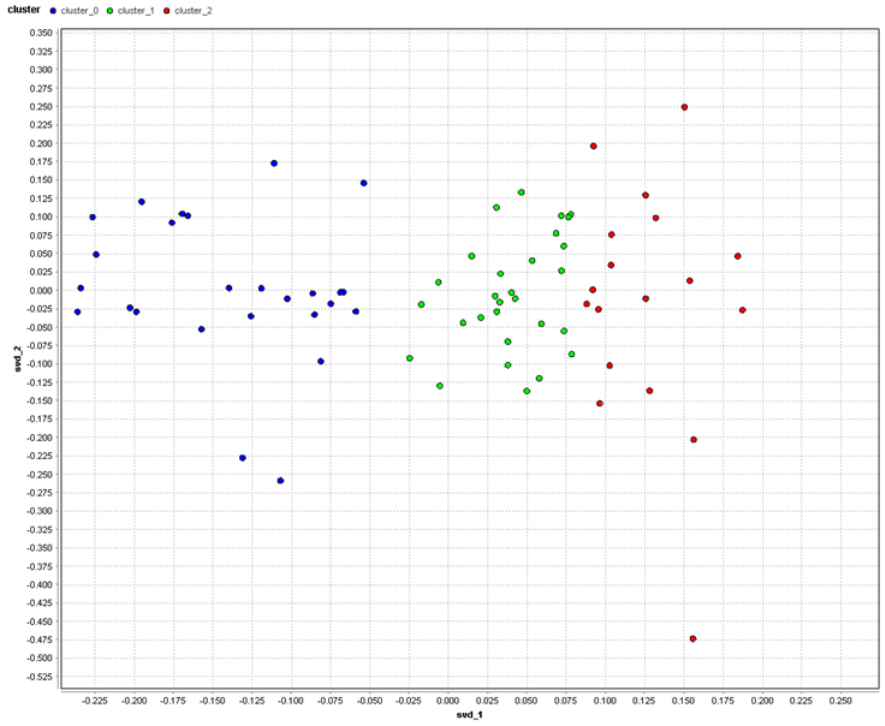

FIGURE 4.18: Objects representation within an identified cluster (working weekdays during non-working hours)

Construction of the classification trees

In order to automate the trend detection process, the next step was to develop a classifier that, on the basis of representative and explanatory variables (predictors), allows to identify one or more clusters of similar power profiles previously characterized. In this phase for each sub-data set a CART classification tree was built. The classification trees allow to estimate the categorical variable linked to the cluster ("Cluster No.") on the basis of the values of the shape factors introduced above. In other words, on the basis of the shape factors each CART classifier identify the homogeneous group of similar profiles belonging to one or more clusters. Simple decision rules to guide the classification process were found out and are listed in Tables 4.10, 4.11 and 4.12 for the three sub-data set analyzed.

The end nodes represent sets of profiles with homogeneous characteristics that can also come from different clusters. Once grouped the profiles belonging to each end node, the benchmark profile was identified by calculating for each hour the median of the average power values of these profiles. In this way a median benchmark profile corresponds to each end node. In order to consider the dispersion of the hourly power values within each end node, a confidence interval was also evaluated representative of the uncertainty band and defined by an upper profile and a lower profile surrounding the benchmark one. The following figures illustrate the benchmark profiles and the relative uncertainty bands for each end node and for each sub-data set. In particular

Rule	Definition	Profile
1	$f_4 > 0.4444$ and $f_3 > 0.8404$	1
2	$f_4 > 0.4444$ and $f_3 > 0.8404$ and $f_5 > 0.0988$	2
3	$f_4 <= 0.4444$ and $f_4 > 0.4302$	3
4	$f_4 <= 0.4302$ and $f_2 > 0.7517$	4
5	$f_4 <= 0.4302$ and $f_2 <= 0.7517$ and $f_4 <= 0.4115$	5
6	$f_4 <= 0.4444$ and $f_3 <= 0.8404$ and $f_5 <= 0.0988$	6
7	$f_4 <= 0.4302$ and $f_2 <= 0.7517$ and $f_4 > 0.4115$ and $f_5 <= 0.0867$	7
8	$f_4 <= 0.4302$ and $f_2 <= 0.7517$ and $f_4 > 0.4115$ and $f_5 > 0.0867$	8

TABLE 4.10: Classification rules: working weekdays during working hours

Rule	Definition	Profile
1	$f_2 <= 0.5920$	1
2	$f_2 > 0.5920$ and $f_1 > 0.9125$	2
3	$f_2 > 0.5920$ and $f_1 <= 0.9125$ and $f_3 <= 0.7747$	3
4	$f_2 > 0.5920$ and $f_1 <= 0.9125$ and $f_3 <= 0.8204$ and $f_3 > 0.7747$	4
5	$f_2 > 0.5920$ and $f_1 <= 0.9125$ and $f_3 > 0.8204$ and $f_2 <= 0.7422$	5
6	$f_2 > 0.5920$ and $f_1 <= 0.9125$ and $f_3 > 0.8204$ and $f_2 > 0.7422$	6

TABLE 4.11: Classification rules: working weekdays during non-working hours

these benchmark profiles were identified: 8 benchmark profiles for the sub-data set related to weekdays and working hours (Fig. 4.19, 4.20, 4.21, 4.22, 4.23, 4.24, 4.25, 4.26); 6 benchmark profiles for the sub-data set related to weekdays and non-working hours (Fig. 4.27, 4.28, 4.29, 4.30, 4.31, 4.32); 4 benchmark profiles for the sub-data set related to public holidays and weekends (Fig. 4.33, 4.34, 4.35, 4.36). Furthermore, in order to verify the trend detection procedure, some testing power profiles, analyzed in the next Section, were identified. For the testing profiles the shape factors were evaluated and on the basis of the classification rules they were associated to the respective benchmark profile. The introduced testing profiles are represented in Fig. 4.20, 4.24, 4.26, 4.29, 4.31, 4.32, 4.33, 4.34, 4.35 with the benchmark profiles to which they have to be compared and to which they were associated through the classifier. In these cases the residuals profile was also calculated as the difference between the power of the testing profile and that relative to the benchmark profile for each hour.

Anomalous trend detection procedure

Once identified the benchmark profiles and the relative uncertainty bands, the trend detection process of a hourly thermal power profile includes two phases:

- the current profile is first associated with a benchmark one through the classifier;

Rule	Definition	Profile
1	$f_3 <= 0.7788$	1
2	$f_3 > 0.7788$ and $f_1 > 0.8957$	2
3	$f_3 > 0.7788$ and $f_1 <= 0.8957$ and $f_2 <= 0.7517$	3
4	$f_3 <= 0.7788$ and $f_1 <= 0.8957$ and $f_2 > 0.7517$	4

TABLE 4.12: Classification rules: public holidays and weekends

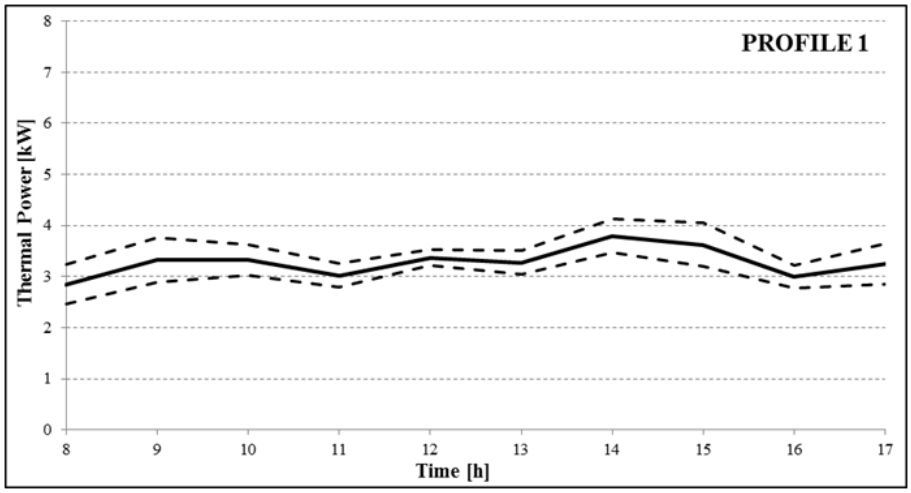

FIGURE 4.19: Hourly average power benchmark profile 1 and uncertainty band (working weekdays and working hours)

- subsequently the profile under observation is compared with the benchmark one to determine the possible "anomaly".

In particular, the comparison between the two profiles is based on the evaluation of two different indicators through which it is possible to define and quantify the potential trend anomaly.

The first indicator (Distance Index, DI) includes the calculation of the residuals norm (square root of the residuals squared sum between benchmark profile and current profile) and provides information on the deviation of the absolute values of thermal power assumed by the testing profile (Eq. 4.8).

$$DI = \sqrt{\sum_{i=1}^{n}(y_{i,bench} - y_{i,test})^2} \tag{4.8}$$

In Eq. 4.8 n are the considered hourly average values of thermal power, $y_{i,bench}$ is the i-th value of the benchmark profile and $y_{i,test}$ is the i-th value of the testing profile.

The second indicator (Similarity Index, SI) consists in the evaluation of the similarity measure between two trends as described in [27, 83, 84]. This measure is the weighted average of the similarity matches S_i between the primitives of the two trends on the

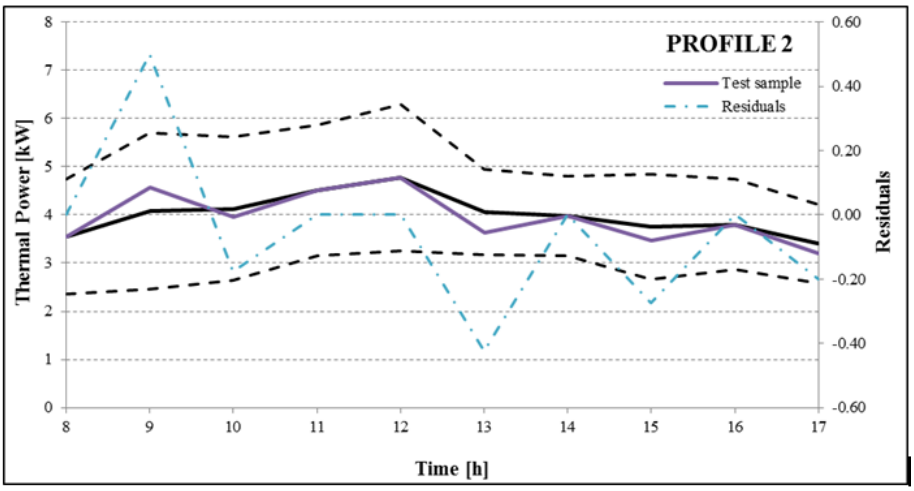

FIGURE 4.20: Hourly average power benchmark profile 2, uncertainty band and testing profile (working weekdays and working hours)

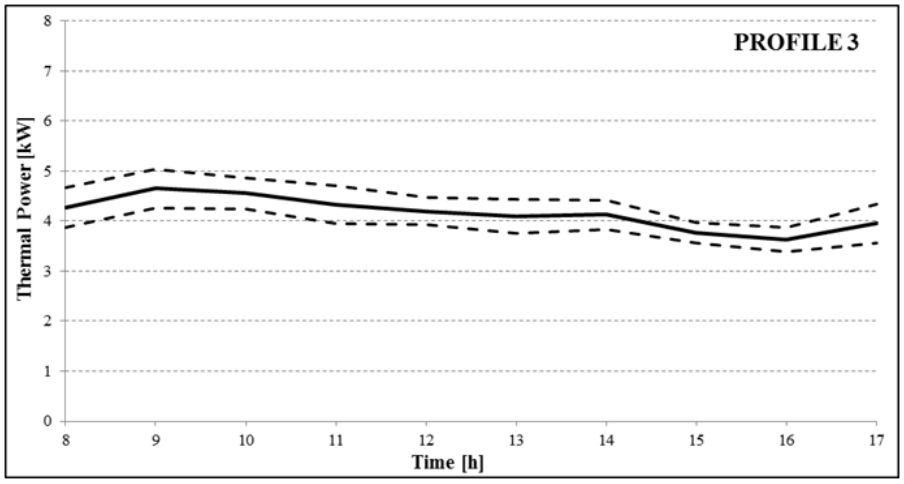

FIGURE 4.21: Hourly average power benchmark profile 3 and uncertainty band (working weekdays and working hours)

different intervals Dt_i of the time period in which the similarity measure has to be calculated (Eq. 4.9).

$$SI = \frac{\sum_{i=1}^{n} S_i \cdot Dt_i}{\sum_{i=1}^{n} Dt_i} \tag{4.9}$$

In this case study the intervals Dt_i always correspond to 1 time unit (1 hour), consequently the similarity measure SI is simply given by the arithmetic average of the similarity matches S_i. It was decided to base the calculation of the similarity matches S_i on the evaluation of the cosine of the incidence angle for each hour between the testing profile y_{test} and the benchmark profile y_{bench}. The incidence angle α can be derived

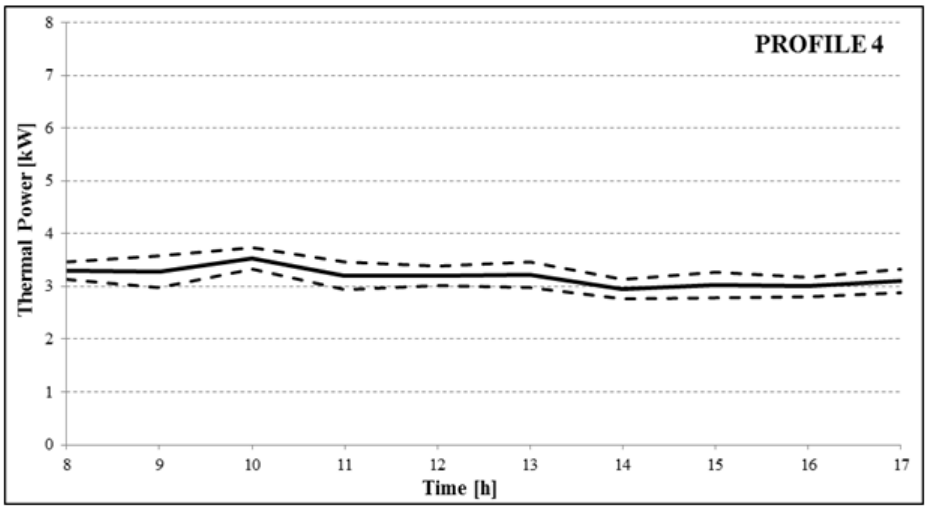

FIGURE 4.22: Hourly average power benchmark profile 4 and uncertainty band (working weekdays and working hours)

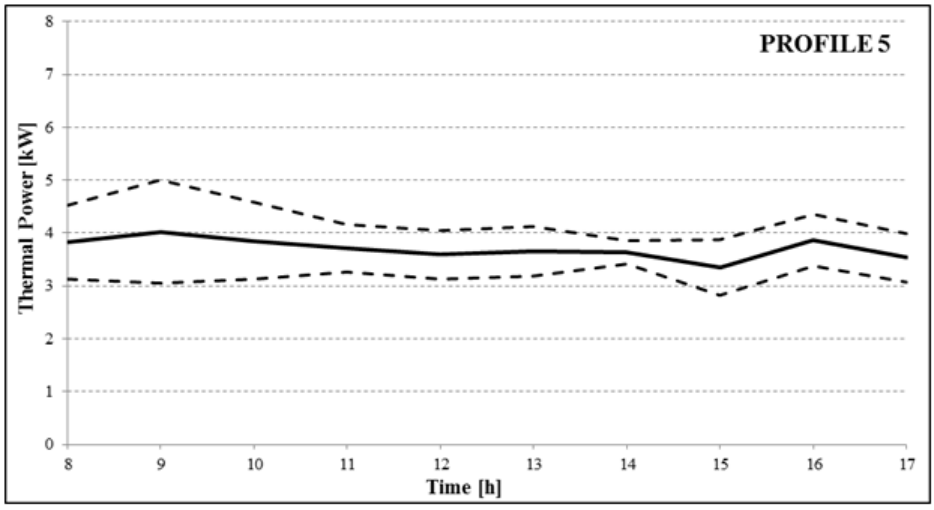

FIGURE 4.23: Hourly average power benchmark profile 5 and uncertainty band (working weekdays and working hours)

through the following relation (Eq. 4.10):

$$\alpha = \arctan\left(\frac{m_{test} - m_{bench}}{1 + m_{test} \cdot m_{bench}}\right) \tag{4.10}$$

where m_{test} and m_{bench} indicate the angular coefficients of the aforesaid profiles respectively. More precisely, the similarity matches S_i are calculated as in the following equation (Eq. 4.11):

$$S_i = \begin{cases} 0, & \text{if } m_{test} \text{ and } m_{bench} \text{ have opposite signs} \\ \cos\alpha, & \text{otherwise} \end{cases} \tag{4.11}$$

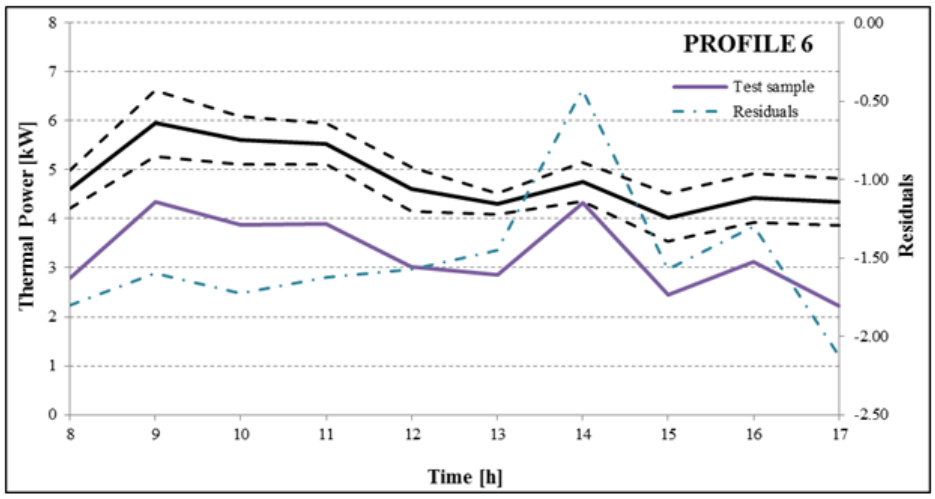

FIGURE 4.24: Hourly average power benchmark profile 6, uncertainty band and testing profile (working weekdays and working hours)

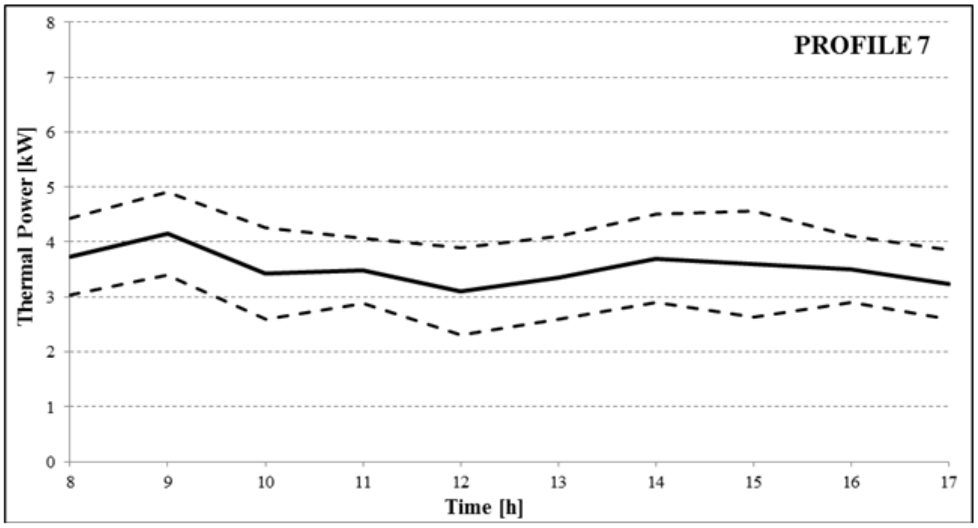

FIGURE 4.25: Hourly average power benchmark profile 7 and uncertainty band (working weekdays and working hours)

Therefore if during an hour opposite trends between benchmark profile and testing profile occur (i.e. a profile increasing and the other decreasing) the corresponding similarity match S_i takes value 0, in all other cases the value given by the incidence angle cosine between the two profiles variable between 0 (when only one of the profiles is constant) and 1 (in the case of profiles with the same trend defined by the angular coefficients). In this way the Similarity Index SI, ranging from 0 to 1, considers altogether if for each hour occur or opposite trends between the benchmark profile and the testing profile or diverging trends (same sign of the angular coefficients of the profiles but different values) and it allows to briefly express how much the trends of the two profiles are similar.

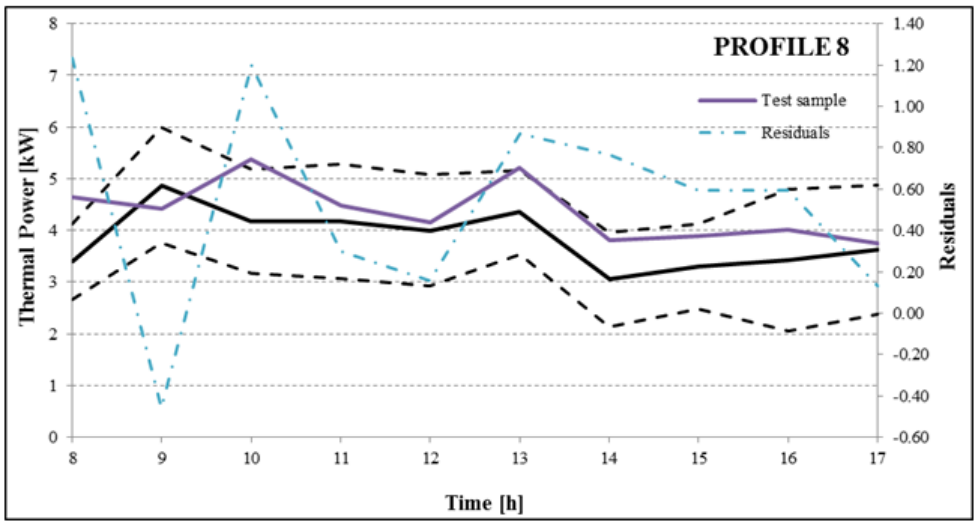

FIGURE 4.26: Hourly average power benchmark profile 8, uncertainty band and testing profile (working weekdays and working hours)

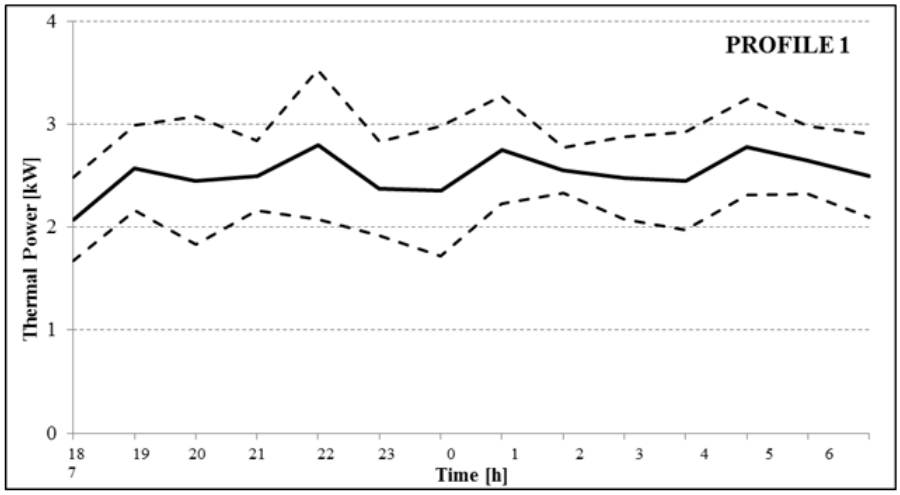

FIGURE 4.27: Hourly average power benchmark profile 1 and uncertainty band (working weekdays and non-working hours)

Once described the indices, the procedure that allows to define and quantify the potential trend anomaly can be fixed. A trend of hourly thermal power is anomalous if:

- the Distance Index of the testing profile is anomalous, i.e. it is greater than the maximum Distance Index of the upper and lower uncertainty profiles. In this case the trend anomaly is a direct and evident finding because the values of the testing trend differ greatly from those of the benchmark one and therefore it is not necessary to assess the Similarity Index. Anyway the Similarity Index can provide indications on the likeness of the profiles trends;

or

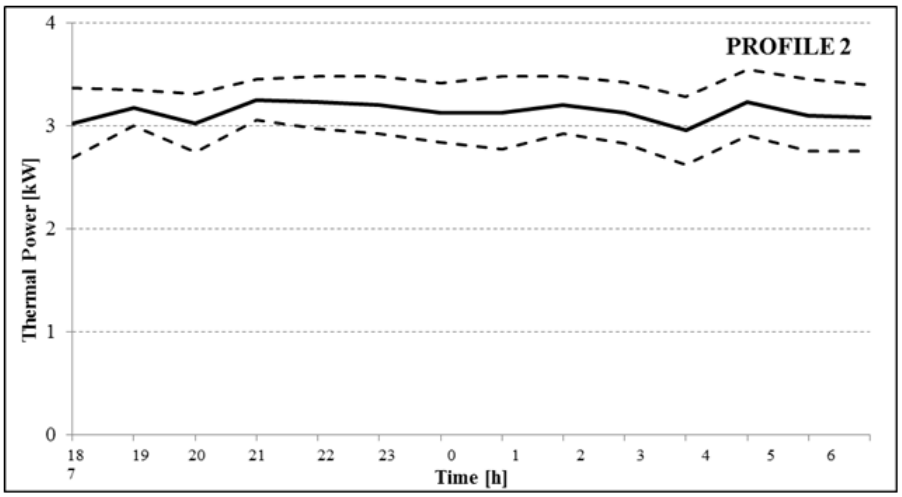

FIGURE 4.28: Hourly average power benchmark profile 2 and uncertainty band (working weekdays and non-working hours)

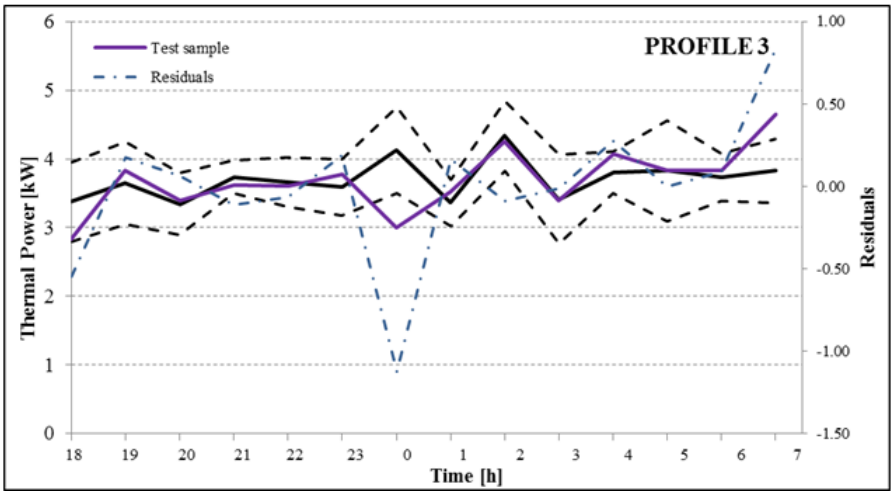

FIGURE 4.29: Hourly average power benchmark profile 3, uncertainty band and testing profile (working weekdays and non-working hours)

- the Distance Index of the testing profile is not anomalous but the Similarity Index is anomalous, i.e. it is lower than a threshold value set at 0.5.

The methodology described above was applied to the testing profiles introduced in the previous Section in order to verify its validity. In Table 4.13 are shown the values of Distance and Similarity Indices of each testing profile and the consequent outcome of the trend detection analysis obtained by the comparison with the corresponding benchmark profile and the related uncertainties.

As also verifiable from the direct observation of the profiles, the profiles 6 (Working Weekdays Working Hours Fig. 4.24), 5 (Working Weekdays Non-Working Hours Fig. 4.31), 1 and 3 (Public Holidays and Weekends Fig. 4.33 and 4.35) are anomalous since the Distance Indices report a significant deviation from the benchmark profiles. In the Profile 5 case also the Similarity Index indicates an anomalous testing trend compared

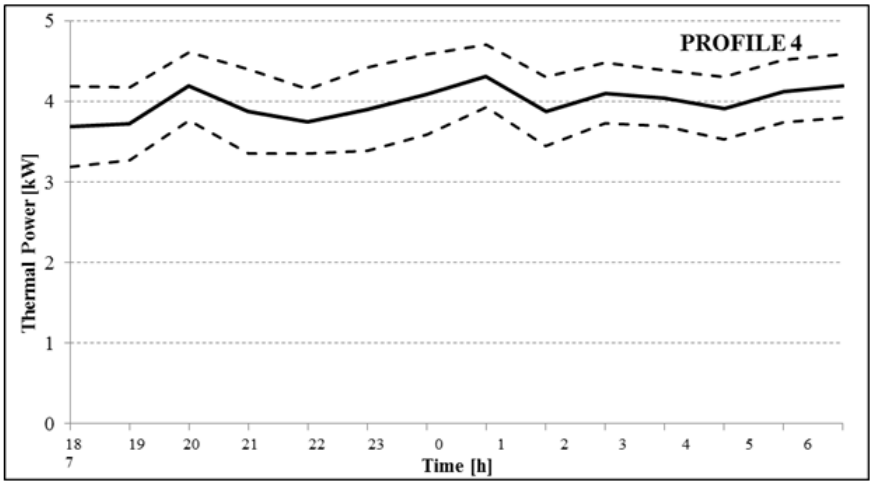

FIGURE 4.30: Hourly average power benchmark profile 4 and uncertainty band (working weekdays and non-working hours)

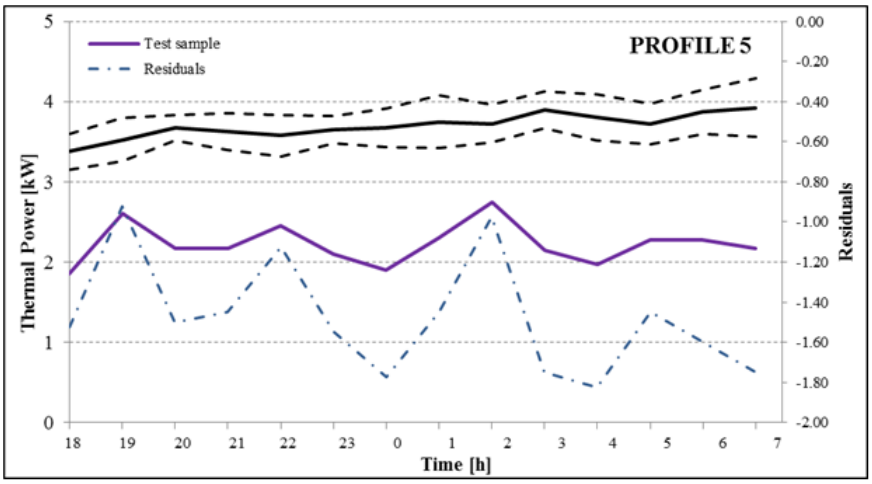

FIGURE 4.31: Hourly average power benchmark profile 5, uncertainty band and testing profile (working weekdays and non-working hours)

to the benchmark one.

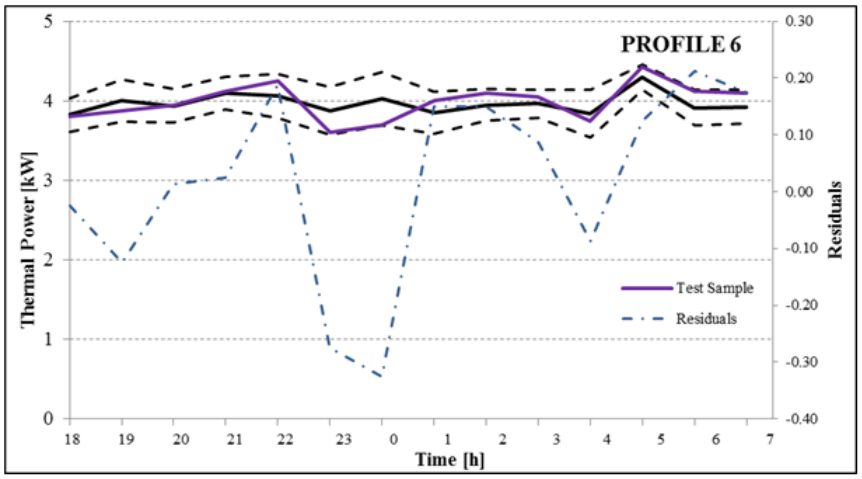

FIGURE 4.32: Hourly average power benchmark profile 6, uncertainty band and testing profile (working weekdays and non-working hours)

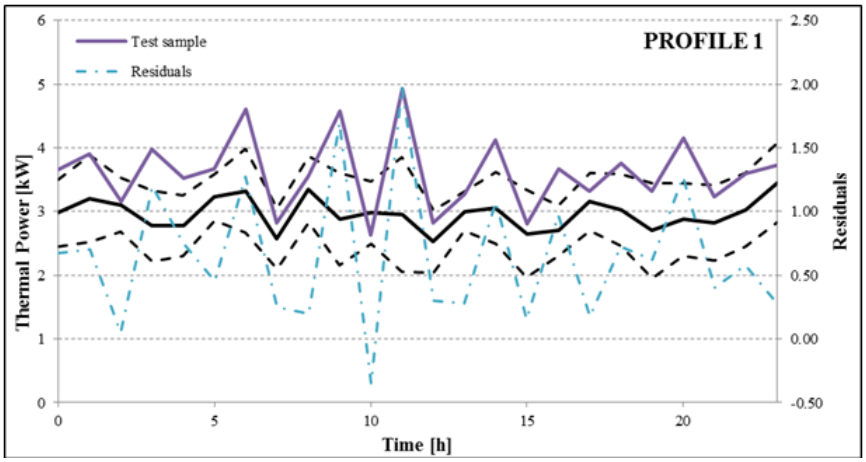

FIGURE 4.33: Hourly average power benchmark profile 1, uncertainty band and testing profile (weekends and public holidays)

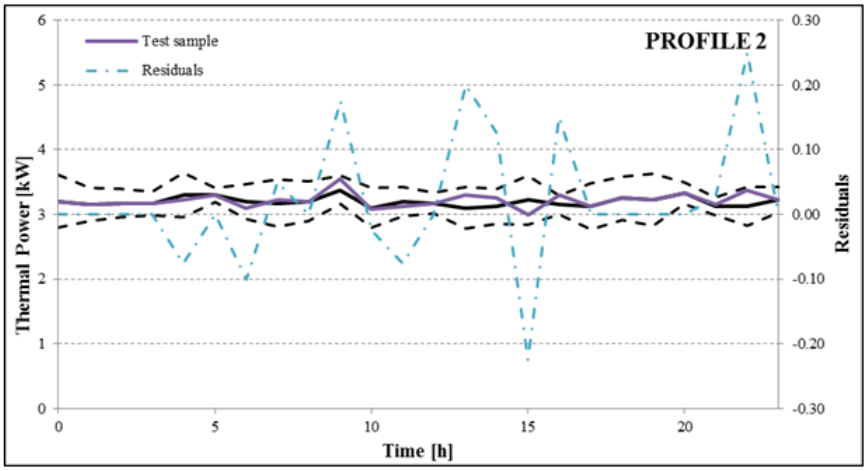

FIGURE 4.34: Hourly average power benchmark profile 2, uncertainty band and testing profile (weekends and public holidays)

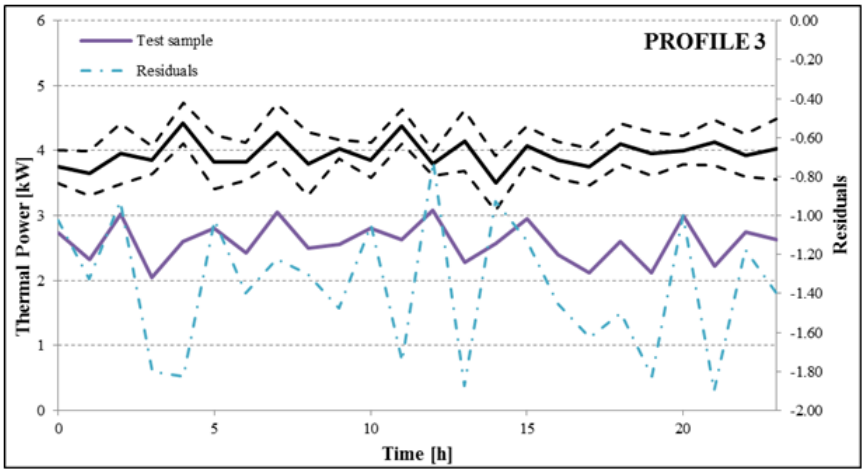

FIGURE 4.35: Hourly average power benchmark profile 3, uncertainty band and testing profile (weekends and public holidays)

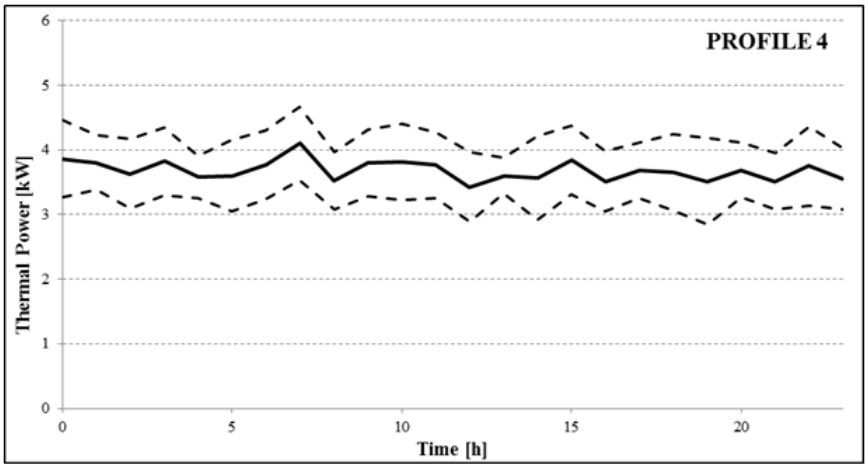

FIGURE 4.36: Hourly average power benchmark profile 4 and uncertainty band (weekends and public holidays)

		Distance Index	Similarity Index	Anomalous Profile
WORKING WEEKDAYS WORKING HOURS	**PROFILE 2**	**0.76**	**0.76**	NO
	UPPER UNCERTAINTY	3.83	-	
	LOWER UNCERTAINTY	3.83	-	
	PROFILE 6	**4.99**	**0.83**	YES
	UPPER UNCERTAINTY	1.46	-	
	LOWER UNCERTAINTY	1.46	-	
	PROFILE 8	**2.31**	**0.54**	NO
	UPPER UNCERTAINTY	3.29	-	
	LOWER UNCERTAINTY	3.29	-	
WORKING WEEKDAYS NON-WORKING HOURS	**PROFILE 3**	**1.57**	**0.65**	NO
	UPPER UNCERTAINTY	1.85	-	
	LOWER UNCERTAINTY	1.85	-	
	PROFILE 5	**5.61**	**0.29**	YES
	UPPER UNCERTAINTY	0.96	-	
	LOWER UNCERTAINTY	0.96	-	
	PROFILE 6	**0.62**	**0.61**	NO
	UPPER UNCERTAINTY	0.91	-	
	LOWER UNCERTAINTY	0.91	-	
WEEKENDS AND PUBLIC HOLIDAYS	**PROFILE 1**	**4.15**	**0.62**	YES
	UPPER UNCERTAINTY	2.81	-	
	LOWER UNCERTAINTY	2.81	-	
	PROFILE 2	**0.50**	**0.56**	NO
	UPPER UNCERTAINTY	1.36	-	
	LOWER UNCERTAINTY	1.36	-	
	PROFILE 3	**6.87**	**0.54**	YES
	UPPER UNCERTAINTY	1.67	-	
	LOWER UNCERTAINTY	1.67	-	

TABLE 4.13: Trend detection analysis of the testing profiles

Chapter 5

Experimentation of fault detection and diagnosis analysis of building electrical consumptions

5.1 Introduction

Energy and economic efficiency are the main targets of BEMS, therefore looking for a valid method for fault detection and diagnosis (FDD) to instruct operation and maintenance is a main mission. At present FDD is mainly based on collecting signals whose analysis and interpretation is left to human experts. Unfortunately, the number of signals is often very high and the relations among them highly non-linear. Thus, human operators are often not capable to detect in time a fault. This is a very critical point, because the early detection of a fault may prevent the building from serious problems.

In the energy optimization field, the evaluation of building actual energy consumptions is a demandable and emerging area of building energy analysis. Therefore, developing automatic, accurate and reliable FDD methods is necessary in order to ensure the optimal operations of systems and to save energy. Research on fault detection and isolation in automated processes has been active over several decades. Different intelligent methods have been used to obtain useful information from building energy consumption data for FDD analysis. A number of methodologies and procedures for optimizing real-time performance, automated fault detection and fault isolation were developed in the IEA ECBCS Annex 25 [75]. Many of these diagnosis methods are later demonstrated in real buildings in the IEA ECBCS Annex 34 [53], which focused on computer-aided fault detection and diagnosis. Annex 40 [134] encompasses commissioning process, building control system, component level models, simulation models at the building level for commissioning. The Executive Committee for the same implementing agreement published Annex 47-report 4 [88] on the use of flow charts and data models in the practice and research of initial commissioning of advanced and low energy building systems in order to improve their operating performance.

Many FDD tools are based on combinations of predicted building performance models and a knowledge-based system. They compare the performances of all or part of the building over a period of time to what is expected, in this way incorrect operation or unsatisfactory performances can be detected. The expected performances can be assumed, desired and model-based [29]. Lai, Magoules, & Lherminier [64], for example, introduce the use of Support Vector Machine (SVM) as a data mining tool applied to buildings energy consumption data from a measurement campaign for the prediction of the electrical consumption of a residential building. Early attempts at displaying energy consumption data for the energy optimization involved the use of graphs to inform the user on the trends within their building systems [13, 41, 42, 40, 110]. The graphical indices can be used to analyze building energy consumption data and to check for errors, but they are usually laborious. Katipamula & Brambley [57, 58] classified the FDD methods for building energy systems and highlighted the strength and weakness of each approach. Most of the research related to FDD focused on the component-level faults [32, 44, 136, 143], and few researchers [141, 30, 48, 71] discussed the FDD strategy for whole building lighting and HVAC systems energy consumption.

A number of papers on the application of artificial intelligence for FDD have been published [70, 140, 94]. Liang, & Due [74] propose an approach that combines the model-based FDD method and the Support Vector Machine (SVM) method for the detection and classification of faults in the HVAC systems.

In the previous Chapter some examples of ANN application for fault detection analysis were presented [30, 85, 118]. In literature many other works of ANNs applied to the entire FDD process can be found. Arseniev et al. [5] provide an approach for building a FDD system based on the ANNs and an automatic training method for such systems. The paper shows that even the usage of the simplest model of ANN such as Rosenblatt's perceptron could provide good results and compliance with rule-based FDD system. Shang et al. [124] introduced an automatic fault detection method for automobile transmission and a fault diagnosis expert system for newly assembled transmission. The order spectrum analysis method was used to analyze vibratory signals of the automobile transmission. Selected feature vector sets were inputted into the neural network for fault identification and classification of the newly assembled automobile transmission. A large number of data was collected and analyzed from an industrial site and the proposed algorithm was verified to be effective and exact. In Kalogirou et al. [56] a fault diagnosis system of an automatic solar water heater was developed. This system consists of a prediction module, a residual calculator and a diagnosis module. In the prediction module an ANN is used to predict the fault-free temperatures that the residual calculator compares with the measurement data, then in the diagnosis module the residuals are compared against three constant threshold values. So, four categories are defined (normal, low probability of failure, high probability of failure, and failure) and three types of faults can be predicted. Other applications of ANNs for building

FDD analysis can be found in [28, 57, 81].

Also fuzzy techniques [61, 144] are very useful for FDD analysis as they allow the integration of human operator knowledge into the fault diagnosis process. The formulation of the decisions is done in a human understandable way such as linguistic rules [104]. In the energy application field these techniques are mainly used in FDD of energy production systems [99, 10, 132] and very few studies are carried out on the building energy consumption. Du, Er, & Rutkowski [31] developed a FDD strategy based on an efficient adaptive Fuzzy Neural Network to assist building automation systems for sensor heath monitoring and fault diagnosis of an Air-Handling Unit (AHU). Pan [103] carried out a hybrid approach employing fuzzy sets and possibility theory: an example of beam failure demonstrates the capability of the model that can help safety operators to effectively assess fault possibilities and better evaluate building performance.

In this Chapter a fault detection analysis based on different neural ensemble and statistical approaches and a fault diagnosis analysis based on fuzzy sets and fuzzy logic are presented. In the first part of the Chapter (Section 5.2) a brief theoretical description of the methods analyzed is presented. Then the proposed methodology is tested on two months monitoring data sets for the lighting energy consumption of an actual office building located at ENEA Casaccia Research Centre. The application of the FDD analysis is shown with the aim to compare the capability of proposed approaches in detecting and diagnosing two artificial faults created in the testing period. On the basis of the proposed methodology, a FDD analysis algorithm was implemented and included in the ICT platform of ENEA Casaccia Research Centre for an on-line and near real-time application to the lighting and fan-coil electrical consumptions, as described in Section 5.3. Experimentation is still ongoing and involves nine actual office buildings of the Centre. The results of the experimentation of a one year time period for these nine buildings are finally shown.

5.2 A methodology for the fault detection and diagnosis analysis: an application example

As shown in Figure 5.1, a soft computing approach in automatic detection and diagnosis of anomalous building lighting consumption is proposed. The capability of different ANNE for artificial lighting fault detection of a real office building is demonstrated. The fault detection is performed first analyzing the magnitude of the residuals generated by ANN BEM through two severity indices related to the peaks detected in the data set. Furthermore a majority voting ensemble method (MVEM) is performed to ensemble the results of different ANN classifiers. Then an innovative fault diagnosis system based on fuzzy sets and fuzzy logic in order to find the cause related to the detected faults is proposed. The method is based on a fuzzyfication of low level signals

(severity indices, percentage of active rooms, hour of the day, etc.) and a fuzzy sets composition producing a single diagnostic index ranging in the lattice [0,1], where 0 and 1 mean respectively the total absence or the maximum faulty alarm for the cause under examination.

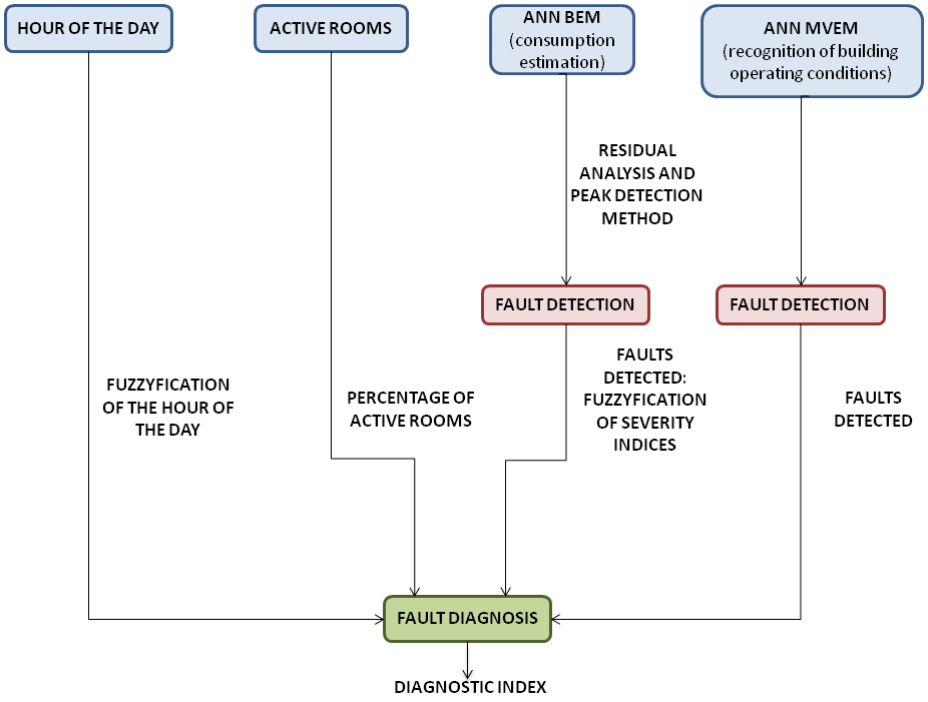

FIGURE 5.1: The proposed fault detection & diagnosis approach

Some theoretical hints on ANNs, ANN BEMs, Peak Detection method and related severity indices were already given in the previous Chapter, ANN MVEM classification approach and fuzzy logic are presented below.

5.2.1 Theoretical description of the proposed methods

Artificial neural network classifier and majority voting ensemble method

Pattern recognition is the study of how machines can observe the environment, learn to distinguish patterns of interest from their background and make decisions about the categories of the patterns [9]. Pattern recognition systems usually learn from a training set and the recognition problem is a classification task: in particular, in the supervised classification the classes are defined by the system designer. The four best known approaches for pattern recognition are template matching, statistical classification, syntactic or structural matching and ANNs. The most commonly used ANN family for pattern classification tasks is the feed-forward networks [129, 49, 43], which includes MLP and Radial-Basis Function (RBF) networks. The increasing popularity of ANNs to solve pattern recognition problems has been primarily due to their low dependence on

domain-specific knowledge and due to the availability of efficient learning algorithms to use [9]. ANN models allow to define nonlinear algorithms for feature extraction and classification. The aim of the training is to ensure that the machine learns to extract relevant information from the training set of possible inputs and corresponding targets (classifications) in order to classify future input patterns.

Combining the decision of several classifiers can lead to improved recognition results: the basic idea is to run not a single network but an ensemble of networks (each of which have been trained on the same data), in order to classify a given input pattern by obtaining a classification from each network and then using a combination scheme to decide the collective classification [45]. Among all the combination methods, the MVEM is by far the simplest one for implementation, and it is as effective as the other more complicated schemes (Bayesian, logistic regression, fuzzy integral, etc.) in improving the recognition rate for the used dataset [65]. By combining the decisions of m experts, the majority vote assign the sample to the class for which at least v (see Equation 5.1) of the experts agree on the identity, where:

$$v = \begin{cases} \frac{m}{2} + 1, & \text{if } m \text{ is even} \\ \frac{m+1}{2}, & \text{if } m \text{ is odd} \end{cases} \tag{5.1}$$

In this study a MVEM is performed to ensemble the results of different ANN classifiers for fault detection analysis. An anomalous consumption detected by ANN MVEM can be also defined "outlier".

Fuzzyfication and fuzzy sets composition

Mathematical developments of the fuzzy set theory advanced in a variety of ways and in many disciplines [142]. Applications of this theory can be found, for example, in artificial intelligence, computer science, medicine, control engineering, decision theory, expert systems, logic, management science, operations research, pattern recognition and robotics [63, 86, 115].

Most of traditional tools for formal modeling, reasoning and computing are deterministic and precise [144], implying that the parameters of the model representing exactly the real system are definitely known. However, these assumptions are not always justified if a good reality description and very detailed data are needed for modeling. To this purpose, fuzzy set theory provides a strict mathematical framework in which vague conceptual phenomena can be precisely and rigorously studied. The axiomatic bases of fuzzy set theory are various, Zimmermann [144] and Gottwald [39] offer a good review.

If J is a collection of objects denoted generically by j, then a fuzzy set A in J is a set of ordered pairs (see Equation 5.2):

$$A = \{(j, \mu_A(j)|j \in J)\} \tag{5.2}$$

where $\mu_A(j)$ is the membership function which maps J to the membership space M. Its range is the subset of non negative real numbers whose supremum is finite. If $sup(\mu_A(j))$ = 1 the fuzzy set is normalized. In fuzzy sets the definition of the membership function (fuzzyfication) is a very important task. This can be any kind of analytical function whose parameters have to be properly tuned according to the meaning of the fuzzy set itself.

A fuzzy set operation is an operation on fuzzy sets. The most widely used operations are called standard fuzzy set operations. There are three standard fuzzy set operations: fuzzy complements, fuzzy intersections and fuzzy unions. The membership function of the intersection (logical and) of two fuzzy sets A and B is defined as (see Equation 5.3):

$$\mu_{A \bigcap B}(j) = min(\mu_A(j), \mu_B(j)), \forall j \in J \tag{5.3}$$

The intersection operation in fuzzy set theory is the equivalent of the AND operation in Boolean algebra.

The membership function of the union (exclusive or) is defined as (see Equation 5.4):

$$\mu_{A \bigcup B}(j) = max(\mu_A(j), \mu_B(j)), \forall j \in J \tag{5.4}$$

The union operation in fuzzy set theory is the equivalent of the OR operation in Boolean algebra.

The membership function of the complement (negation) is defined as (see Equation 5.5):

$$\mu_{-A}(j) = 1 - \mu_A(j), \forall j \in J \tag{5.5}$$

The complement operation in fuzzy set theory is the equivalent of the NOT operation in Boolean algebra.

These definitions have also been extended. The 'logical and' (intersection) can also be modeled as a t-norm [33] and the 'inclusive or' (union) as a t-conorm [6]. Both types are monotonic, commutative and associative. Finally, a class of 'averaging operators'

[138] were defined, which do not have the mathematical properties of the t-norms and t-conorms.

5.2.2 Case study and data set description

An actual office building (building F40) located at ENEA Casaccia Research Centre (Rome, Italy) was considered as a case study (see Fig. 5.2). The building is composed of three floors and a basement connected through the larger side with a second building. The building is equipped with an advanced monitoring system aimed at collecting energy consumption (electrical and thermal) and the environmental conditions.

FIGURE 5.2: The case study building for the application example of the fault detection & diagnosis analysis

Artificial lighting energy consumption and maximum power of the building first floor were analyzed and considered in this experimentation with an hourly timestamp. Furthermore people presence, number of active rooms (a room is considered active if at least one person is present), global solar radiation, time, date and day of the week, were recorded with an hourly time step and considered as independent variables. A dataset of about two months (December 2012 - January 2013) was considered for the analysis. In order to verify the reliability and the effectiveness of the proposed FDD approach, two artificial faults were created in the last week of the dataset (on Thursday 24th and Friday 25th of January). In those days, at the end of the working time with a low people presence (between 17:30 and 18:00), all the offices artificial lights of the first floor were switched on creating an anomalous peak of energy demand. In the floor there are 13 offices of different size with a floor area ranging from 14 to 36 m^2 and 2 CED rooms each of about 20 m^2. Different number of fluorescent lamps (each 55 W) ranging from 4 to 8 are installed in each office/room. In the 2 CED rooms 12 lamps, each 55 W, are installed.

5.2.3 Framework of the fault detection analysis and development of the models

In order to build the ANN ensemble models, the monitored variables to be used as inputs and outputs were selected (see Table 5.1). Two ANN ensembles were built according to BEM and MVEM methods respectively. The methods were tested on the week "Testing Set 2" (see Figure 5.3) for the fault detection analysis.

ANN BEM		ANN MVEM	
Input	**Output**	**Input**	**Output**
Day of the week (1-7)	Lighting active electrical energy	Day of the week (1-7)	Flag fault (0-1)
Time (hour)	Lighting maximum active electrical power	Time (hour)	
People presence (floor level)		People presence (floor level)	
"Active" rooms (floor level)		"Active" rooms (floor level)	
Global solar radiation		Global solar radiation	
		Lighting active electrical energy	
		Lighting maximum active electrical power	

TABLE 5.1: Inputs and outputs of ANN BEM and ANN MVEM models

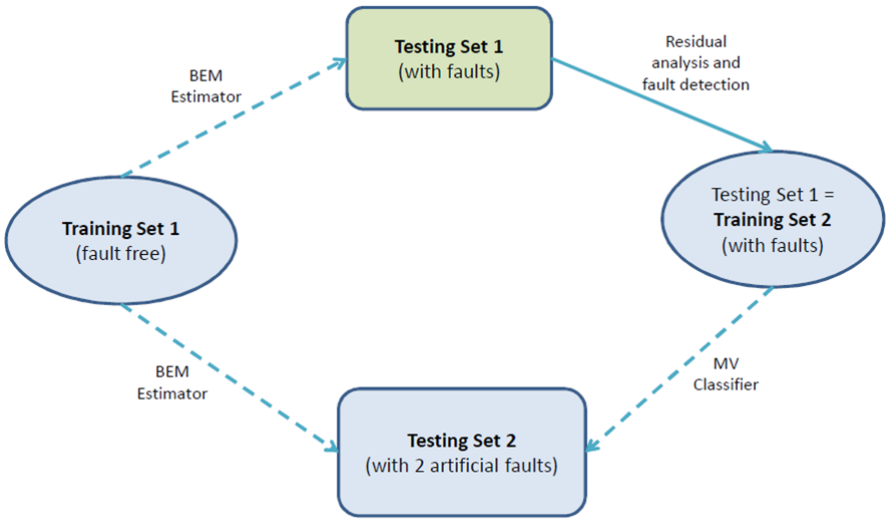

FIGURE 5.3: Data-set splitting

First, in order to estimate a normal pattern for the artificial lighting, the training of the ANN BEM was performed considering a 2 weeks "fault free" data-set ("Training Set 1"): the "fault free" hypothesis was based on the pattern observations of the electrical energy consumption for lighting and energy manager experience. In this case ANNs were used as consumption estimators, not as consumption predictors: the neural model inputs are only the building operating conditions without dynamics (the consumption

data). The "fault free" hypothesis of the training set is fundamental in order to guarantee that high differences between the consumption estimated by the neural model and the real consumption in the testing set effectively correspond to an anomalous consumption in relation to the building operating conditions. Combining the outputs of several ANNs through BEM is very simple (the estimation of BEM is the mean of the estimations of all the ANNs) and allows to obtain better results than those which could be obtained from any of the constituent neural models. Starting from a good estimation of normal operation, a robust fault detection through BEM was carried out with a residual analysis.

Furthermore in order to develop an ANN ensemble for classification of operational data, the ANNs were trained using two weeks data that are representatives of normal as well as faulty operating conditions ("Training Set 2"). The output of the training data set ("Training Set 2"), indeed, was characterized by faults detected applying the Peak Detection Method on the residual set: the residuals were calculated by the difference between the real consumption in the same period ("Testing Set 1") and the consumption estimated by an ANN BEM, as shown in Figure 5.3. It should be noticed that Lighting active electrical energy and Lighting maximum electrical active power, used as inputs of ANN MVEM, are real consumption measurements. The aim of the training is to ensure that the neural model learns to identify "normal" and "anomalous" operating situations of the building in order to classify future input patterns. Combining the decision of several ANN classifiers through MVEM is very simple and effective (the decision of MVEM is the decision of at least half of all the classifiers) and can lead to improved recognition rate than the individual neural models. Once the ANNs were trained, the fault detection through MVEM becomes a pattern recognition task. The ANN MVEM was used as a further fault detection method in order to assure a better robustness of the whole methodology.

The considered ANN features were feed-forward MLP, with 1 hidden layer consisting of 15 neurons, hyperbolic tangent as activation function for the hidden neurons and linear for the output. Training was performed with MATLAB through the Levenberg-Marquardt algorithm stopping after 1000 iterations.

5.2.4 Results: application of estimation and classification models for the fault detection analysis

As described above, an ANN BEM model was built. The results related to "Training Set 1" and "Testing Set 1" are reported in Table 5.2. In particular the performances of the models have been evaluated according to the MAE (Eq. 5.6) and the MAX (Eq.

5.7) errors:

$$MAE = \frac{1}{n}\sum_{i=1}^{n}|y_i - \hat{y}_{BEM,i}| \tag{5.6}$$

$$MAX = max\{|y_i - \hat{y}_{BEM,i}|\}_{i=1}^{n} \tag{5.7}$$

		TRAINING SET 1		TESTING SET 1	
		ANN	**BEM**	**ANN**	**BEM**
Active Energy	**MAE (kWh)**	0.18 (±0.02)	0.15	0.73 (±0.02)	0.71
	MAX (kWh)	1.45	1.11	5.02	3.81
Maximum Active Power	**MAE (kW)**	0.20 (±0.03)	0.16	0.87 (±0.01)	0.84
	MAX (kW)	1.80	1.40	5.71	5.47

TABLE 5.2: ANN BEM results (Training Set 1 and Testing Set 1)

where y_i is the real output, $\hat{y}_{BEM,i}$ is the estimated output and n is the size of the real data set. The reported results were averaged over 10 different runs (standard deviation in brackets) and the ensemble was built by the same 10 models. As shown in Table 5.2, the results obtained with ANN BEM perform always better than those obtained with individual networks. Training and testing trends are shown in Figure 5.4 and Figure 5.5 for lighting active energy and maximum active power demand respectively. The estimated energy and maximum power follow quite well the real ones, except for some "anomalous" real consumption values in the testing period.

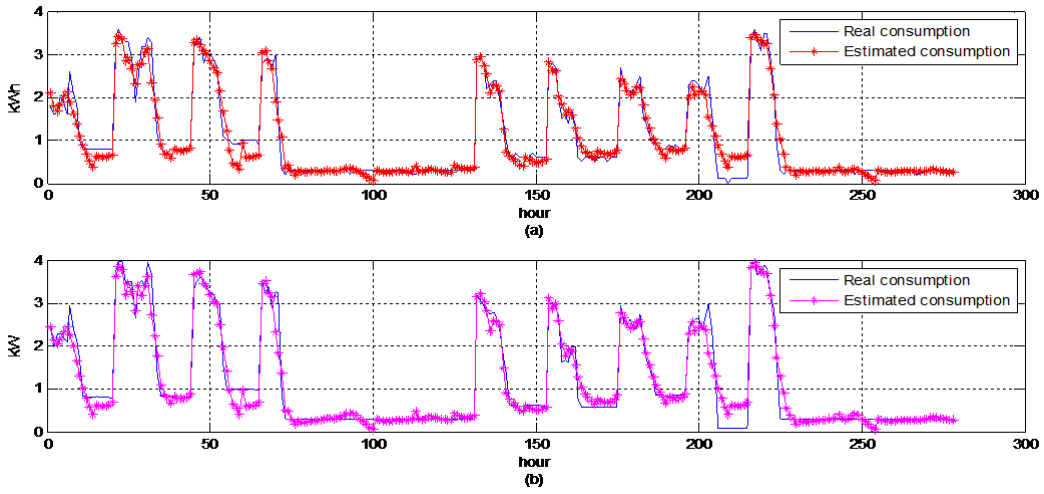

FIGURE 5.4: ANN BEM (Training Set 1) – Active Energy (a) and Maximum Active Power (b)

A residual analysis on maximum active power was conducted: Figure 5.6 shows the Testing Set 1 residuals both for energy and maximum power. Then, the Peak Detection Method was applied to maximum active power residuals: the detected faults, reported in Table 5.3, were used to build the Classifier Training Set (Training Set 2).

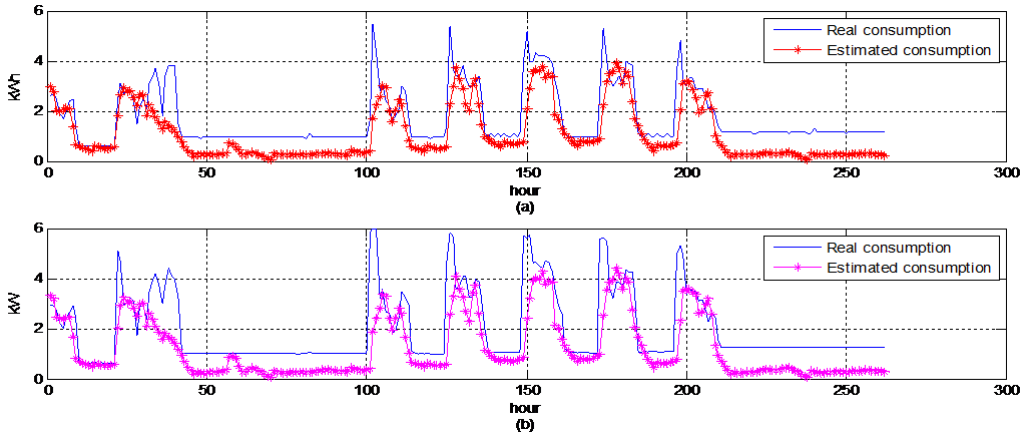

FIGURE 5.5: ANN BEM (Testing Set 1) – Active Energy (a) and Maximum Active Power (b)

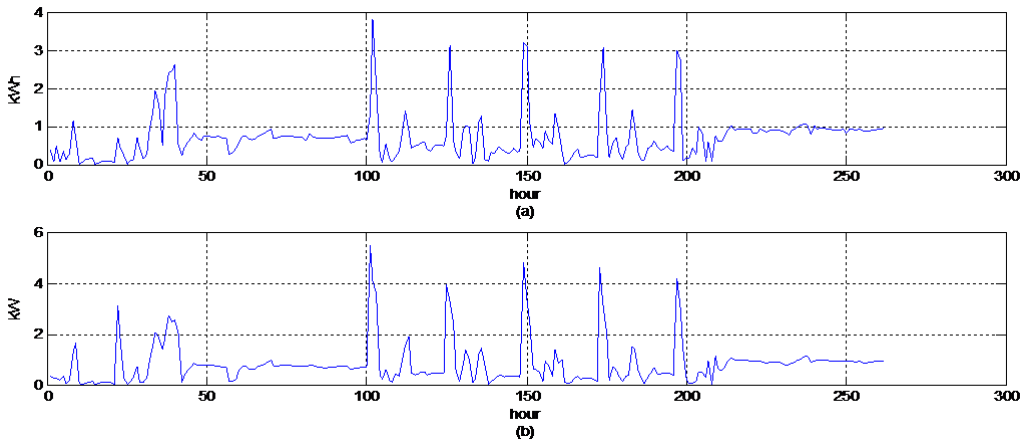

FIGURE 5.6: Testing set 1 residuals - Active Energy (a) and Maximum Active Power (b)

The inputs of the ANN MVEM (see Table 5.1) are a set of features that define the output of the network, i.e. the operating state of the system as "normal" or "anomalous". The output data associated were chosen to enable the ANN to perform pattern recognition. Thus, by codifying the output data using a unique numerical pattern, the condition 'normal operation' was defined. In order to codify output data, the numerical values 0 (normal operation) and 1 (faulty operation) were used to develop a totally single numerical pattern. The ensemble technique used is the MVEM. The neural classifier was built in the training period (Training Set 2, see Figure 5.7) and it was applied using hourly data in the testing period (Testing Set 2, see Figure 5.8).

As shown in Figure 5.8, using the MVEM to combine the results of ANN classifiers, the two artificial faults and some other actual anomalous power consumption values were detected. These actual faults correspond to very high power demand observed with few people presence usually out of the working hour (especially in the early morning when only the cleaning staff is present in the building). Table 5.4 shows all the faults

Outlier Data	Outlier Hour	Maximum Power Residual Value [kW]	S Function Value	MZScore Value
07/01/2013	18:00	1,66	1,62	1,65
08/01/2013	7:00	3,10	3,07	4,17
11/01/2013	17:00	2,56	1,58	3,23
14/01/2013	6:00	5,47	4,94	8,29
14/01/2013	8:00	3,61	3,15	5,04
14/01/2013	18:00	1,91	1,54	2,09
15/01/2013	6:00	3,96	3,45	5,65
15/01/2013	8:00	2,41	2,09	2,96
16/01/2013	6:00	4,82	4,34	7,16
16/01/2013	8:00	2,52	2,12	3,16
17/01/2013	6:00	4,59	4,43	6,75
17/01/2013	8:00	2,00	1,84	2,24
18/01/2013	6:00	4,19	3,90	6,06

TABLE 5.3: Residual analysis and fault detection on Testing Set 1 with ANN BEM

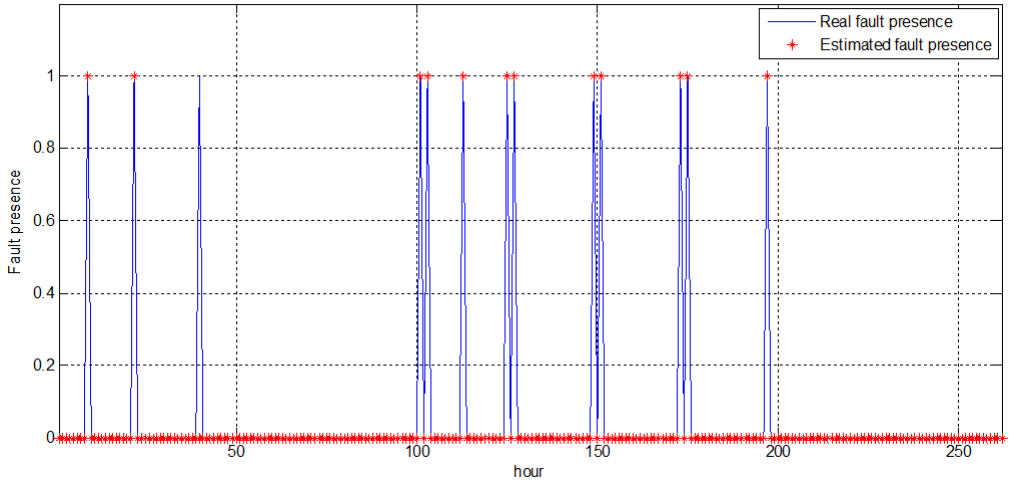

FIGURE 5.7: ANN majority voting ensemble classifier (training)

detected. In Table 5.5 the classification error (defined as the percentage relative magnitude of classification error) in the training period is reported. It can be observed that an ANN MVEM performs slightly better than using a single network.

Then, the ANN BEM trained with the Training Set 1 (see Figure 5.4) was applied to Testing Set 2 (see Figure 5.9): the results obtained are reported in Table 5.6. Even in this case, the ANN BEM always outperforms the single ANN. The lighting energy and power demand was estimated with an high accuracy through the ANN BEM in the training period. In the testing period the estimated energy and power follow quite well the monitored ones, with the exception of the 2 artificial faults and some other evident abnormal values.

The magnitude of the difference over the time between the actual and estimated power demand (see Figure 5.10) was analyzed for detecting faulty operation or anomalous

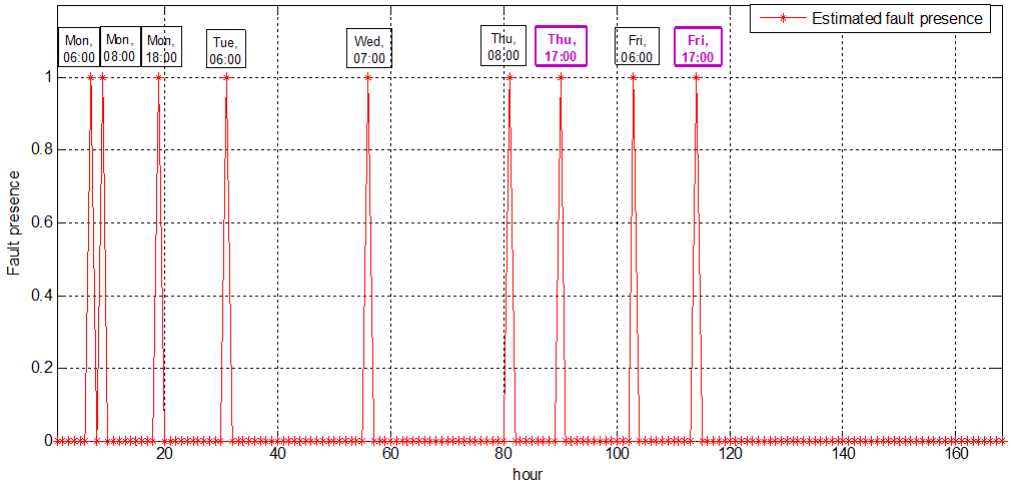

FIGURE 5.8: ANN majority voting ensemble classifier (testing). The two artificial faults are in bold

Outlier Data	Outlier Hour	Maximum Active Power [kW]
21/01/2013	06:00	4,17
21/01/2013	08:00	5,23
21/01/2013	18:00	3,84
22/01/2013	06:00	5,26
23/01/2013	07:00	5,2
24/01/2013	08:00	5,19
24/01/2013	**17:00**	**5,86**
25/01/2013	06:00	5,34
25/01/2013	**17:00**	**5,55**

TABLE 5.4: Fault detection on Testing Set 2 with ANN MVEM

values through the peak detection method. Since maximum active power is more representative of variations than active energy, only the analysis performed on the maximum power for lighting is presented.

To this purpose the Peak Detection Method was applied to the residuals data set in the testing period. In Figure 5.11 the trend of residuals over the time is shown and the common detected faults with ANN MVEM are circled.

As well as for the MVEM, the identified residual peaks include the "early morning faults" and the two artificial faults (see Table 5.7). Even in this case, the "early morning faults" are actual "systematic" faults due to an high power demand observed in the early morning, when usually many lights are on and only the cleaning staff is present in the building. However both proposed methods are able to detect also faults related to other anomalous use of artificial lighting considering, for example, the available natural lighting. The results confirm that the analysis of residual generated through the ANN BEM and the application of the Peak Detection Method represents a useful and powerful technique for the peak building lighting fault detection.

Training	Percentage Error
Best ANN	0,38
Worst ANN	2,29
ANN Average	0,95
Classifier	0,38

TABLE 5.5: Classification error percentage (training)

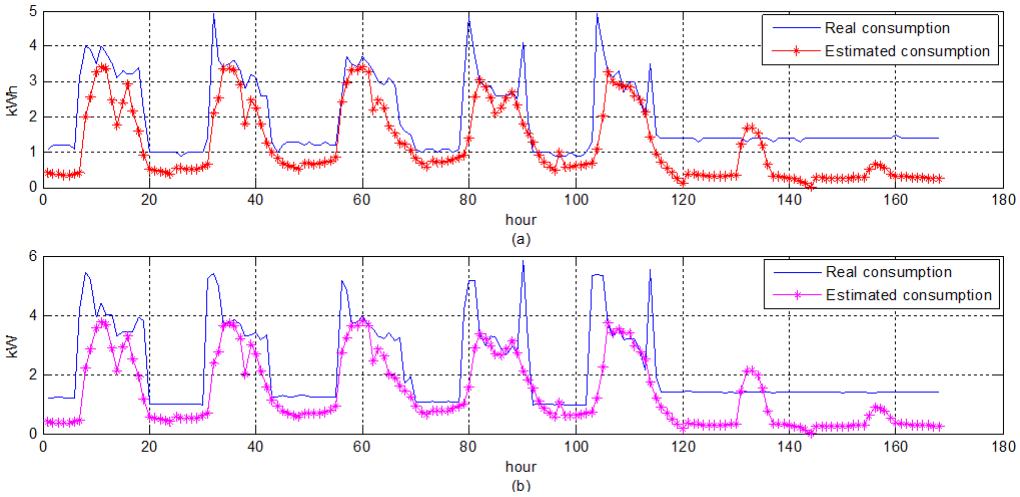

FIGURE 5.9: ANN BEM (Testing Set 2) – Active Energy (a) and Maximum Active Power (b)

The Peak Detection Method was also directly applied to the sequence maximum power demand data. In Figure 5.12 the outliers detected for testing period (Testing Set 2) are shown with the trends of $Mzscore$ and $Sfunction$ indices. Circled faults (the 2 artificial faults) are the common faults with the two previous methods.

It can be observed that the method allows to detect the two artificial faults and some other real faults in early morning. In this situations the relative severity indices correctly assume higher value (see Figure 5.12). However, the data analysis showed that power is related to other variables i.e. people, solar radiation, day and active rooms, so it can be inferred that the extreme values are not always definite faults. Therefore some false positives can be found when an "univaried" outlier detection method is applied without taking into account the effect of the independent variables on the pattern recognition. For this reason, an FDD process performed through a residual ANN BEM analysis is always recommended to avoid the occurrence of false positive faults.

5.2.5 Diagnostic process with a fuzzy analysis

Finally, the experimentation concerned the application of the Fault Diagnosis method on the selected testing week is proposed. The Fault Diagnosis system is based on fuzzy sets and fuzzy logic. A fuzzyfication of low level signals and a fuzzy sets composition

		TRAINING SET 1		TESTING SET 2	
		ANN	**BEM**	**ANN**	**BEM**
Active Energy	**MAE (kWh)**	0.20 (±0.03)	0.17	0.84 (±0.06)	0.77
	MAX (kWh)	1.70	1.24	4.08	3.81
Maximum Active Power	**MAE (kW)**	0.21 (±0.03)	0.17	1.01 (±0.06)	0.92
	MAX (kW)	2.15	1.44	4.75	4.59

TABLE 5.6: ANN BEM results (Training Set 1 and Testing Set 2)

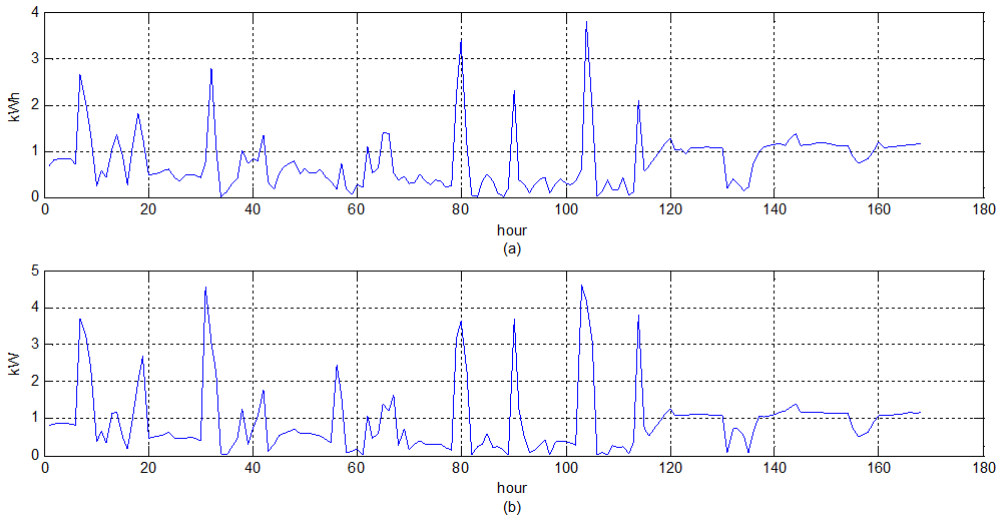

FIGURE 5.10: Testing 2 residuals - Active Energy (a) and Maximum Active Power (b)

providing a real value, in the lattice [0,1], were conducted. This value is capable of indicating the seriousness or the alarm degree (1 maximum alarm degree, 0 no alarm degree) of the detected fault with the cause under examination.

Thus, in order to characterize the diagnostic index which represents the alarm degree of the detected faults for the **cause**:

"An anomalous lighting energy demand out of the working hours"

the main criterion and the process variables were defined. The main criterion is: "IF a fault in lighting energy consumption occurs AND people presence in the building is low AND NOT in working hours THEN the diagnostic index is high". In terms of fuzzy sets, the diagnostic index that corresponds to the cause under examination can be translated in one of the two ways (Eq. 5.8 and Eq. 5.9):

$$C_1 = min(S_1, S_2) \tag{5.8}$$

$$C_2 = w \cdot S_1 + (1 - w) \cdot S_2 \tag{5.9}$$

where w is a real number in [0,1] (in the experimentation w = 0.7). S_1 and S_2 are the **situations**:

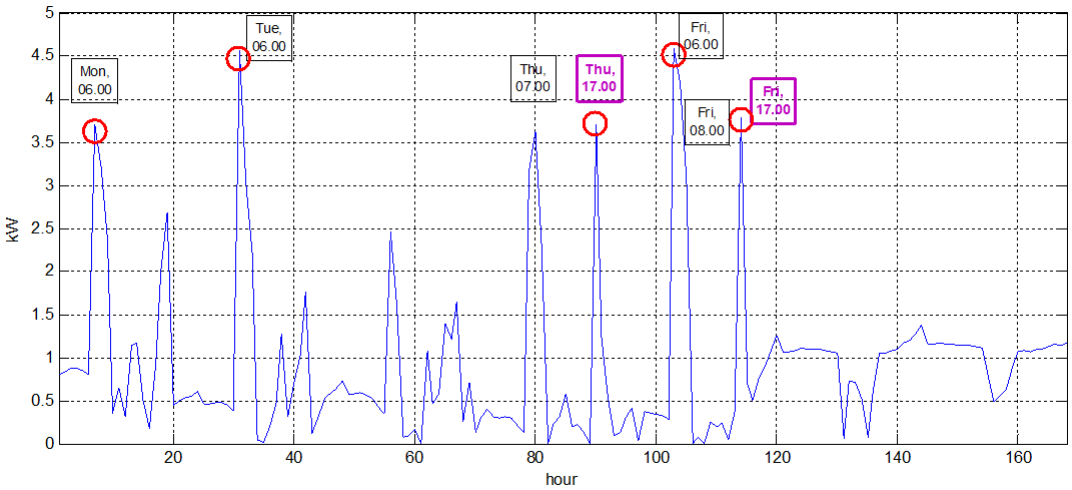

FIGURE 5.11: Testing Set 2 residuals (maximum active power) and detected peaks

Outlier Data	Outlier Hour	Maximum Power Residual Value [kW]	S Function Value	MZScore Value
21/01/2013	06:00	3,70	3,11	4,34
22/01/2013	06:00	4,56	4,36	5,62
24/01/2013	07:00	3,63	3,56	4,24
24/01/2013	**17:00**	**3,71**	**3,66**	**4,35**
25/01/2013	06:00	4,59	4,44	5,66
25/01/2013	08:00	3,07	2,92	3,39
25/01/2013	**17:00**	**3,79**	**3,51**	**4,47**

TABLE 5.7: Residual analysis and fault detection on Testing Set 2 with ANN BEM (the 2 artificial faults are in bold)

S_1 = "A fault in lighting energy consumption occurs"

S_2 = "People presence in the building is low AND NOT in working hours"

which are defined as expressed in Eq. 5.10 and Eq. 5.11 (see Table 5.8).

$$S_1 = (F_1)AND(F_2) \tag{5.10}$$

$$S_2 = NOT(F_3)AND(F_4) \tag{5.11}$$

Fuzzy set	Linguistic value	Membership function $\mu_{Fi}(j_i)$	Parameters
F_1	Neural classifier fault detection is positive	$y_F = \hat{y}_{MVEM}$	
F_2	$Sfunction$ value is high	Sigmoid	c = 0,10; t = 0,08
F_3	Working hours	Gaussian	q = 12; r = 4
F_4	Active rooms	y_F = 1 - p	

TABLE 5.8: Fuzzy sets, linguistic values, membership functions and parameters

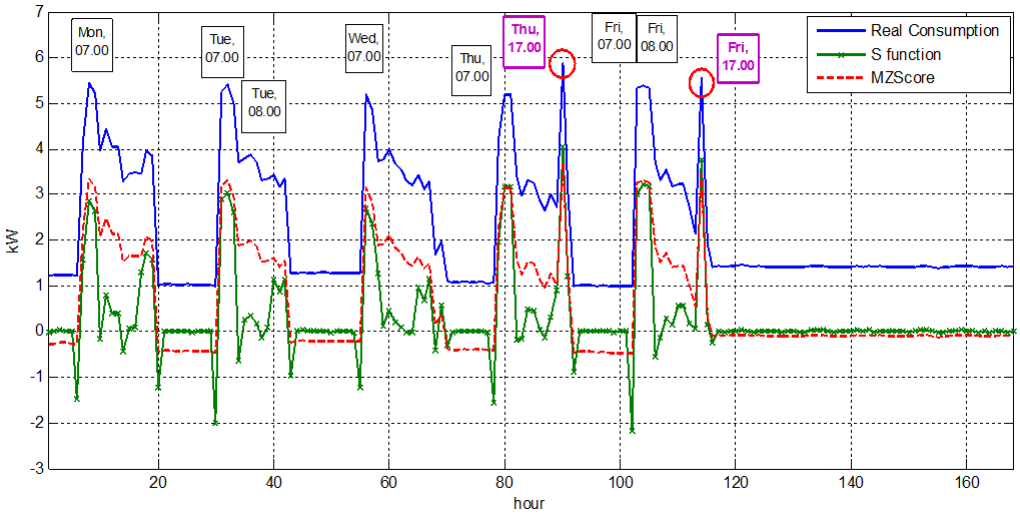

FIGURE 5.12: Maximum active power (Testing Set 2), $Sfunction$ and $Mzscore$ values and detected peaks (common peaks are circled)

The fuzzy sets F_1, F_2, F_3 and F_4 are derived from the membership functions reported in Table 5.8 and consist of values ranging from 0 to 1 obtained from variables which represent measured evidences (**preprocessing**). In particular, $\hat{y}_{MVEM}$ is the MVEM output (which is by itself a value in the lattice [0,1]), p is the percentage of the rooms given by the monitoring system where at least one person is present (active rooms), Sigmoid and Gaussian functions are defined by Eq. 5.12 and Eq. 5.13 respectively where for the Sigmoid function j is the S function value and for the Gaussian function j is the hour of the day.

$$Sigmoid = \frac{1}{1 + e^{\frac{c-j}{t}}} \tag{5.12}$$

$$Gaussian = e^{\left(\frac{-(j-q)^2}{2r^2}\right)} \tag{5.13}$$

The presented fault detection and diagnosis approach is therefore an analysis consisting of the three conceptual steps: preprocessing, situation assessment and diagnosis of the cause. In the following (Table 5.9), the results of the fuzzy diagnostic process on a testing day where some faults occurred are reported in bold. Table 5.9 shows that the index C_2 (Eq. 5.9) performs much better than C_1 (Eq. 5.8) because it assumes higher values in the situations where power is too high with respect to the hour of the day and the percentage of active rooms. In Figure 5.13 the FDD diagnostic index behavior (red dashed line) with respect to the normalized power consumption (blue line) over four days of the testing week is reported.

Time	Power [kW]	Active rooms (%)	F_1	F_2	F_3	F_4	S_1	S_2	C_1	C_2
5:00	1,07	0,00%	0	0,00	0,78	1,00	0,00	0,78	0,00	0,24
6:00	**4,20**	0,00%	1	1,00	0,68	1,00	1,00	0,68	**0,68**	**0,90**
7:00	**5,20**	6,12%	1	1,00	0,54	0,94	1,00	0,54	**0,54**	**0,86**
8:00	**5,19**	17,35%	1	1,00	0,39	0,83	1,00	0,39	**0,39**	**0,82**
9:00	3,39	21,43%	0	0,06	0,25	0,79	0,00	0,25	0,00	0,07
10:00	2,97	27,55%	0	0,09	0,12	0,72	0,00	0,12	0,00	0,04
11:00	3,31	28,57%	0	0,99	0,03	0,71	0,00	0,03	0,00	0,01
12:00	3,27	29,59%	0	0,98	0,00	0,70	0,00	0,00	0,00	0,00
13:00	2,86	28,57%	0	0,43	0,03	0,71	0,00	0,03	0,00	0,01
14:00	2,65	27,55%	0	0,10	0,12	0,72	0,00	0,12	0,00	0,04
15:00	3,00	27,55%	0	0,91	0,25	0,72	0,00	0,25	0,00	0,07
16:00	2,72	26,53%	0	1,00	0,39	0,73	0,00	0,39	0,00	0,12
17:00	**5,86**	20,41%	1	1,00	0,54	0,80	1,00	0,54	**0,54**	**0,86**
18:00	3,08	14,29%	0	1,00	0,68	0,86	0,00	0,68	0,00	0,20

TABLE 5.9: Fault Diagnosis results on a testing day

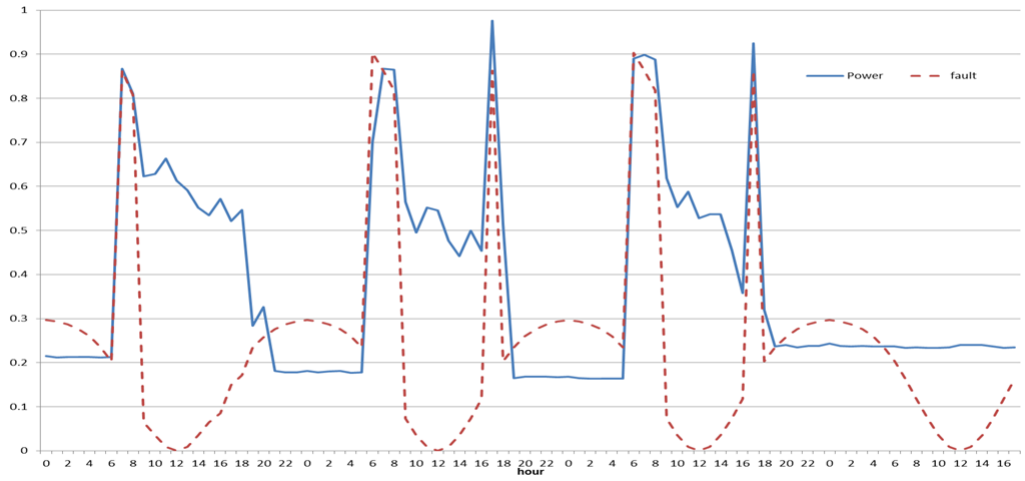

FIGURE 5.13: FDD index behavior with respect to the normalized power consumption

5.3 On-line experimentation of fault detection and diagnosis analysis

5.3.1 The ENEA Smart Village project

The "Smart Village" is a research project carried out by ENEA Casaccia Research Center, where the project is also realized, in partnership with Politecnico di Torino, Roma Tre University and Università Politecnica delle Marche. The experimental project is aimed to develop a Smart City reference model for real urban districts, based on the three pillars Smart Building, Smart Lighting and Smart Mobility. In the "Smart Village" different technologies are integrated, in particular monitoring, data elaboration and data storage, actuation systems, with the main purpose to offer services on demand to users. This results in a more efficient resource management and in an improved user comfort and social participation. The activities related to the different aspects of the

FIGURE 5.14: The Control Room of the ENEA Smart Village

project are centrally coordinated: in the Control Room (see Fig. 5.14), located in one of the buildings involved in the project, the monitored data of the "Smart Village" are stored and then elaborated by the several applications hosted on the "Smart Village" ICT Platform.

Regarding to the Smart Building aspect of the experimentation, several buildings of the ENEA R. C. are involved in the "Smart Village" project as shown in Fig. 5.15. In these buildings BEMSs by different companies are installed aimed to monitor electrical and thermal consumptions and environmental conditions and to define the desired optimized control logics. In particular the F40 building (presented in Paragraph 5.2.2) is equipped with sensors and actuators at room level, while the F64 building and the cluster of buildings (presented in Section 4.2) are equipped with sensors and actuators at building level: in this way it will be possible to compare the long term results of the two energy management strategies. So far in the F40 building the lighting and fan-coil electrical devices are controlled at room level on the basis of the hour of the day, the day of the week and the employee presence. The objective is to apply this control logic for the lighting and fan-coil electrical devices at building level to F64 building and to the cluster of buildings. From the thermal point of view the main idea to realize is to control the valves of the thermal plants that serve the buildings on the basis of the hour of the day, the day of the week, the external temperature and the employee presence. Furthermore, in the near future, the cluster of building will be equipped with RES generation and energy storage elements in order to realize a complete energy micro district in the Centre.

5.3.2 Experimentation results

Starting from the findings experience of Section 5.2 and works [59, 66, 82, 68], an application tool was implemented and included in the ICT platform of the "Smart Village" project aimed to obtain the on-line and near real-time FDD analysis of the lighting and

FIGURE 5.15: Smart Buildings of the ENEA Smart Village

fan-coil anomalous electrical consumptions of the buildings involved in the project. In particular the considered anomalies are caused by the improper use of the employees and are below indicate as "lights on in absence of people" and "fan-coils on in absence of people".

Figures 5.16, 5.17, 5.18 and 5.19 provide some implementation step on the "smarttowndb" database in the ICT platform, according to the three-steps procedure Preprocessing (Fig. 5.16, 5.17, 5.18), Situation Assessment, Causes (Fig. 5.19) presented in Paragraph 5.2.5.

```
SELECT *
FROM smarttowndb.processmethods_parameters;
```

idprocessmethod	idBuilding	Parametro1	Parametro2
1	1	3	2
1	4	3	2
1	5	3	2.5
1	6	3	2
1	7	3	2
1	8	3	2.5
1	9	3	2
1	10	3	2
1	11	3	2
7	1	4	1
7	4	3	2
7	5	4	1
7	6	4	1
7	7	4	1
7	8	4	1
7	9	4	1
7	10	3	2
7	11	3	1

FIGURE 5.16: *processmethods_parameters* Table in *smarttowndb* DB

The testing phase of the diagnostic models was carried out. The period of experimentation starts from January 26, 2013 for the F40 building and from April 1, 2013 for the cluster of buildings (dates when the data acquisition periods start, respectively) and is

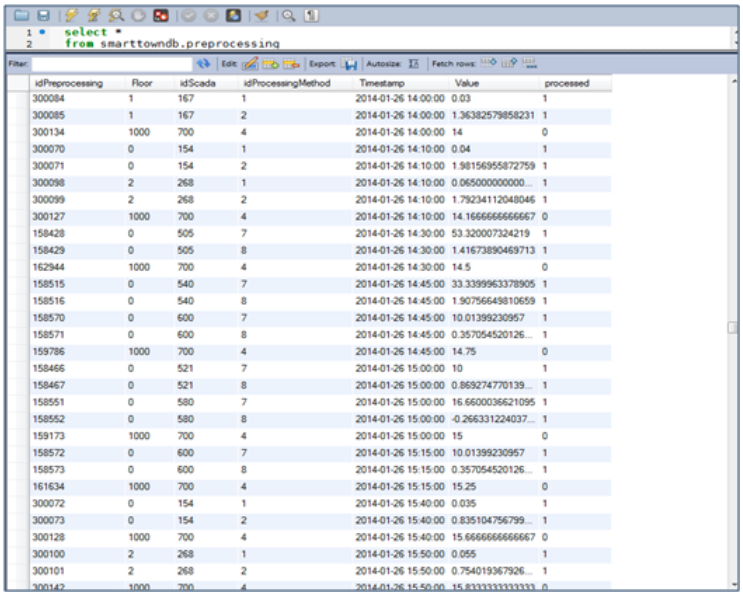

idPreprocessing	Floor	idScada	idProcessingMethod	Timestamp	Value	processed
300084	1	167	1	2014-01-26 14:00:00	0.03	1
300085	1	167	2	2014-01-26 14:00:00	1.36382579858231	1
300134	1000	700	4	2014-01-26 14:00:00	14	0
300070	0	154	1	2014-01-26 14:10:00	0.04	1
300071	0	154	2	2014-01-26 14:10:00	1.98156955872759	1
300098	2	268	1	2014-01-26 14:10:00	0.065000000000...	1
300099	2	268	2	2014-01-26 14:10:00	1.79234112048046	1
300127	1000	700	4	2014-01-26 14:10:00	14.1666666666667	0
158428	0	505	7	2014-01-26 14:30:00	53.320007324219	1
158429	0	505	8	2014-01-26 14:30:00	1.41673890469713	1
162944	1000	700	4	2014-01-26 14:30:00	14.5	0
158515	0	540	7	2014-01-26 14:45:00	33.3399963378905	1
158516	0	540	8	2014-01-26 14:45:00	1.90756649810659	1
158570	0	600	7	2014-01-26 14:45:00	10.01399230957	1
158571	0	600	8	2014-01-26 14:45:00	0.357054520126...	1
159786	1000	700	4	2014-01-26 14:45:00	14.75	0
158466	0	521	7	2014-01-26 15:00:00	10	1
158467	0	521	8	2014-01-26 15:00:00	0.869274770139...	1
158551	0	580	7	2014-01-26 15:00:00	16.6600036621095	1
158552	0	580	8	2014-01-26 15:00:00	-0.266331224037...	1
159173	1000	700	4	2014-01-26 15:00:00	15	0
158572	0	600	7	2014-01-26 15:15:00	10.01399230957	1
158573	0	600	8	2014-01-26 15:15:00	0.357054520126...	1
161634	1000	700	4	2014-01-26 15:15:00	15.25	0
300072	0	154	1	2014-01-26 15:40:00	0.035	1
300073	0	154	2	2014-01-26 15:40:00	0.835104756799...	1
300128	1000	700	4	2014-01-26 15:40:00	15.6666666666667	0
300100	2	268	1	2014-01-26 15:50:00	0.055	1
300101	2	268	2	2014-01-26 15:50:00	0.754019367926...	1

FIGURE 5.17: Part of *preprocessing* Table in *smarttowndb* DB

still continuing. In F40 building, however, some problems in the acquisition of electrical measurements were encountered and fixed in July 2014, then the values of lighting and fan coil consumption are reliable only from that period.

For each building the analysis of anomalies consisted in their distribution by year, by month, by time slots and by severity. Only the anomalies with a diagnostic index value greater or equal to 0.5 are considered.

Figures 5.20, 5.21, 5.22 and 5.23 show the results obtained in the case of distribution by time slots of the anomalies "fan-coils on in absence of people" and "lights on in absence of people" for the cluster of buildings (Figure 5.20 and Figure 5.22) and the F40 building (Figure 5.21 and Figure 5.23) in the year June 2014 (July 2014 for the F40 building) - June 2015. The anomalies related to the lights in the building F40 (Figure 5.23) are almost absent during the night as in this building is applied an adaptive control of the lights based on the people presence. A similar situation occurs for the fan-coils on/off during the heating and cooling periods of the F40 building: the control is carried out by setting the temperature set-point for each room on the basis of the corresponding employee presence and ensuring the fan-coils on during the early morning and the lunch time. According to this, the fan-coils anomalies in the building F40, illustrated in Figure 5.21, are characterized by a clear decrease in the night hours. The distribution of the anomalies changes considerably in the cluster buildings, where no electrical and thermal utilities control is applied: the anomalies related to the fan coils (Figure 5.20) and lights (Figure5.22) occur even at night and increase in correspondence of the entrance and the exit of the employees from the buildings.

Figures 5.24, 5.25, 5.26 and 5.27show the distribution of anomalies for diagnostic index value. The number of anomalies with high diagnostic index value (index> = 0.8) is

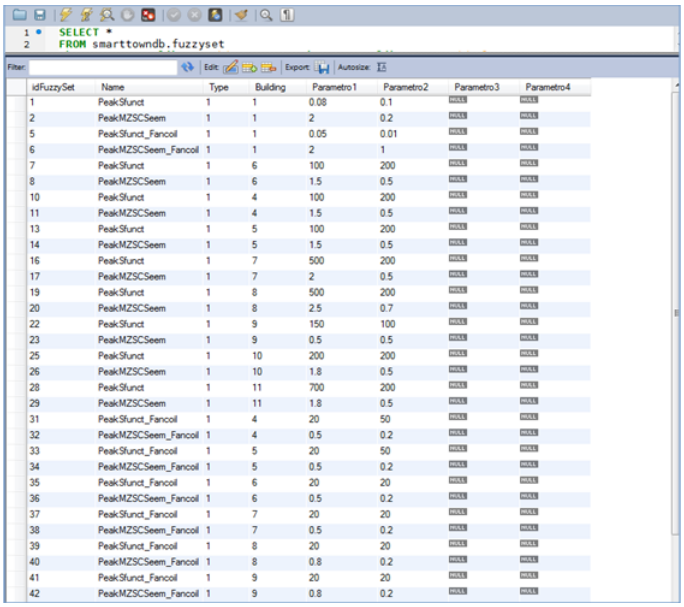

```
SELECT *
FROM smarttowndb.fuzzyset
```

idFuzzySet	Name	Type	Building	Parametro1	Parametro2	Parametro3	Parametro4
1	PeakSfunct	1	1	0.08	0.1	NULL	NULL
2	PeakMZSCSeem	1	1	2	0.2	NULL	NULL
5	PeakSfunct_Fancoil	1	1	0.05	0.01	NULL	NULL
6	PeakMZSCSeem_Fancoil	1	1	2	1	NULL	NULL
7	PeakSfunct	1	6	100	200	NULL	NULL
8	PeakMZSCSeem	1	6	1.5	0.5	NULL	NULL
10	PeakSfunct	1	4	100	200	NULL	NULL
11	PeakMZSCSeem	1	4	1.5	0.5	NULL	NULL
13	PeakSfunct	1	5	100	200	NULL	NULL
14	PeakMZSCSeem	1	5	1.5	0.5	NULL	NULL
16	PeakSfunct	1	7	500	200	NULL	NULL
17	PeakMZSCSeem	1	7	2	0.5	NULL	NULL
19	PeakSfunct	1	8	500	200	NULL	NULL
20	PeakMZSCSeem	1	8	2.5	0.7	NULL	NULL
22	PeakSfunct	1	9	150	100	NULL	NULL
23	PeakMZSCSeem	1	9	0.5	0.5	NULL	NULL
25	PeakSfunct	1	10	200	200	NULL	NULL
26	PeakMZSCSeem	1	10	1.8	0.5	NULL	NULL
28	PeakSfunct	1	11	700	200	NULL	NULL
29	PeakMZSCSeem	1	11	1.8	0.5	NULL	NULL
31	PeakSfunct_Fancoil	1	4	20	50	NULL	NULL
32	PeakMZSCSeem_Fancoil	1	4	0.5	0.2	NULL	NULL
33	PeakSfunct_Fancoil	1	5	20	50	NULL	NULL
34	PeakMZSCSeem_Fancoil	1	5	0.5	0.2	NULL	NULL
35	PeakSfunct_Fancoil	1	6	20	20	NULL	NULL
36	PeakMZSCSeem_Fancoil	1	6	0.5	0.2	NULL	NULL
37	PeakSfunct_Fancoil	1	7	20	20	NULL	NULL
38	PeakMZSCSeem_Fancoil	1	7	0.5	0.2	NULL	NULL
39	PeakSfunct_Fancoil	1	8	20	20	NULL	NULL
40	PeakMZSCSeem_Fancoil	1	8	0.8	0.2	NULL	NULL
41	PeakSfunct_Fancoil	1	9	20	20	NULL	NULL
42	PeakMZSCSeem_Fancoil	1	9	0.8	0.2	NULL	NULL

FIGURE 5.18: Part of $fuzzyset$ Table in $smarttowndb$ DB

generally lower than the number of anomalies with low diagnostic index value (index between 0.5 and 0.7).

In Figures 5.28, 5.29, and 5.30 the fan-coils anomalies distributions by month and by year for F40 building are illustrated. The results are affected by problems in consumption data acquisition.

Figures 5.31, 5.32 and 5.33 show the lighting anomalies distributions by month and by year for F40 building. As in the previous case, the results are affected by problems in consumption data acquisition.

In Figures 5.34 and 5.35 the number of anomalies related to fan-coils and to light for each building of the cluster and for each year during the period April 2013 - June 2015 is shown respectively. The F68 building is characterized by the greatest number of fan-coils anomalies (1930 total), while the F72 building is the most virtuous (626 Total anomalies). The F71 building shows the greatest number of lighting anomalies (978 total), the building F70 the lowest number (77 total).

```
1 •  SELECT * FROM smarttowndb.historianc
```

idhistorianc	idcauses	label	meaning	Floor	idBuilding	time	value	sync
63925	1	C13a	Luci accese in assenza di persone	0	1	2014-02-19 09:50:00	0.996981583675292	0
63927	1	C13a	Luci accese in assenza di persone	1	1	2014-02-19 12:00:00	0.961538461538462	0
63931	1	C13a	Luci accese in assenza di persone	0	10	2014-02-19 12:45:00	0.862652768462569	0
63944	1	C13a	Luci accese in assenza di persone	2	1	2014-02-19 15:50:00	0.667747718620518	0
63926	1	C13a	Luci accese in assenza di persone	0	1	2014-02-19 16:30:00	0.5	0
63941	1	C13a	Luci accese in assenza di persone	0	9	2014-02-19 16:30:00	0.733333333333333	0
52446	3	C27	Fancoil accesi in assenza di persone	0	8	2014-02-20 00:00:00	0.977229467314245	0
52447	3	C27	Fancoil accesi in assenza di persone	0	8	2014-02-20 00:30:00	0.970101229524984	0
52501	3	C27	Fancoil accesi in assenza di persone	0	11	2014-02-20 00:45:00	0.622482818376449	0
63937	1	C13a	Luci accese in assenza di persone	1	1	2014-02-20 07:00:00	0.995920242191949	0
63938	1	C13a	Luci accese in assenza di persone	1	1	2014-02-20 07:10:00	0.975769856872619	0
52448	3	C27	Fancoil accesi in assenza di persone	0	8	2014-02-20 07:15:00	0.960830962325743	0
52449	3	C27	Fancoil accesi in assenza di persone	0	8	2014-02-20 07:30:00	0.970101229524984	0
63942	1	C13a	Luci accese in assenza di persone	0	11	2014-02-20 07:45:00	0.692307692307692	0
63940	1	C13a	Luci accese in assenza di persone	0	7	2014-02-20 08:00:00	0.727272727272727	0
52520	3	C27	Fancoil accesi in assenza di persone	0	1	2014-02-20 08:10:00	0.982013790037908	0
63939	1	C13a	Luci accese in assenza di persone	1	1	2014-02-20 08:20:00	0.807692307692308	0
63943	1	C13a	Luci accese in assenza di persone	1	1	2014-02-20 08:30:00	0.807692307692308	0
63945	1	C13a	Luci accese in assenza di persone	2	1	2014-02-20 08:30:00	0.666666666666667	0
63932	1	C13a	Luci accese in assenza di persone	0	1	2014-02-20 09:40:00	0.996722136180157	0
63933	1	C13a	Luci accese in assenza di persone	0	1	2014-02-20 10:10:00	0.75	0
63947	1	C13a	Luci accese in assenza di persone	0	6	2014-02-20 10:30:00	0.75	0
63949	1	C13a	Luci accese in assenza di persone	0	10	2014-02-20 10:45:00	0.6	0
63934	1	C13a	Luci accese in assenza di persone	0	1	2014-02-20 11:00:00	0.75	0
63950	1	C13a	Luci accese in assenza di persone	0	10	2014-02-20 11:00:00	0.6	0
63935	1	C13a	Luci accese in assenza di persone	0	1	2014-02-20 12:50:00	0.625	0
63936	1	C13a	Luci accese in assenza di persone	0	1	2014-02-20 14:20:00	0.625	0
52473	3	C27	Fancoil accesi in assenza di persone	0	9	2014-02-20 18:00:00	0.791270446595408	0
52450	3	C27	Fancoil accesi in assenza di persone	0	8	2014-02-20 21:45:00	0.813521448484973	0
52502	3	C27	Fancoil accesi in assenza di persone	0	11	2014-02-21 03:15:00	0.54157875438918	0

FIGURE 5.19: Part of *historianc* Table in *smarttowndb* DB

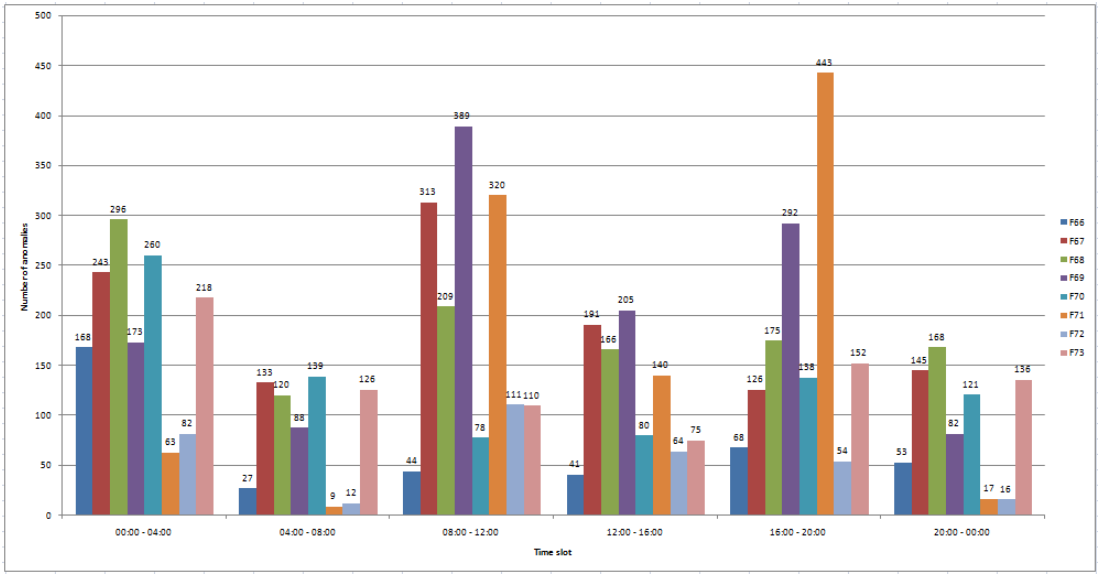

FIGURE 5.20: Cluster of buildings, fan-coils on in absence of people: time slots when anomalies occur per building in the year June 2014 - June 2015

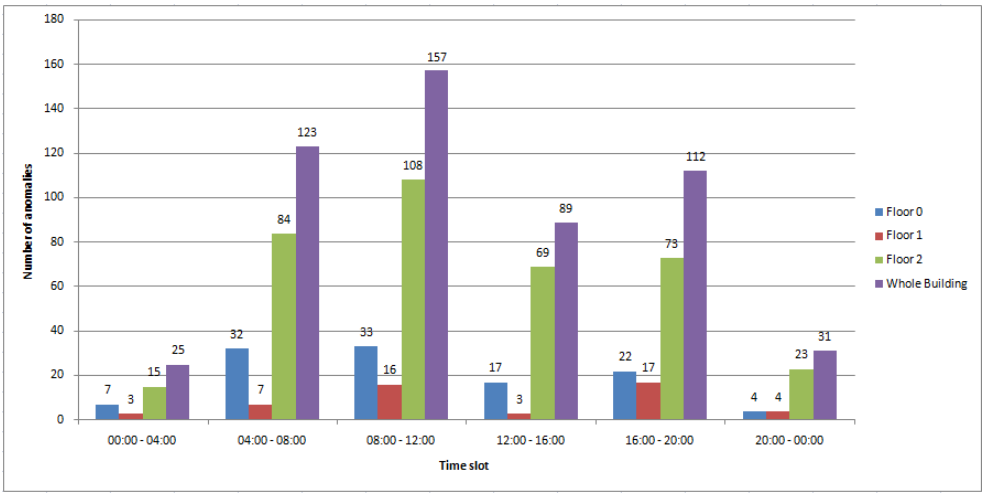

FIGURE 5.21: Building F40, fan-coils on in absence of people: time slots when anomalies occur per floor and in the whole building in the period July 2014 – June 2015

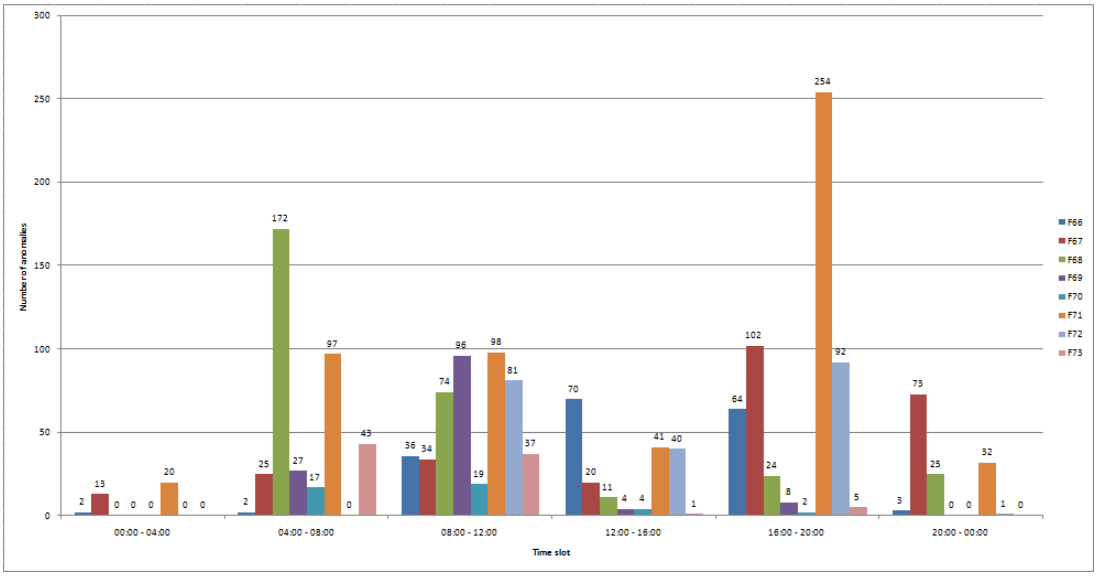

FIGURE 5.22: Cluster of buildings, lights on in absence of people: time slots when anomalies occur per building in the year June 2014 - June 2015

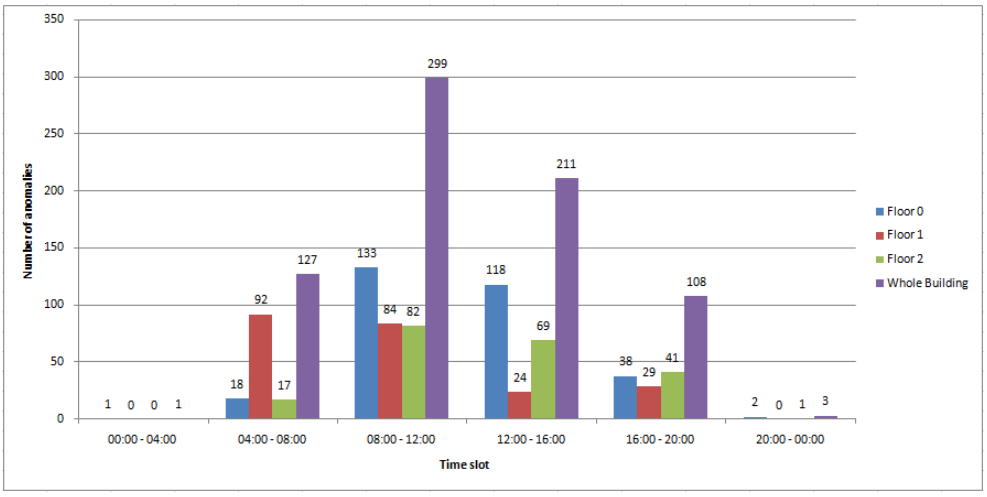

FIGURE 5.23: Building F40, lights on in absence of people: time slots when anomalies occur per floor and in the whole building in the period July 2014 – June 2015

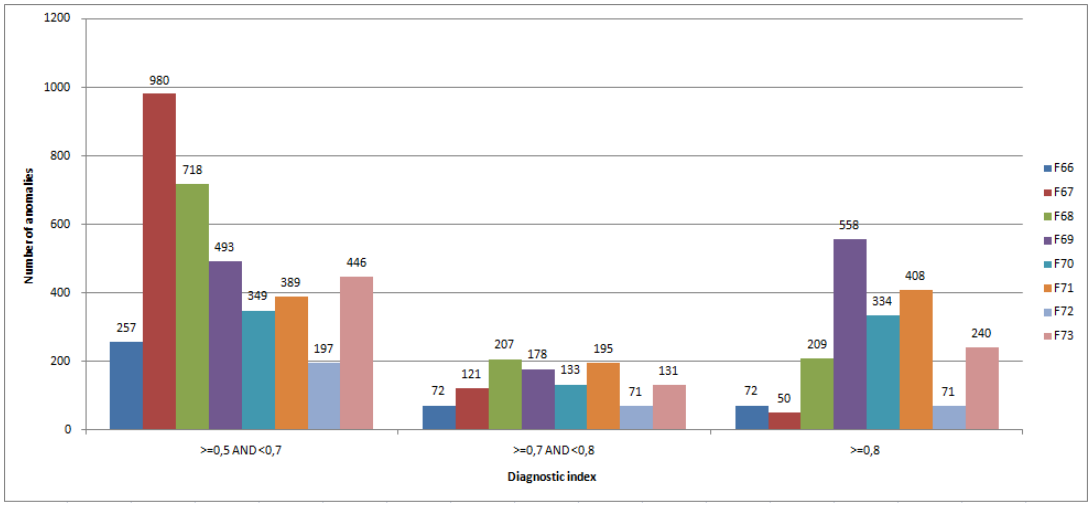

FIGURE 5.24: Cluster of buildings, fan-coils on in absence of people: diagnostic index of the anomalies per building in the year June 2014 - June 2015

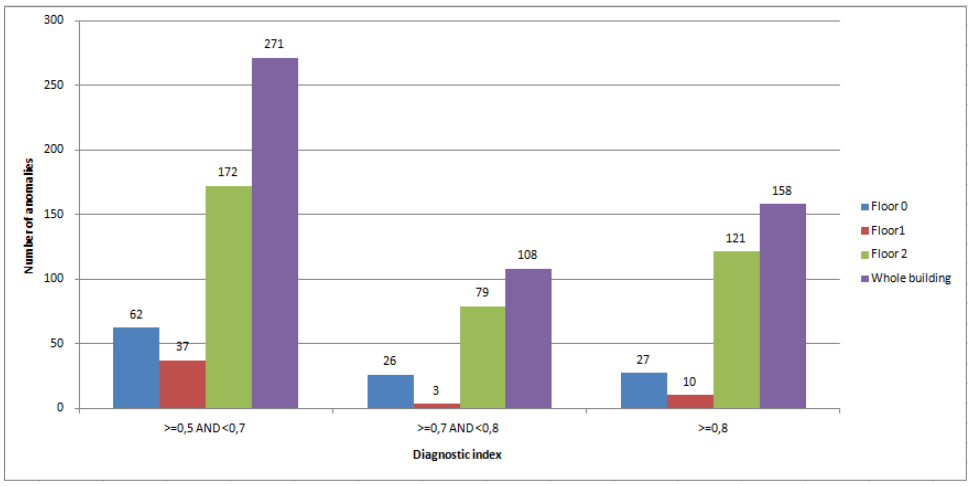

FIGURE 5.25: Building F40, fan-coils on in absence of people: diagnostic index of the anomalies per floor and in the whole building in the period July 2014 – June 2015

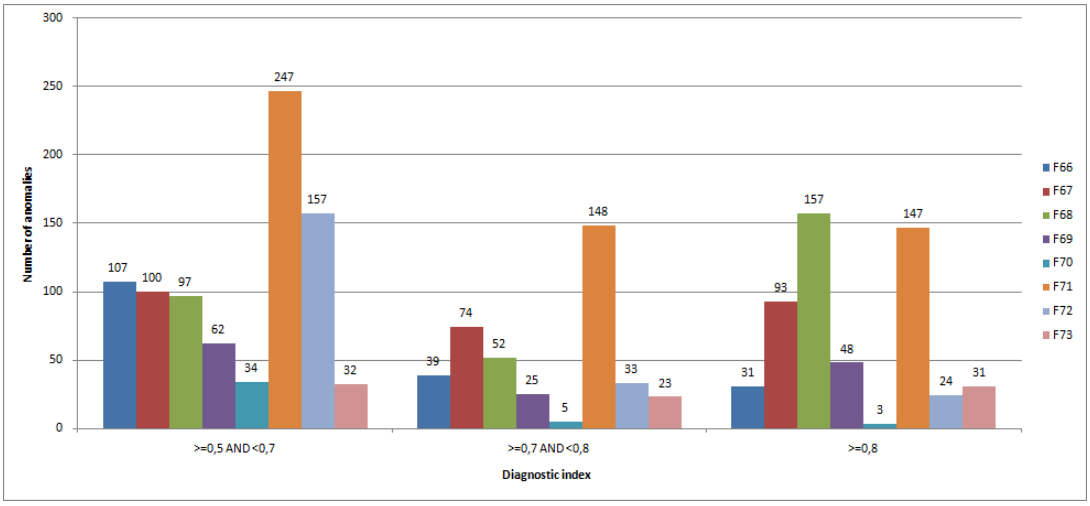

FIGURE 5.26: Cluster of buildings, lights on in absence of people: diagnostic index of the anomalies per building in the year June 2014 - June 2015

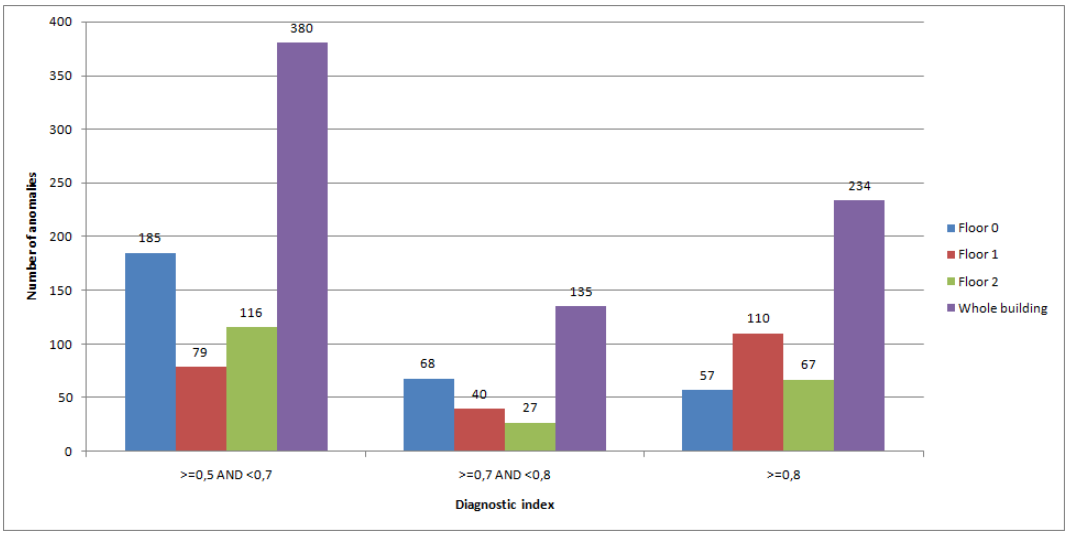

FIGURE 5.27: Building F40, lights on in absence of people: diagnostic index of the anomalies per floor and in the whole building in the period July 2014 – June 2015

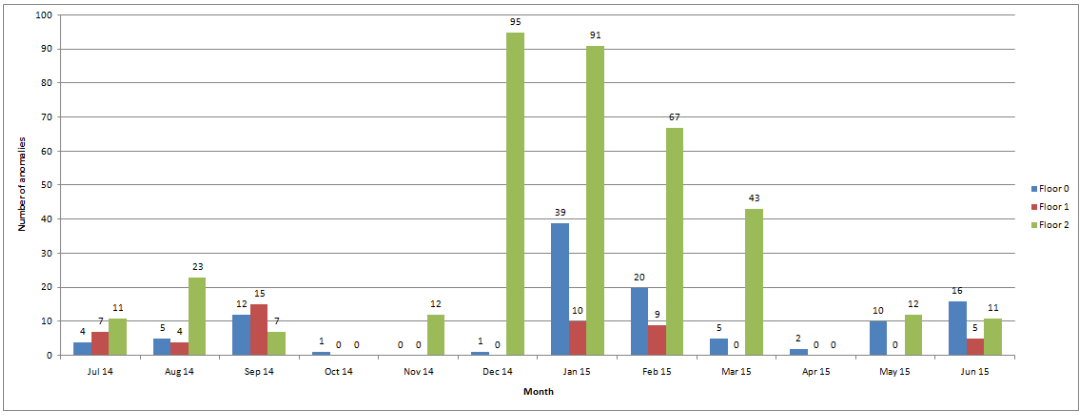

FIGURE 5.28: Building F40, fan-coils on in absence of people: monthly distribution of the anomalies per floor in the period July 2014 – June 2015

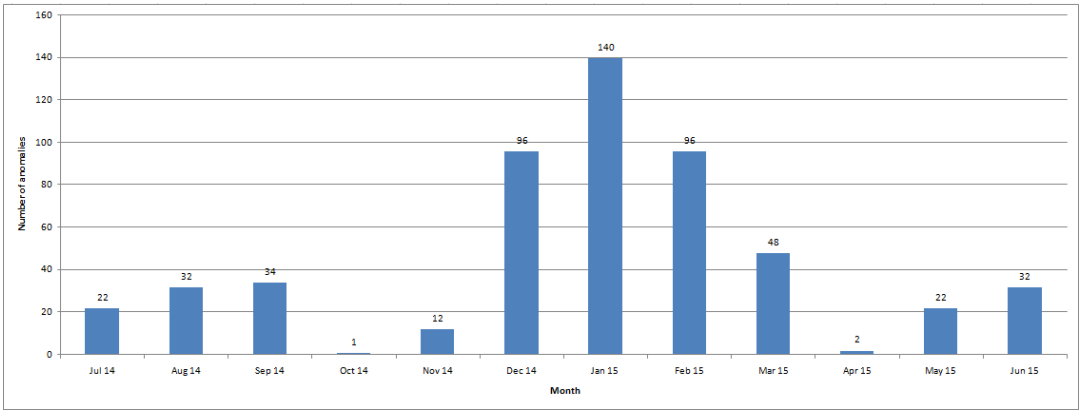

FIGURE 5.29: Building F40, fan-coils on in absence of people: monthly distribution of total anomalies in the period July 2014 – June 2015

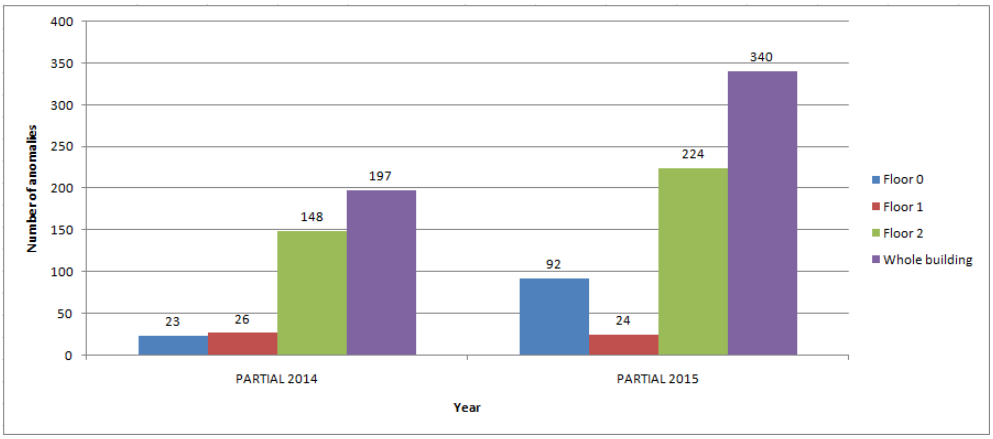

FIGURE 5.30: Building F40, fan-coils on in absence of people: yearly number of anomalies per floor and in the whole building in the period July 2014 – June 2015

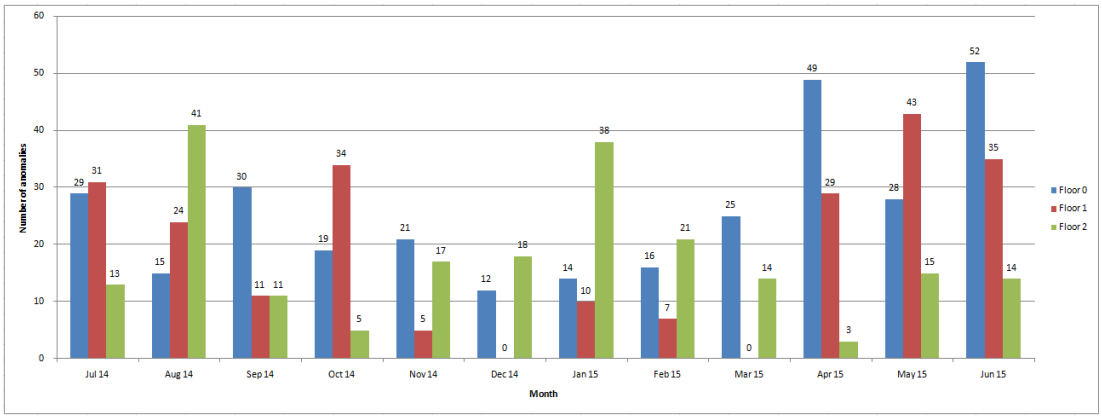

FIGURE 5.31: Building F40, lights on in absence of people: monthly distribution of the anomalies per floor in the period July 2014 – June 2015

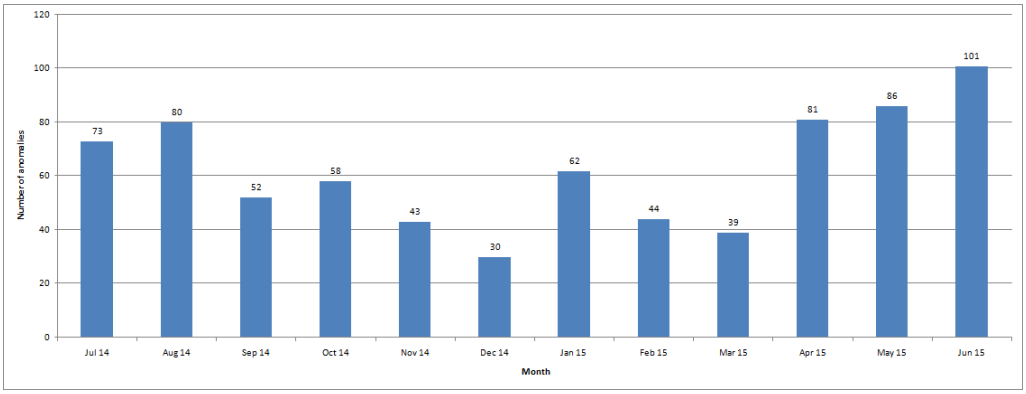

FIGURE 5.32: Building F40, lights on in absence of people: monthly distribution of total anomalies in the period July 2014 – June 2015

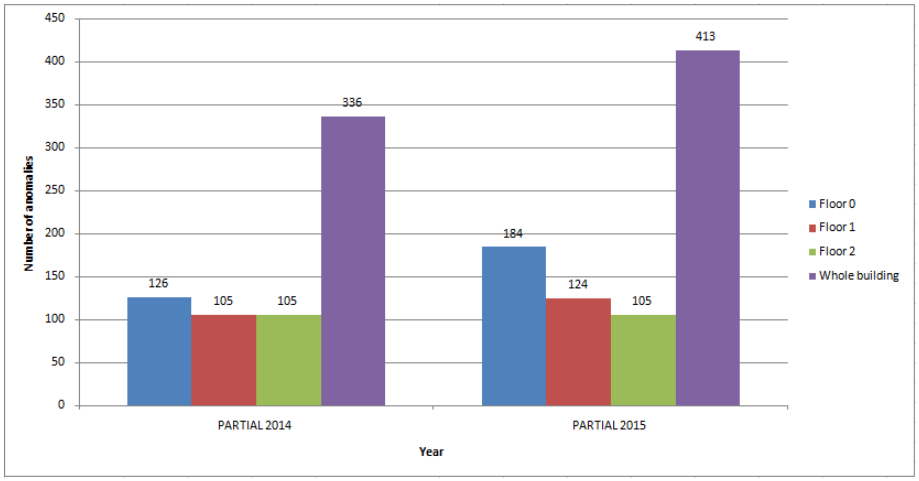

FIGURE 5.33: Building F40, lights on in absence of people: yearly number of anomalies per floor and in the whole building in the period July 2014 – June 2015

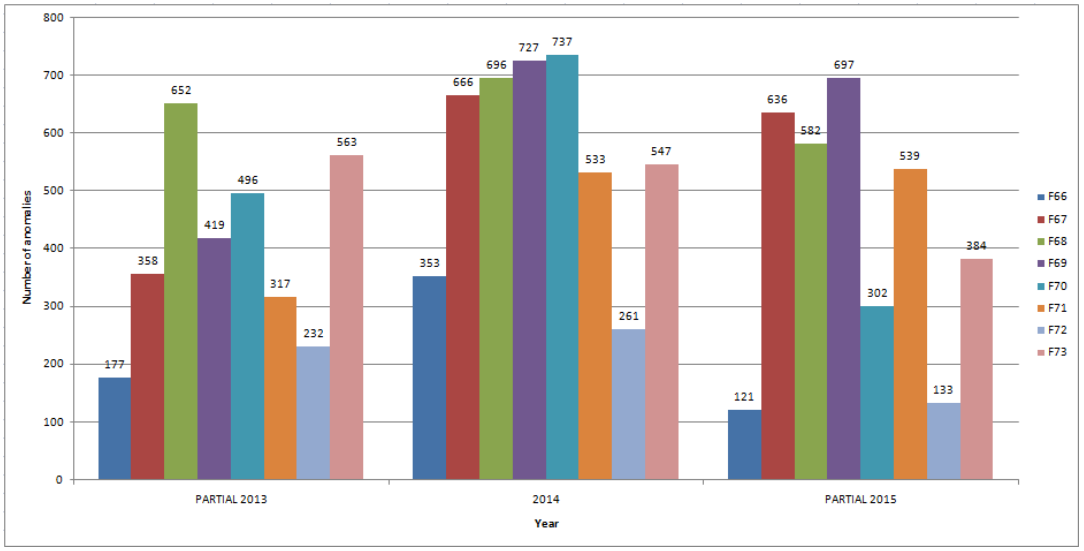

FIGURE 5.34: Cluster of buildings, fan-coils on in absence of people: yearly number of anomalies per building in the period April 2013 – June 2015

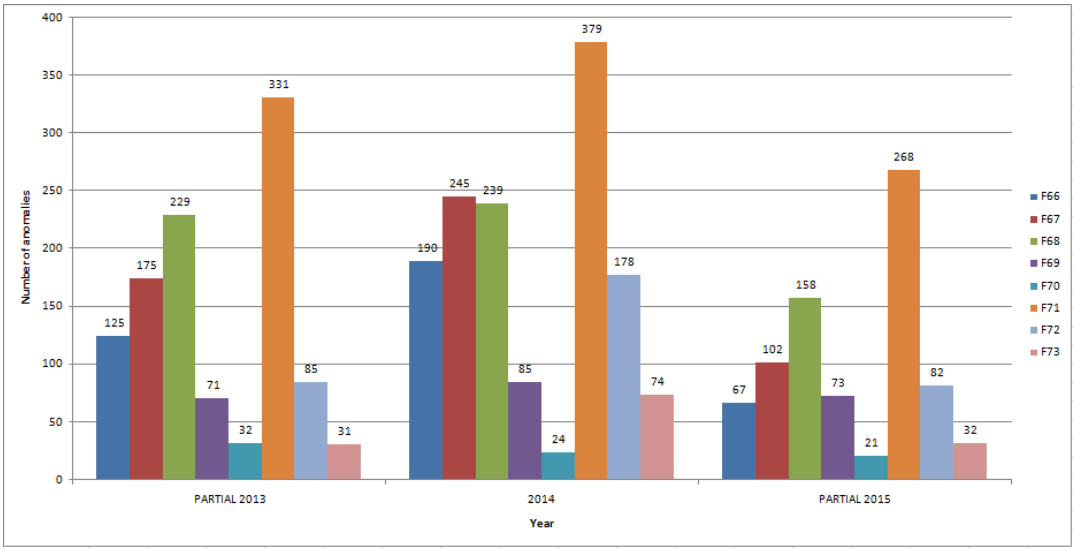

FIGURE 5.35: Cluster of buildings, lights on in absence of people: yearly number of anomalies per building in the period April 2013 – June 2015

Chapter 6

Conclusions

Smart Buildings go beyond energy savings and contributions to sustainability goals. They impact the management, security and safety of all resources, enable innovation by creating a platform for accessible information, and turn buildings into virtual power generators by allowing operators to reduce the electric load and sell the energy into the market. Smart Buildings are a key component of the future where information technology and energy sector combine to produce a robust and low-carbon economy.

This dissertation proposes a BEMS model for a Smart Building of the tertiary sector that interacts with the energy market with a classic consumer profile. In future works the suggested BEMS model can be extended to the cases of micro-grids (districts) where buildings and other consumers (classic and flexible), generation and storage elements, thus prosumers, are present. In this last cases BEMSs can take into account information from the rest of the district, thus contributing to the micro-grid management in a distributed way. This perspective assumes a rethinking of the concept of building, that deals with its management and at the same time is active element of a district context.

The proposed BEMS architecture is modular from the features point of view and hierarchical depending on the control frequency and the specific objective. The research experiences carried out in this work represent implementation and application examples of different modules operating at different levels.

In particular, two innovative and adaptive MPC strategies for multi-zone building temperature regulation using electrical heaters were proposed in Chapter 3. In order to reduce the energy consumption, at every simulation step the information about the occupancy level of each zone and the energy price profile were used. The experimentation was carried out considering the thermal coupling between the zones, thus comparing two possible MPC architectures (distributed and decentralized) in order to evaluate the best one in terms of control results (consumed energy and comfort). The distributed MPC with dynamic temperature set-points according to occupancy and energy price levels was proved to be the best MPC configuration in terms of consumed energy. This positive aspect corresponds to a slight disadvantage in discomfort terms (distance from the ideal indoor comfort temperature). Future work will focus on the analysis of the

asymptotic stability of the system and on the non-linear MPC implementation for the results comparison with the linear version presented in this work.

The research carried out in Chapter 4 was aimed at testing the potential of using data mining, artificial intelligence and statistical techniques for automated fault detection of both singular values and trends of anomalous consumption for a cluster of buildings. The methods proposed and implemented in the first part of the Chapter have proven adequate for the detection of anomalous values of lighting consumption with different potentials and limitations. In the context of Smart Buildings, the common detected outliers in the cluster of buildings demonstrate that the management of a Smart District can be operated with the whole cluster of buildings approach. The second part of the Chapter focused on the detection of anomalous trends of heating thermal power considering daily profiles with a hourly average timestamp. The application of the proposed approaches can improve fault detection processes in building context by reducing the number of false anomalies. The study will help BEMS by tracking and detecting anomalous energy consumption in building overall energy system. The methodology can be easily integrated with the BEMS to perform fault detection in "near" real time and can be applied to the buildings with similar end-uses. The developed methodology is already partially implemented and will be completed in the informatics infrastructure in ENEA Casaccia to supervise the building electrical and thermal energy consumptions of the cluster of buildings.

Chapter 5 starts demonstrating the effectiveness and usefulness of several techniques (ANN Estimator, BEM, Residual Analysis, Peak Detection, ANN Classifier, MVEM, Fuzzy Logic) for the FDD analysis of lighting energy consumption of an office building considering its operating conditions. The results show that ANN BEM always outperforms individual networks in artificial lighting power demand estimation. The fault detection, performed trough the analysis of the magnitude of residuals using a peak detection method, allowed to detect two artificial faults and some other actual anomalous power values in the testing data set. An ANN ensemble for classification of operational data has been also developed, considering as output of the network the operating state of the system as "normal" or "anomalous". A very high accuracy of the developed classifier was verified in detecting anomalous artificial lighting power values using a MVEM. Finally, a diagnostic index ranging from 0 to 1 indicates the severity degree of an anomalous energy consumption associated to a particular cause. This index was implemented using fuzzy sets, which provide a transparent model easy to be interpreted, where several process variables like hour of the day, active rooms percentage and power consumption are combined. The lighting energy consumption profile of the building is strictly dependent on the external lighting conditions that were considered through the global solar radiation data. The global solar radiation changes considerably on the basis of the season. The proposed methodology is really transferable to the

building operation in other months because it's possible to build (train) the neural models for every season of the year and apply (test) them in the corresponding season. In particular the diagnosis process (identification of the cause) was related to anomalous lighting energy values out of the working hours. In further studies the methodologies here proposed can be effectively used also for the diagnosis of anomalous trends (and not only of peaks) of building consumptions (e. g. "after a work day some users have forgotten to turn off their lights") since the residual analysis and the pattern recognition methods proposed are able to detect consecutive anomalous values and consequently begin the diagnostic process. In the second part of the Chapter a FDD analysis algorithm based on the proposed methodology was implemented and included in the ICT platform of the "Smart Village" project of the ENEA Casaccia Research Centre. The aim was to obtain for the buildings involved in the project an on-line and near real-time application tool for the FDD analysis of the lighting and fan-coil anomalous electrical consumptions caused by the improper use of the employees. The one year experimentation results demonstrate the effectiveness of the implemented application as a powerful tool for the Energy Manager: in fact it proves to be useful for the short-term diagnosis of anomalous consumption related to the occupant bad behavior, and indirectly in the medium/long period it provides feedback on possible device failures and on the proper application of the building control strategies.

Appendix A

Publications

- Journals
  - Lauro, F., Moretti, F., Capozzoli, A., Khan, I., Pizzuti, S., Macas, M., & Panzieri, S. (2014). Building fan coil electric consumption analysis with fuzzy approaches for fault detection and diagnosis. Energy Procedia, 62, 411-420.
  - Capozzoli, A., Lauro, F., & Khan, I. (2015). Fault detection analysis using data mining techniques for a cluster of smart office buildings. Expert Systems with Applications, 42(9), 4324-4338.
  - Lauro, F., Moretti, F., Capozzoli, A., & Panzieri, S. (2015). Model Predictive Control for Building Active Demand Response Systems. Energy Procedia, 83, 494-503.
- Conference Proceedings
  - Lauro, F., Capozzoli, A., & Pizzuti, S. (2013). Building Energy Consumption Modeling with Neural Ensembling Approaches for Fault Detection Analysis. Sustainability in Energy and Buildings: Research Advances, KES Open Access LibrAry, Special Edition - Mediterranean Green Energy Forum 2013 (MGEF-13), (2), pp. 7-12.
  - Marino, F., Capozzoli, A., Grossoni, M., Lauro, F., Leccese, F., Moretti, F., Panzieri, S. & Pizzuti, S. (2014). Indoor lighting fault detection and diagnosis using a data fusion approach. Energy Production and Management in the 21st Century: The Quest for Sustainable Energy, 190, 183.
  - Macas, M., Moretti, F., Lauro, F., Pizzuti, S., Annunziato, M., Fonti, A., Comodi, G. & Giantomassi, A. (2014). Importance of Feature Selection for Recurrent Neural Network Based Forecasting of Building Thermal Comfort. In Adaptive and Intelligent Systems (pp. 11-19). Springer International Publishing.

  - Macas, M., Lauro, F., Moretti, F., Pizzuti, S., Annunziato, M., Fonti, A., Comodi, G. & Giantomassi, A. (2014, January). Sensitivity based feature selection for recurrent neural network applied to forecasting of heating gas consumption. In International Joint Conference SOCO'14-CISIS'14-ICEUTE'14 (pp. 259-268). Springer International Publishing.
  - Khan, I., Capozzoli, A., Lauro, F., Corgnati, S. P., & Pizzuti, S. (2014). Building Energy Management Through Fault Detection Analysis Using Pattern Recognition Techniques Applied on Residual Neural Networks. In Advances in Artificial Life and Evolutionary Computation (pp. 1-12). Springer International Publishing.
  - Lauro, F., Longobardi, L., & Panzieri, S. (2014, October). An adaptive distributed predictive control strategy for temperature regulation in a multizone office building. In Intelligent Energy Systems (IWIES), 2014 IEEE International Workshop on (pp. 32-37). IEEE.

- Technical Reports
  - Corgnati, S. P., Capozzoli, A., Khan, I., Lauro, F., Raimondo, D., & Talà, N. (2013). Metodi per l'analisi prestazionale di reti di edifici e test su dati sperimentali e simulatore. Technical Report for "Ricerca di Sistema Elettrico" Project. RdS/2012/121. (Italian)
  - Capozzoli, A., Corgnati, S. P., Khan, I., Lauro, F., & Raimondo, D. (2014). Validazione, analisi e modelli di diagnostica energetica avanzata di reti di edifici. Technical Report for "Ricerca di Sistema Elettrico" Project". RdS/2013/061. (Italian)
  - Capozzoli, A., Corgnati, S. P., Fabi, V., Lauro, F., & Raimondo, D. (2015). Validazione, analisi, sviluppo ed implementazione di modelli di diagnostica orientata a reti di edifici. Technical Report for "Ricerca di Sistema Elettrico" Project. (Italian)

Bibliography

[1] International Energy Agency. "World Energy Outlook 2008". In: *IEA* (2008).

[2] Oral Alan and Cagatay Catal. "Thresholds based outlier detection approach for mining class outliers: An empirical case study on software measurement datasets". In: *Expert Systems with Applications* 38.4 (2011), pp. 3440–3445.

[3] Michael A Arbib. *The handbook of brain theory and neural networks*. MIT press, 2003.

[4] Andreas Arning, Rakesh Agrawal, and Prabhakar Raghavan. "A Linear Method for Deviation Detection in Large Databases." In: *KDD*. 1996, pp. 164–169.

[5] Dmitry G Arseniev, Boris E Lyubimov, and Vyacheslav P Shkodyrev. "Intelligent fault detection and diagnostics system on rule-based neural network approach". In: *2009 IEEE Control Applications,(CCA) &Intelligent Control,(ISIC)*. 2009.

[6] T Bag and SK Samanta. "A comparative study of fuzzy norms on a linear space". In: *Fuzzy Sets and Systems* 159.6 (2008), pp. 670–684.

[7] VSKM Balijepalli et al. "Review of demand response under smart grid paradigm". In: *Innovative Smart Grid Technologies-India (ISGT India), 2011 IEEE PES*. IEEE. 2011, pp. 236–243.

[8] Yves Bamberger et al. *STRATEGIC RESEARCH AGENDA FOR EUROPE'S ELECTRICITY NETWORKS OF THE FUTURE*. Office for Official Publications of the European Communities, 2007.

[9] Jayanta Kumar Basu, Debnath Bhattacharyya, and Tai-hoon Kim. "Use of artificial neural network in pattern recognition". In: *International journal of software engineering and its applications* 4.2 (2010).

[10] Ilaria Bertini et al. "Rotor imbalance detection in gas turbines using fuzzy sets". In: *Distributed Computing, Artificial Intelligence, Bioinformatics, Soft Computing, and Ambient Assisted Living*. Springer, 2009, pp. 1195–1204.

[11] Christopher M Bishop. *Neural networks for pattern recognition*. Oxford university press, 1995.

[12] Leo Breiman. "Combining predictors". In: *Combining artificial neural nets* 31 (1999).

[13] DE Calridge et al. "Monitored commercial building energy data: reporting the results." In: *ASHRAE Winter Meeting, Anaheim, CA, USA, 01/25-29/92*. 1992, pp. 887–889.

[14] Francesco Calvino et al. "The control of indoor thermal comfort conditions: introducing a fuzzy adaptive controller". In: *Energy and Buildings* 36.2 (2004), pp. 97–102.

[15] Eduardo F Camacho and Carlos Bordons Alba. *Model predictive control*. Springer Science & Business Media, 2013.

[16] Hui Cao et al. "Enhancing effectiveness of density-based outlier mining scheme with density-similarity-neighbor-based outlier factor". In: *Expert Systems with Applications* 37.12 (2010), pp. 8090–8101.

[17] Alfonso Capozzoli, Fiorella Lauro, and Imran Khan. "Fault detection analysis using data mining techniques for a cluster of smart office buildings". In: *Expert Systems with Applications* 42.9 (2015), pp. 4324–4338.

[18] VJ Carey et al. "Resistant and test-based outlier rejection: effects on Gaussian one-and two-sample inference". In: *Technometrics* 39.3 (1997), pp. 320–330.

[19] M Castilla et al. "A comparison of thermal comfort predictive control strategies". In: *Energy and buildings* 43.10 (2011), pp. 2737–2746.

[20] Shuyan Chen, Wei Wang, and Henk van Zuylen. "A comparison of outlier detection algorithms for ITS data". In: *Expert Systems with Applications* 37.2 (2010), pp. 1169–1178.

[21] Yumin Chen, Duoqian Miao, and Hongyun Zhang. "Neighborhood outlier detection". In: *Expert Systems with Applications* 37.12 (2010), pp. 8745–8749.

[22] Albert Chiu et al. "Framework for Integrated Demand Response (DR) and Distributed Energy Resources (DER) Models". In: *NAESB & UCAIug. September* (2009).

[23] Jiří Cigler et al. "Optimization of predicted mean vote index within model predictive control framework: Computationally tractable solution". In: *Energy and Buildings* 52 (2012), pp. 39–49.

[24] Smart Energy Demand Coalition. "Mapping demand response in Europe today". In: *Tracking Compliance with Article* 15 (2014).

[25] Wesley J Cole, David P Morton, and Thomas F Edgar. "Optimal electricity rate structures for peak demand reduction using economic model predictive control". In: *Journal of Process Control* 24.8 (2014), pp. 1311–1317.

[26] European Commission. "Energy yearly statistics 2007". In: *EUROSTAT* (2009).

[27] Sourabh Dash, Raghunathan Rengaswamy, and Venkat Venkatasubramanian. "Fuzzy-logic based trend classification for fault diagnosis of chemical processes". In: *Computers & Chemical Engineering* 27.3 (2003), pp. 347–362.

[28] Arthur Dexter, Jouko Pakanen, et al. "Demonstrating automated fault detection and diagnosis methods in real buildings". In: *VTT Building Technology, Finland (ISBN 951-38-5726-3), ANNEX* 34 (2001).

[29] Natasa Djuric and Vojislav Novakovic. "Review of possibilities and necessities for building lifetime commissioning". In: *Renewable and Sustainable Energy Reviews* 13.2 (2009), pp. 486–492.

[30] Robert H Dodier and Jan F Kreider. "Detecting whole building energy problems". In: *ASHRAE transactions* 105 (1999), p. 579.

[31] Juan Du, Meng Joo Er, and Leszek Rutkowski. "Fault diagnosis of an air-handling unit system using a dynamic fuzzy-neural approach". In: *Artificial Intelligence and Soft Computing*. Springer. 2010, pp. 58–65.

[32] Zhimin Du, Xinqiao Jin, and Yunyu Yang. "Fault diagnosis for temperature, flow rate and pressure sensors in VAV systems using wavelet neural network". In: *Applied energy* 86.9 (2009), pp. 1624–1631.

[33] Didier Dubois and Henri Prade. "A CLASS OF FUZZY MEASURES BASED ON TRIANGULAR NORMS† A general framework for the combination of uncertain information". In: *International Journal Of General System* 8.1 (1982), pp. 43–61.

[34] Matthew S Elliott and Bryan P Rasmussen. "Decentralized model predictive control of a multi-evaporator air conditioning system". In: *Control Engineering Practice* 21.12 (2013), pp. 1665–1677.

[35] Martin Ester et al. "A density-based algorithm for discovering clusters in large spatial databases with noise." In: *Kdd*. Vol. 96. 34. 1996, pp. 226–231.

[36] Pedro Faria et al. "Demand response management in power systems using a particle swarm optimization approach". In: *IEEE Intelligent Systems* 28.4 (2013), pp. 43–51.

[37] Romain Fontugne et al. "Strip, bind, and search: a method for identifying abnormal energy consumption in buildings". In: *Proceedings of the 12th international conference on Information processing in sensor networks*. ACM. 2013, pp. 129–140.

[38] Linas Gelazanskas and Kelum AA Gamage. "Demand side management in smart grid: a review and proposals for future direction". In: *Sustainable Cities and Society* 11 (2014), pp. 22–30.

[39] Siegfried Gottwald. "Foundations of a set theory for fuzzy sets. 40 years of development". In: *International journal of general systems* 37.1 (2008), pp. 69–81.

[40] J Haberl, R Sparks, and C Culp. "Exploring new techniques for displaying complex building energy consumption data". In: *Energy and buildings* 24.1 (1996), pp. 27–38.

[41] JS Haberl and M Abbas. "Development of graphical indices for viewing building energy data: Part I". In: *Journal of solar energy engineering* 120.3 (1998), pp. 156–161.

[42] JS Haberl and M Abbas. "Development of graphical indices for viewing building energy data: Part II". In: *Journal of solar energy engineering* 120.3 (1998), pp. 162–167.

[43] AK Halm-Owoo and KO Suen. "Applications of fault detection and diagnostic techniques for refrigeration and air conditioning: A review of basic principles". In: *Proceedings of the Institution of Mechanical Engineers, Part E: Journal of Process Mechanical Engineering* 216.3 (2002), pp. 121–132.

[44] Hua Han et al. "PCA-SVM-based automated fault detection and diagnosis (AFDD) for vapor-compression refrigeration systems". In: *HVAC&R Research* 16.3 (2010), pp. 295–313.

[45] Lars Kai Hansen and Peter Salamon. "Neural network ensembles". In: *IEEE Transactions on Pattern Analysis & Machine Intelligence* 10 (1990), pp. 993–1001.

[46] Philip Haves. "Overview of diagnostic methods". In: *Proceedings of the workshop on diagnostics for commercial buildings: From research to practice*. 1999, pp. 16–17.

[47] Philip Haves. "Study of on-line simulation for whole building level energy consumption fault detection and optimization". In: (2004).

[48] Daniel Holcomb, Wenchao Li, and Sanjit A Seshia. "Algorithms for green buildings: Learning-based techniques for energy prediction and fault diagnosis". In: *Google Scholar, UCB/EECS-2009-138* (2009).

[49] John M House, Won Yong Lee, and Dong Ryul Shin. "Classification techniques for fault detection and diagnosis of an air-handling unit". In: *ASHRAE Transactions* 105 (1999), p. 1087.

[50] J Hyvärinen and S Kärki. "Building Optimization and Fault Diagnosis Source Book, IEA Annex 25". In: *Finland: VTT* (1996).

[51] Lucia Igualada et al. "Optimal energy management for a residential microgrid including a vehicle-to-grid system". In: *Smart Grid, IEEE Transactions on* 5.4 (2014), pp. 2163–2172.

[52] Global eSustainability Initiative et al. *SMART 2020: Enabling the low carbon economy in the information age*. Climate Group, 2008.

[53] R Jagpal. "Computer aided evaluation of HVAC system performance: Technical synthesis report". In: *International Energy Agency* (2006).

[54] Rod Janssen. "Towards energy efficient buildings in Europe". In: *London: The European Alliance of Companies for Energy Efficiency in Buildings* (2004).

[55] Biing-Hwang Juang and Lawrence R Rabiner. "The segmental K-means algorithm for estimating parameters of hidden Markov models". In: *Acoustics, Speech and Signal Processing, IEEE Transactions on* 38.9 (1990), pp. 1639–1641.

[56] Soteris Kalogirou et al. "Development of a neural network-based fault diagnostic system for solar thermal applications". In: *Solar Energy* 82.2 (2008), pp. 164–172.

[57] Srinivas Katipamula and Michael R Brambley. "Review article: methods for fault detection, diagnostics, and prognostics for building systems—a review, Part I". In: *HVAC&R Research* 11.1 (2005), pp. 3–25.

[58] Srinivas Katipamula and Michael R Brambley. "Review article: Methods for fault detection, diagnostics, and prognostics for building systems—a review, part ii". In: *HVAC&R Research* 11.2 (2005), pp. 169–187.

[59] Imran Khan et al. "Building energy management through fault detection analysis using pattern recognition techniques applied on residual neural networks".

In: *Advances in Artificial Life and Evolutionary Computation*. Springer, 2014, pp. 1–12.

[60] Imran Khan et al. "Fault detection analysis of building energy consumption using data mining techniques". In: *Energy Procedia* 42 (2013), pp. 557–566.

[61] Bart Kosko. "Neural networks and fuzzy systems: a dynamical systems approach to machine intelligence/book and disk". In: *Vol. 1Prentice hall* (1992).

[62] Anders Krogh, Jesper Vedelsby, et al. "Neural network ensembles, cross validation, and active learning". In: *Advances in neural information processing systems* 7 (1995), pp. 231–238.

[63] Hakan Kuşan, Osman Aytekin, and İlker Özdemir. "The use of fuzzy logic in predicting house selling price". In: *Expert systems with Applications* 37.3 (2010), pp. 1808–1813.

[64] Florence Lai, Frederic Magoules, and Fred Lherminier. "Vapnik's learning theory applied to energy consumption forecasts in residential buildings". In: *International Journal of Computer Mathematics* 85.10 (2008), pp. 1563–1588.

[65] Louisa Lam and Ching Y Suen. "Application of majority voting to pattern recognition: an analysis of its behavior and performance". In: *Systems, Man and Cybernetics, Part A: Systems and Humans, IEEE Transactions on* 27.5 (1997), pp. 553–568.

[66] Fiorella Lauro, Alfonso Capozzoli, and Stefano Pizzuti. "Building energy consumption modeling with neural ensembling approaches for fault detection analysis". In: *Sustainability in Energy and Buildings: Research Advances ISSN 2054-3743* 2 (2012), p. 7.

[67] Fiorella Lauro, Luigi Longobardi, and Stefano Panzieri. "An adaptive distributed predictive control strategy for temperature regulation in a multizone office building". In: *Intelligent Energy Systems (IWIES), 2014 IEEE International Workshop on*. IEEE. 2014, pp. 32–37.

[68] Fiorella Lauro et al. "Building fan coil electric consumption analysis with fuzzy approaches for fault detection and diagnosis". In: *Energy Procedia* 62 (2014), pp. 411–420.

[69] Fiorella Lauro et al. "Model Predictive Control for Building Active Demand Response Systems". In: *Energy Procedia* 83 (2015), pp. 494–503.

[70] Shun Li and Jin Wen. "A model-based fault detection and diagnostic methodology based on PCA method and wavelet transform". In: *Energy and Buildings* 68 (2014), pp. 63–71.

[71] Xiaoli Li, Chris P Bowers, and Thorsten Schnier. "Classification of energy consumption in buildings with outlier detection". In: *Industrial Electronics, IEEE Transactions on* 57.11 (2010), pp. 3639–3644.

[72] Xiwang Li and Jin Wen. "Review of building energy modeling for control and operation". In: *Renewable and Sustainable Energy Reviews* 37 (2014), pp. 517–537.

[73] J Liang and R Du. "Design of intelligent comfort control system with human learning and minimum power control strategies". In: *Energy conversion and management* 49.4 (2008), pp. 517–528.

[74] Jian Liang and Ruxu Du. "Model-based fault detection and diagnosis of HVAC systems using support vector machine method". In: *International Journal of refrigeration* 30.6 (2007), pp. 1104–1114.

[75] Martin W Liddament. "Real Time Simulation of HVAC Systems for Building Optimisation". In: *Fault Detection and Diagnostics, ECBCS, Coventry* (1999).

[76] Dandan Liu et al. "A method for detecting abnormal electricity energy consumption in buildings". In: *Journal of Computational Information Systems* 6.14 (2010), pp. 4887–4895.

[77] Yong Liu and Xin Yao. "Ensemble learning via negative correlation". In: *Neural Networks* 12.10 (1999), pp. 1399–1404.

[78] Jingran Ma, S Joe Qin, and Timothy Salsbury. "Application of economic MPC to the energy and demand minimization of a commercial building". In: *Journal of Process Control* 24.8 (2014), pp. 1282–1291.

[79] Jingran Ma et al. "Demand reduction in building energy systems based on economic model predictive control". In: *Chemical Engineering Science* 67.1 (2012), pp. 92–100.

[80] Ookie Ma et al. "Demand response for ancillary services". In: *Smart Grid, IEEE Transactions on* 4.4 (2013), pp. 1988–1995.

[81] Frédéric Magoulès, Hai-xiang Zhao, and David Elizondo. "Development of an RDP neural network for building energy consumption fault detection and diagnosis". In: *Energy and Buildings* 62 (2013), pp. 133–138.

[82] F Marino et al. "Indoor lighting fault detection and diagnosis using a data fusion approach". In: *Energy Production and Management in the 21st Century: The Quest for Sustainable Energy* 190 (2014), p. 183.

[83] Mano Ram Maurya, Raghunathan Rengaswamy, and Venkat Venkatasubramanian. "Fault diagnosis using dynamic trend analysis: A review and recent developments". In: *Engineering applications of artificial intelligence* 20.2 (2007), pp. 133–146.

[84] Mano Ram Maurya et al. "A framework for on-line trend extraction and fault diagnosis". In: *Engineering Applications of Artificial Intelligence* 23.6 (2010), pp. 950–960.

[85] Georgios Mavromatidis, Salvador Acha, and Nilay Shah. "Diagnostic tools of energy performance for supermarkets using Artificial Neural Network algorithms". In: *Energy and Buildings* 62 (2013), pp. 304–314.

[86] Patricia Melin and Oscar Castillo. "A review on the applications of type-2 fuzzy logic in classification and pattern recognition". In: *Expert Systems with Applications* 40.13 (2013), pp. 5413–5423.

[87] David I Mendoza-Serrano and Donald J Chmielewski. "Smart grid coordination in building HVAC systems: EMPC and the impact of forecasting". In: *Journal of Process Control* 24.8 (2014), pp. 1301–1310.

[88] N Milesi Ferretti and D Choiniere. "Annex 47 Extended Project Summary". In: *NIST TN* (1750).

[89] Rim Missaoui et al. "Managing energy smart homes according to energy prices: analysis of a building energy management system". In: *Energy and Buildings* 71 (2014), pp. 155–167.

[90] P Morosan et al. "Distributed model predictive control for building temperature regulation". In: *American Control Conference (ACC), 2010*. IEEE. 2010, pp. 3174–3179.

[91] Petru-Daniel Moroşan et al. "A distributed MPC strategy based on Benders' decomposition applied to multi-source multi-zone temperature regulation". In: *Journal of Process Control* 21.5 (2011), pp. 729–737.

[92] Petru-Daniel Moroşan et al. "A dynamic horizon distributed predictive control approach for temperature regulation in multi-zone buildings". In: *Control & Automation (MED), 2010 18th Mediterranean Conference on*. IEEE. 2010, pp. 622–627.

[93] Petru-Daniel Morosan et al. "Distributed MPC for multizone temperature regulation with coupled constraints". In: *IFAC World Congress*. 2011, pp. 729–737.

[94] Timothy Mulumba et al. "Robust model-based fault diagnosis for air handling units". In: *Energy and Buildings* 86 (2015), pp. 698–707.

[95] Nabil Nassif, Stanislaw Kajl, and Robert Sabourin. "Optimization of HVAC control system strategy using two-objective genetic algorithm". In: *HVAC&R Research* 11.3 (2005), pp. 459–486.

[96] Rudy R Negenborn and JM Maestre. "Distributed model predictive control: An overview and roadmap of future research opportunities". In: *Control Systems, IEEE* 34.4 (2014), pp. 87–97.

[97] TT Nguyen and Ashkan Yousefi. "Multi-objective demand response allocation in restructured energy market". In: *Innovative Smart Grid Technologies (ISGT), 2011 IEEE PES*. IEEE. 2011, pp. 1–8.

[98] Tuan Anh Nguyen and Marco Aiello. "Energy intelligent buildings based on user activity: A survey". In: *Energy and buildings* 56 (2013), pp. 244–257.

[99] SOT Ogaji et al. "Gas-turbine fault diagnostics: a fuzzy-logic approach". In: *Applied Energy* 82.1 (2005), pp. 81–89.

[100] Frauke Oldewurtel et al. "Reducing peak electricity demand in building climate control using real-time pricing and model predictive control". In: *Decision and Control (CDC), 2010 49th IEEE Conference on*. IEEE. 2010, pp. 1927–1932.

[101] V Palade, CD Bocaniala, and L Iain. *Computational intelligence in fault diagnosis, 2006*.

[102] G Palshikar et al. "Simple algorithms for peak detection in time-series". In: *Proc. 1st Int. Conf. Advanced Data Analysis, Business Analytics and Intelligence*. 2009.

[103] Nang-Fei Pan. "Evaluation of building performance using fuzzy FTA". In: *Construction Management and Economics* 24.12 (2006), pp. 1241–1252.

[104] NF Pan, RJ Dzeng, and MD Yang. "Performance evaluation of constructed facilities through linguistic judgment". In: *Industrial Engineering and Engineering Management, 2009. IEEM 2009. IEEE International Conference on*. IEEE. 2009, pp. 827–831.

[105] Alessandra Parisio et al. "A scenario-based predictive control approach to building HVAC management systems". In: *Automation Science and Engineering (CASE), 2013 IEEE International Conference on*. IEEE. 2013, pp. 428–435.

[106] RJ Patton, CJ Lopez-Toribio, and FJ Uppal. "Artificial intelligence approaches to fault diagnosis for dynamic systems". In: *International Journal of applied mathematics and computer science* 9.3 (1999), pp. 471–518.

[107] Michael P Perrone and Leon N Cooper. *When networks disagree: Ensemble methods for hybrid neural networks*. Tech. rep. DTIC Document, 1992.

[108] Pierre Pinson, Henrik Madsen, et al. "Benefits and challenges of electrical demand response: A critical review". In: *Renewable and Sustainable Energy Reviews* 39 (2014), pp. 686–699.

[109] Phetkeo Poumanyvong and Shinji Kaneko. "Does urbanization lead to less energy use and lower CO 2 emissions? A cross-country analysis". In: *Ecological Economics* 70.2 (2010), pp. 434–444.

[110] L Prazeres and JA Clarke. "Communicating building simulation outputs to users". In: *Proceedings of Building Simulation*. 2003.

[111] Vamsi Putta et al. "A distributed approach to efficient model predictive control of building HVAC systems". In: (2012).

[112] Sridhar Ramaswamy, Rajeev Rastogi, and Kyuseok Shim. "Efficient algorithms for mining outliers from large data sets". In: *ACM SIGMOD Record*. Vol. 29. 2. ACM. 2000, pp. 427–438.

[113] Roozbeh Razavi-Far, Enrico Zio, and Vasile Palade. "Efficient residuals preprocessing for diagnosing multi-class faults in a doubly fed induction generator, under missing data scenarios". In: *Expert Systems with Applications* 41.14 (2014), pp. 6386–6399.

[114] Jakob Rehrl and Martin Horn. "Model Predictive Control for Heating Ventilating and Air Conditioning Systems". In: *PAMM* 11.1 (2011), pp. 833–834.

[115] James A Rodger. "A fuzzy nearest neighbor neural network statistical model for predicting demand for natural gas and energy cost savings in public buildings". In: *Expert Systems with Applications* 41.4 (2014), pp. 1813–1829.

[116] F Rosemblat. "The perceptron: A perceiving and recognizing automation". In: *Cornell Aeronautical Laboratory Report* (1957).

[117] Frank Rosenblatt. *Principles of neurodynamics. perceptrons and the theory of brain mechanisms*. Tech. rep. DTIC Document, 1961.

[118] Francesco Rossi et al. "Artificial neural networks and physical modeling for determination of baseline consumption of CHP plants". In: *Expert Systems with Applications* 41.10 (2014), pp. 4658–4669.

[119] Nader Samaan and Chanan Singh. "A new method for composite system annualized reliability indices based on genetic algorithms". In: *Power Engineering Society Summer Meeting, 2002 IEEE*. Vol. 2. IEEE. 2002, pp. 850–855.

[120] Luigi Schibuola, Massimiliano Scarpa, and Chiara Tambani. "Demand response management by means of heat pumps controlled via real time pricing". In: *Energy and Buildings* 90 (2015), pp. 15–28.

[121] John E Seem. "Pattern recognition algorithm for determining days of the week with similar energy consumption profiles". In: *Energy and Buildings* 37.2 (2005), pp. 127–139.

[122] John E Seem. "Using intelligent data analysis to detect abnormal energy consumption in buildings". In: *Energy and Buildings* 39.1 (2007), pp. 52–58.

[123] Pervez Hameed Shaikh et al. "A review on optimized control systems for building energy and comfort management of smart sustainable buildings". In: *Renewable and Sustainable Energy Reviews* 34 (2014), pp. 409–429.

[124] Wenli Shang, Xiaofeng Zhou, and Jie Yuan. "An intelligent fault diagnosis system for newly assembled transmission". In: *Expert Systems with Applications* 41.9 (2014), pp. 4060–4072.

[125] Pierluigi Siano. "Demand response and smart grids—A survey". In: *Renewable and Sustainable Energy Reviews* 30 (2014), pp. 461–478.

[126] Haykin Simon. *Neural Networks: A Comprehensive Foundation. 1999*.

[127] ASHRAE Standard. "55: Thermal Environmental Conditions for Human Occupancy American Society of Heating". In: *Refrigeration and Air Conditioning Engineers, Atlanta, USA* (1992).

[128] Goran Strbac. "Demand side management: Benefits and challenges". In: *Energy policy* 36.12 (2008), pp. 4419–4426.

[129] Marco Henrique Terra and Renato Tinós. "Fault detection and isolation in robotic manipulators via neural networks: A comparison among three architectures for residual analysis". In: *Journal of Robotic Systems* 18.7 (2001), pp. 357–374.

[130] Paul Thorsnes, John Williams, and Rob Lawson. "Consumer responses to time varying prices for electricity". In: *Energy Policy* 49 (2012), pp. 552–561.

[131] Roman Timofeev. "Classification and regression trees (cart) theory and applications". In: (2004).

[132] Andrea Toffolo. "Fuzzy Expert Systems for the Diagnosis of Component and Sensor Faults in Complex Energy Systems". In: *Journal of Energy Resources Technology* 131.4 (2009), p. 042002.

[133] ENISO UNI. "7730 (1997)-Ambienti termici moderati". In: *Determinazione degli indici PMV e PPD e specifica delle condizioni di benessere termico* (1997).

[134] JC Visier et al. "Commissioning tools for improved energy performance". In: *Results of IEA ECBCS Annex* 40 (2005).

[135] Don Von Dollen. "Report to NIST on the smart grid interoperability standards roadmap". In: *Electric Power Research Institute (EPRI) and National Institute of Standards and Technology* (2009).

[136] Shengwei Wang and Fu Xiao. "AHU sensor fault diagnosis using principal component analysis method". In: *Energy and Buildings* 36.2 (2004), pp. 147–160.

[137] Siyu Wu and Jian-Qiao Sun. "Cross-level fault detection and diagnosis of building HVAC systems". In: *Building and Environment* 46.8 (2011), pp. 1558–1566.

[138] Ronald R Yager and Janusz Kacprzyk. *The ordered weighted averaging operators: theory and applications*. Springer Science & Business Media, 2012.

[139] Kenji Yamanishi and Jun-ichi Takeuchi. "Discovering outlier filtering rules from unlabeled data: combining a supervised learner with an unsupervised learner". In: *Proceedings of the seventh ACM SIGKDD international conference on Knowledge discovery and data mining*. ACM. 2001, pp. 389–394.

[140] Ke Yan et al. "ARX model based fault detection and diagnosis for chillers using support vector machines". In: *Energy and Buildings* 81 (2014), pp. 287–295.

[141] Bing Yu and DH van Paassen. "Fuzzy neural networks model for building energy diagnosis". In: *8th International IBPSA Conference*. 2003, pp. 1459–1466.

[142] Lotfi A Zadeh. "Fuzzy sets". In: *Information and control* 8.3 (1965), pp. 338–353.

[143] Yang Zhao, Shengwei Wang, and Fu Xiao. "Pattern recognition-based chillers fault detection method using support vector data description (SVDD)". In: *Applied Energy* 112 (2013), pp. 1041–1048.

[144] Hans-Jürgen Zimmermann. *Fuzzy set theory—and its applications*. Springer Science & Business Media, 2011.

[145] Yi Zong et al. "Model predictive controller for active demand side management with pv self-consumption in an intelligent building". In: *Innovative Smart Grid Technologies (ISGT Europe), 2012 3rd IEEE PES International Conference and Exhibition on*. IEEE. 2012, pp. 1–8.